Category UC-92a

SAND83-7121
Unlimited Release
Printed April 1984

DEVELOPMENT OF A DOWNHOLE STEAM GENERATOR SYSTEM

Prepared for
Sandia National Laboratories
Albuquerque, NM 87185
Contract #74-8794

by

Foster-Miller, Inc.
350 Second Avenue
Waltham, MA 02154

ABSTRACT

This report describes the development of a downhole steam generator system for use in enhanced oil recovery. The system is composed of four major components: the steam generator, packer, tube string and control system. A state-of-the-art review indicated that advances in technology would be necessary in two areas (high pressure combustion and high temperature packer seals) in order to fabricate a field-worthy system. As a result, two tasks were undertaken which resulted in the development of a novel ceramic-lined combustor and a unique all-metal packer. These elements were incorporated into an overall system design. Key system components were built and tested in the laboratory. The program culminated in a successful simulated downhole test of the entire system, less tube string, at Sandia National Laboratories.

TABLE OF CONTENTS

TABLE OF CONTENTS (Continued)

LIST OF ILLUSTRATIONS

LIST OF ILLUSTRATIONS (Continued)

LIST OF TABLES

1. INTRODUCTION

Steam stimulation is already a leading enhanced oil recovery technique, and its importance over the next decade is expected to increase. At present, the steam is generated at the surface and injected into the reservoir through a tube string. As producing reservoirs become depleted, interest is shifting to other, fundamentally different applications of steam stimulation. In such applications, surface-generated steam appears to be at a disadvantage, and a new approach -- downhole steam generation -- deserves evaluation. The applications in question, along with some reasons why conventional steam stimulation appears unsuitable, are given below.

- Deep wells. Wells as deep as 3000 to 5000 ft are now candidates for steam stimulation, and at these depths, wellbore heat losses may be unacceptably high for surface-generated steam.

- Environmentally impacted areas. Locations where the surface equipment must be minimized (or remotely located) and/or areas where no exhaust emissions are allowed.

- Arctic applications. Regions in the far North where the cold environment (surface and subsurface) will lead to increased heat loss, and where thermal impact on the permafrost overburden must be minimized, to prevent any destabilization of the ground around the wellbore.

- Offshore applications - Situations where the highly deviated (long) wells may result in excessive wellbore heat loss. In addition, space constraints may require the surface equipment to be located some distance from the wellhead.

Recognizing the need for a new approach to steam stimulation, the U. S. Department of Energy (DOE) initiated Project Deep Steam and appointed Sandia National Laboratories, Albuquerque, New Mexico, (Sandia) as project manager. One of the main objectives of this project was to develop the technology base needed to make downhole steam generation a viable commercial proposition. The work described herein was carried out in pursuit of this objective under contract to Sandia. Initial specifications for the system were broad enough to cover a wide range of potential applications. Key requirements (maximum values) included:

Firing Rate	-	15 MMBTU/hr
Steam Output	-	900 Bbl/day
Injection Pressure	-	3000 psi
Depth	-	5000 ft

In addition, the downhole components were to be compatible for use with 7" well casing. The initial choice of fuel was diesel oil (#2 fuel), but it was recognized that to be commercially attractive, the system should be able to run on heavier fuels. This factor played an important role in the selection of the combustor concept, as described later.

Four components were identified as being crucial to the success of downhole steam. They are the steam generator, packer, tube string and control system. The steam generator produces steam downhole and injects it into the formation. The packer seals the wellbore and prevents steam from leaking up to the surface. The tube string carries fuel, air and water down the well to the steam generator. The control system regulates the fuel, air and water flow and controls the steaming operation.

At the start of the program, a state-of-the-art review was carried out to assess the technologies needed to develop the system. This review indicated that advances in technology would be necessary in two areas: high pressure combustion and high temperature packer seals. As a result, two developmental tasks were undertaken initially; tasks which resulted in the development of a novel ceramic-lined combustor and a unique all-metal packer seal*. These elements were incorporated into an overall system design. The key system components were then built and tested in the laboratory. The program culminated in a successful 140 hour simulated downhole test (4-10 MMBTU/hr; 250-1300 psi) which was started at Foster-Miller and then continued at Sandia to demonstrate system performance.

---

* Patents covering the novel aspects of these components have been applied for; one has issued, two are pending.

The work carried out during this program is described in the sections that follow. This work includes:

- The development and testing of a high-pressure steam generator that incorporates the ceramic-lined combustor.

- The analysis, design and testing of the all-metal packer seal.

- The design and specification of the major components of the downhole steam generation system, including the steam generator, packer, tube string and control system.

The success of this and other programs carried out under Project Deep Steam led DOE to conclude that a sound technology base had been developed, and that further refinement and testing of the downhole steam generation system should proceed under commercial sponsorship.

2. SYSTEM DESCRIPTION

2.1 Methods of Steam Generation

For an oil-fired system, there are two basic methods of steam generation depending on how the heat is transferred from the hot combustion gas to the feedwater. These methods are shown in Figure 2-1. In the direct method (Figure 2-1a), water mixes with the hot gas and heat transfer by direct contact causes it to vaporize into steam. In the indirect method (Figure 2-1b), the hot gas and water are prevented from physical contact, while heat is transferred across a heat exchanger wall. When adapted for downhole use, the direct method requires that combustion take place at the injection pressure and that the combustion gas (mixed with steam) be injected into the formation. With the indirect method, however, combustion can take place at atmospheric pressure, with the combustion gas brought up to the surface and released to the atmosphere.

At the start of this program, a key decision was made to develop the direct type of steam generator*. The reasons for this choice include:

---

* Another contractor pursued development of an indirect system.

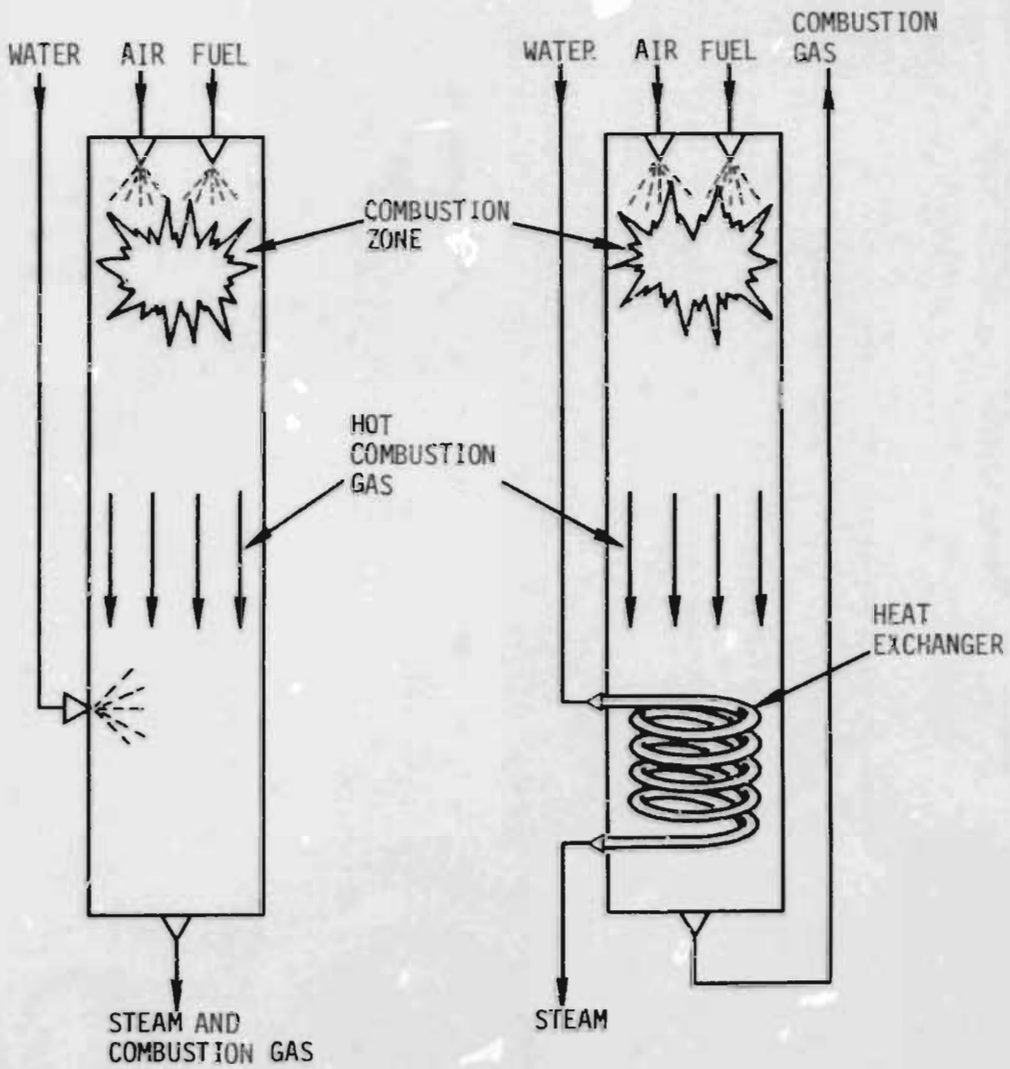

Figure 2-1. Basic Steam Generation Methods

1. Supression of Atmospheric Pollution. Because the combustion gas is injected into the formation (instead of being brought up and released at the surface), atmospheric pollution is suppressed.

2. Simpler Downhole Hardware. Direct contact heat transfer eliminates the need for a downhole heat exchanger. In addition, since the combustion gas is not brought up to the surface, the tube string configuration is simpler.

3. Reduced Corrosion Potential. Because transport of the combustion gas is not required, exposure of system hardware to this highly corrosive product is greatly reduced.

The main drawback of the direct method is that combustion takes place at the injection pressure and so the power required to compress the combustion oxidizer is higher than with the indirect method. This increase in compression power -- which is a fundamental consequence of the injection of combustion gas into the formation -- represents the price to be paid for the aforementioned, and any other desirable features of the direct system.

2.2 System Configuration

Steam is generated at the reservoir sandface by means of a downhole steam generator (Figure 2-2). The oxidizer, fuel and water flows required by the steam generator are established and controlled at the surface and supplied through a multi-string tubing system. Although either air or oxygen can be used as the oxidizer, this development program considers only air which is supplied by a compressor that provides the flow at the required injection pressure. The control system monitors this flow at the required injection pressure. The control system monitors this flow and regulates the fuel and water flow to maintain the precise air-fuel and air-water ratios needed for clean combustion and high quality steam generation. The air, fuel and water then flow to the steam generator through the multi-string tubing system. At the steam generator, the fuel burns in the presence of air and the resulting hot combustion gases then mix with the sprayed water, causing it to vaporize into steam. The mixture of steam and combustion gases then enters into the formation. The packer is included in the system to prevent the steam and combustion gases from leaking back up the wellbore.

2.2.1 The Steam Generator

A key component of the system is the downhole steam generator. The present design (Figure 2-3) has undergone many days of simulated downhole testing using #2 fuel. An early prototype of the combustor section was also run for a brief period (about 1 hour) on heated Kern River Crude (12^{o} API).

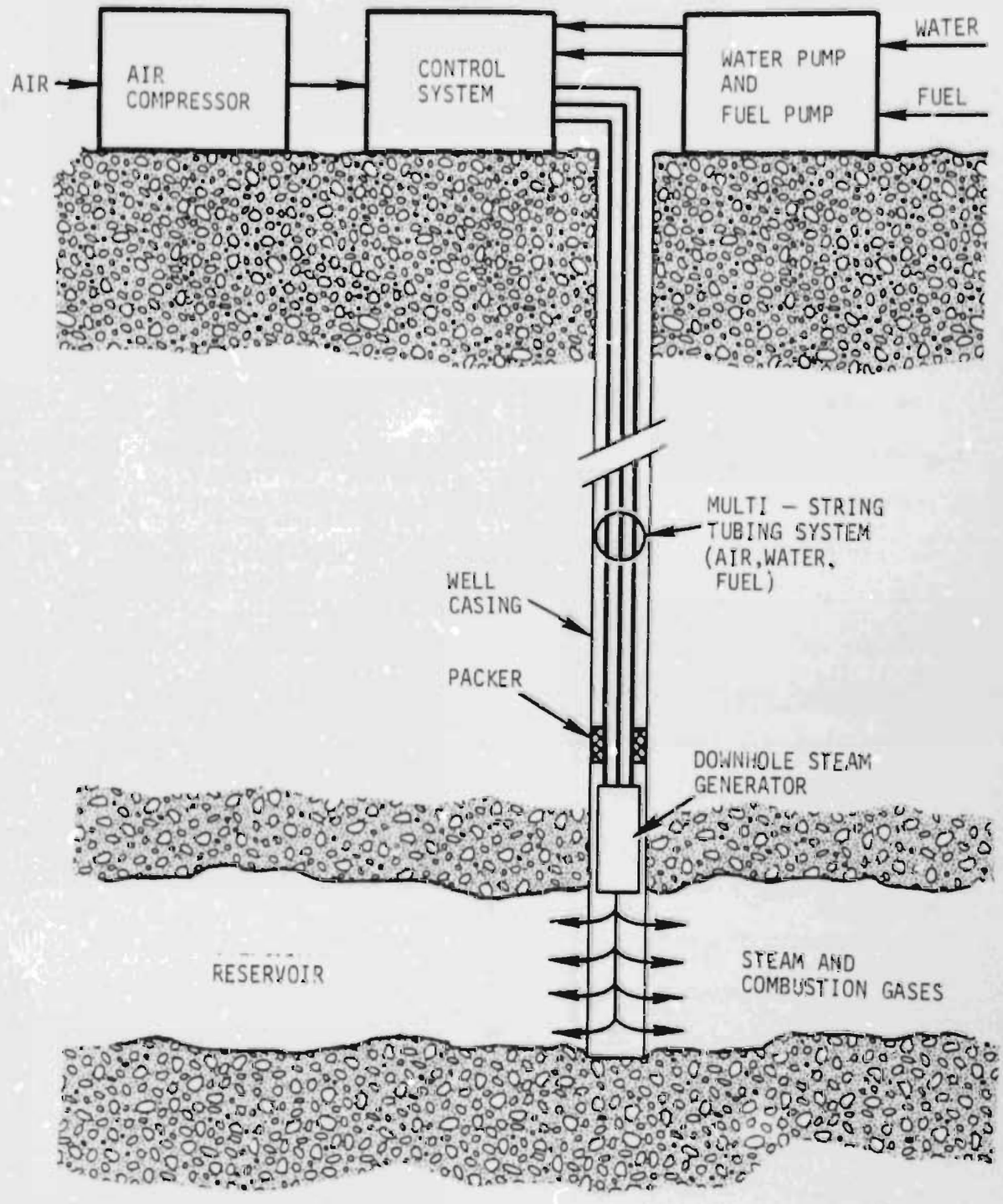

Figure 2-2. The Downhole Steam Generation System

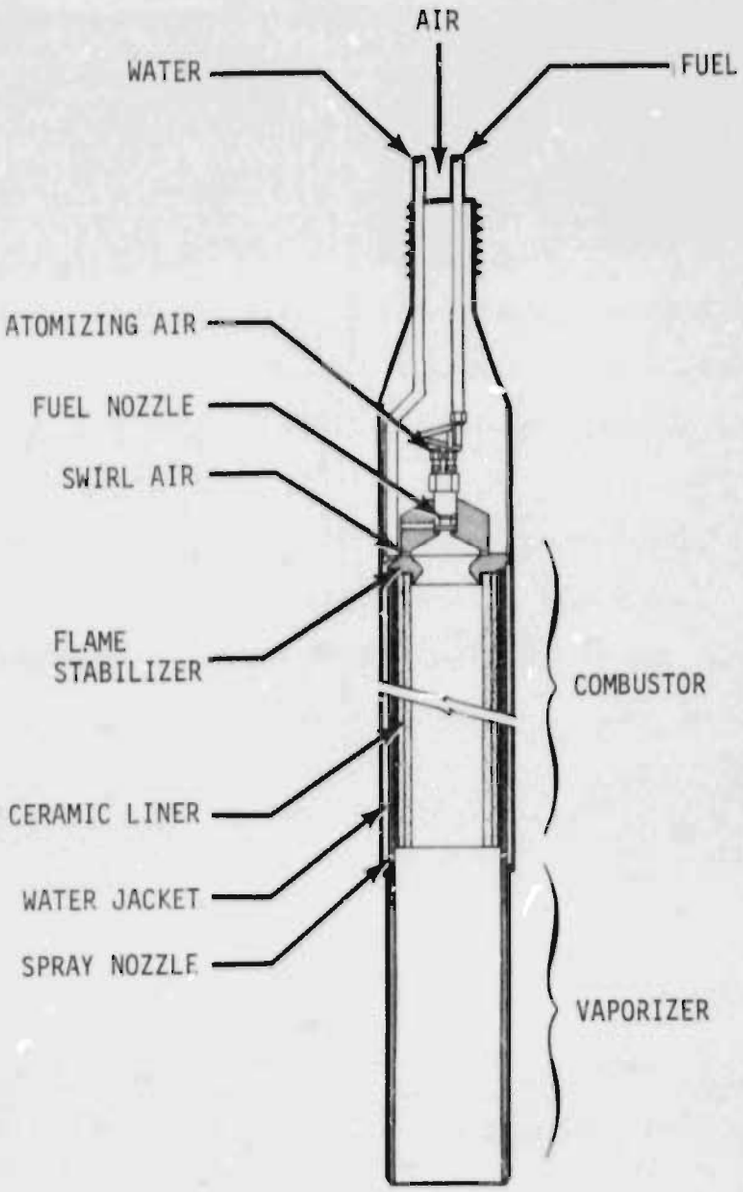

Figure 2-3. Prototype Steam Generator

The steam generator is divided into two sections: the combustor and the vaporizer. Pressurized fuel is sprayed into the combustor through an atomizing nozzle. Approximately 15 percent of the combustion air flows axially around the fuel nozzle and helps carry the atomized fuel into the combustion zone. In this zone, it mixes with the remainder of the combustion air which is injected through tangential orifices. The mixture than ignites and passes through a flame-stabilizing venturi. The function of the venturi is to ensure that the flame is not blown back or blown out under changing conditions. The hot combustion gases, including any unburnt hydrocarbons, now pass through a long hot ceramic-lined section of the combustor. The swirl and long residence time in this hot zone promote the complete combustion of any unburnt hydrocarbons. The hot combustion gases then enter the vaporizer. Preheated water from the surrounding jacket is injected into this section and vaporizes into steam. Finally, the steam and combustion gases exit from the steam generator and enter into the formation.

Because the combustor, under optimum operating conditions, produces practically no soot, the exhaust products can be injected into the reservoir without fear of degrading the natural porosity of the formation. This reduces the pollutants that would otherwise be released to the atmosphere. In addition, the exhaust gases may interact with the oil and produce a faster reservoir response.

2.2.2 The Packer

The packer assembly is shown in Figure 2-4(a). It consists of two components: a tubing anchor and a seal module. The anchor is of conventional design; almost any commercial unit can be used. The seal module consists of a set of annular dies that holds two metal sealing rings. The rings are expanded hydraulically by pressurized fluid (at about 10,000 psi) supplied through a 1/4 in. dia. control line from the surface. As the fluid enters the seal module, the inner section of the ring extrudes through the die and forces the outer section to increase in diameter until it contacts the well casing to form the seal (Figure 2-4(b)).

The rings are of a composite construction; three different materials are used in their manufacture. The inner section (aluminum) forms the hydraulic seal and prevents fluid from leaking past the die. Aluminum provides the plasticity (low yield strength and ductility) needed for reliable sealing. The ring body (titanium) serves as the main load-carrying member that resists steam pressure. Titanium provides the necessary combination of high-temperature strength, ductility and corrosion resistance. The outer lip (copper) serves as a soft metal seal between the packer and the casing. The lip material and configuration provide a tight seal in irregular, worn and out-of-round casing, and permit the packer to be retrieved (by upward pull) without excessive force. The use of copper also protects

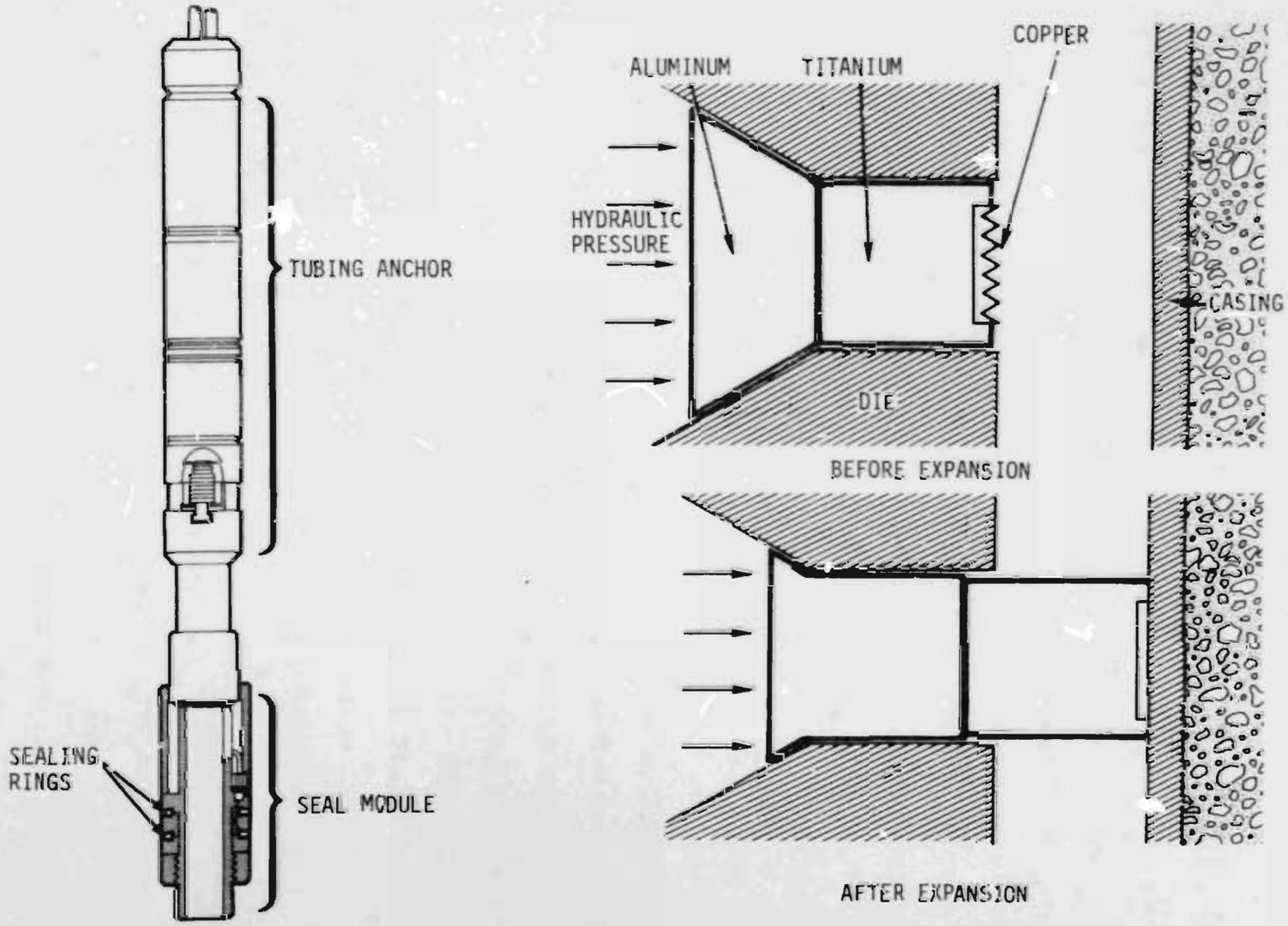

Figure 2-4. High Temperature Packer

the lip from galvanic corrosion when in contact with the steel casing.

2.2.3 The Control System

The control system for the steam generator has three parts: two equipment skids and a control console. The system is shown schematically in Figure 2-5. The equipment skids are made up of the pumps, valves and other items needed to supply the steam generator with air, fuel and water. All flows are controlled by flow regulators which consist of electropneumatic control valves connected to flow sensors in a closed loop configuration. This ensures that the flow is accurately regulated in spite of any disturbances in the system.

The first equipment skid (air skid) controls the airflow. Pressurized air from the air compressor is brought to this skid and goes through an air dump valve. Airflow to the burner is thus regulated by venting any excess air from the compressor to the atmosphere. The dump valve control signal is generated at the control console by comparing the measured flow with the controller setpoint. The second equipment skid (fuel and water skid) establishes and controls the fuel and water flow. Fuel from the tank goes through a filter and is pressurized by a positive displacement pump. A backup fuel pump, connected in parallel, switches on automatically in case the primary pump fails. The pressurized fuel then passes through a flow regulator that is controlled from the control console. The regulated fuel flow is then delivered to the steam generator. The water supply

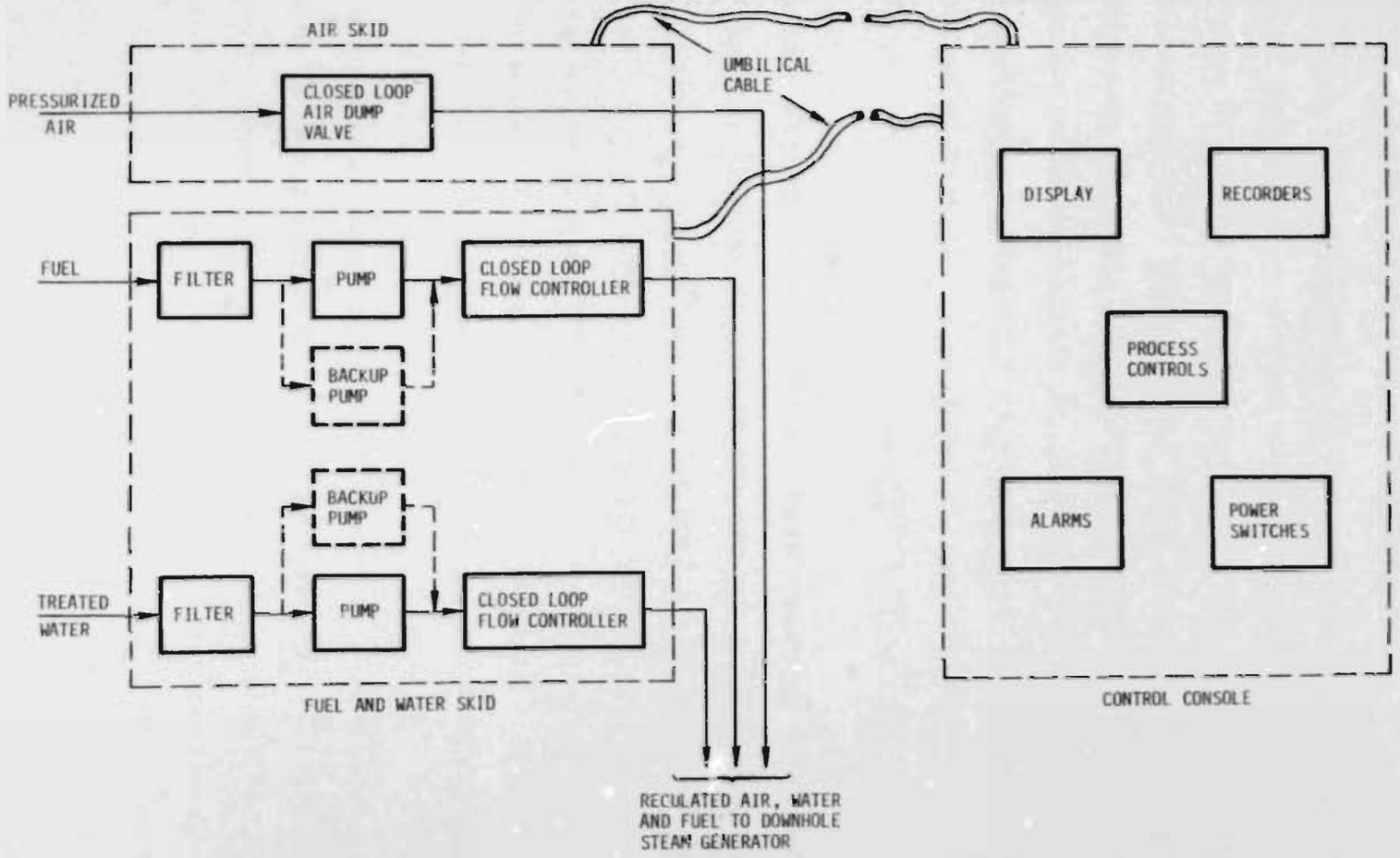

Figure 2-5. The Control System

system is similar to the fuel system. T eated water is brought to the skid, passes through a filter, is pressurized by a pump, controlled by the flow regulator, and delivered to the steam generator.

The control console allows the operator to control the steam generation system, and monitor and record the important variables. It also alerts the operator by means of audible and visual alarms of any system abnormality, and automatically takes appropriate action, when necessary, to avert catastrophic system failure. The console is connected to the equipment skids by means of umbilical cables.

The required values of the process control variables are established by indicating set-point controllers, which allow a given parameter level to be set on a dial. The measured value of the variable is also displayed to check controller operation. The main control variable is airflow, which establishes the firing rate. The other control variables are the air-fuel and air-water ratios. The air-fuel ratio, which for stoichiometric combustion is a characteristic of a given fuel, is only changed when the type of fuel is changed. The air-water ratio sets the water flow (for a given heat output) and thus determines the rate of steam generation and the steam quality. These parameters (firing rate, steam output and quality) are also displayed, along with several other variables such as fuel flow, water flow, system pressures, etc. Key variables are also recorded by

three multi-channel strip-chart recorders. An alarm system with an annunciator is provided to alert the operator to abnormal conditions. The annunciator provides visual and aural alerting signals for seven system abnormalities, including low fuel or water flow, filter blockage, system overpressure, etc. Certain conditions, such as low fuel flow causes the backup pump to take over automatically. Other conditions like low water flow, if left uncorrected, cause the system to shut down to avoid combustor burnout.

The power switches that activate the various parts of the system (pumps, controllers, etc.) are also located on the control console to maximize operator convenience.

2.2.4 The Tube String

The tube string design contains several features found in offshore risers and other systems where industry has successfully used multiple string tubing for a number of years. The basic configuration (Figure 2-6) consists of a side-by-side arrangement of jointed API pipe for the air and water supply. The larger tube (2-7/8 in. dia.) is for the air; its diameter chosen as large as space allows to reduce the pressure drop. The smaller tube (1-1/4 in. dia.) is for the water. The fuel and packer hydraulic fluid are supplied through small dia. continuous tubing (3/4 in. and 1/4 in. dia. respectively) strung alongside the jointed pipe and restrained at regular intervals by a banded collar. The function of the collar is to support the tubing and center the tube bundle. An optional electrical conduit (not shown in Figure 2-6) is also included in the design to connect with any downhole instrumentation (thermocouples).

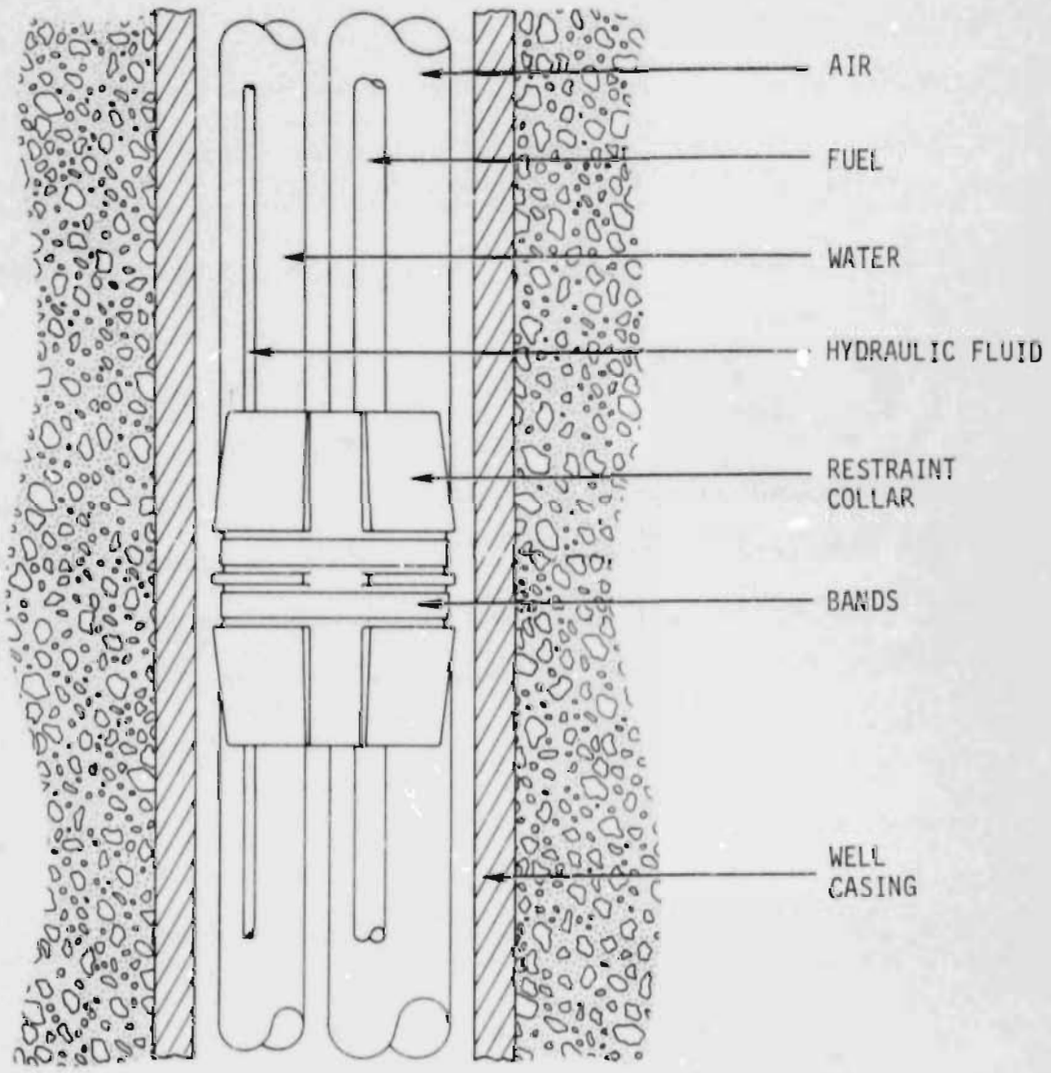

Figure 2-6. The Tube String

2.3 Thermodynamic Analysis

A thermodynamic analysis of the downhole steam generation system has been carried out. A summary of the analytical model is given in Appendix A. Figure 2-7 gives an indication of the thermal efficiency of the system as a function of the injection pressure. As can be seen, about 50-60% of the heat in the fuel appears as heat (enthalpy) in the steam. The remaining heat is used to run the prime mover and compress the air to injection pressure (35-40%), and heat the products of combustion (~5%). Another characteristic of note is that the steam (partial) pressure is less than the injection pressure because the steam is mixed with the exhaust gases (N_2 and CO_2) and hence has a partial pressure lower than the total pressure of the mixture (Law of Partial Pressures). The steam partial pressure as a function of the injection pressure is shown in Figure 2-8. The corresponding partial pressures for N_2 and CO_2 are also shown. By definition (Appendix A), the sum of the three partial pressures equals the total injection pressure. The steam temperature, which is the same as the mixture temperature, is also shown in Figure 2-8.

The following conclusions emerge from the analysis of downhole steam generation.

a. The thermal efficiency of the process lies between 55-65% if both the heat in the steam and exhaust gas are

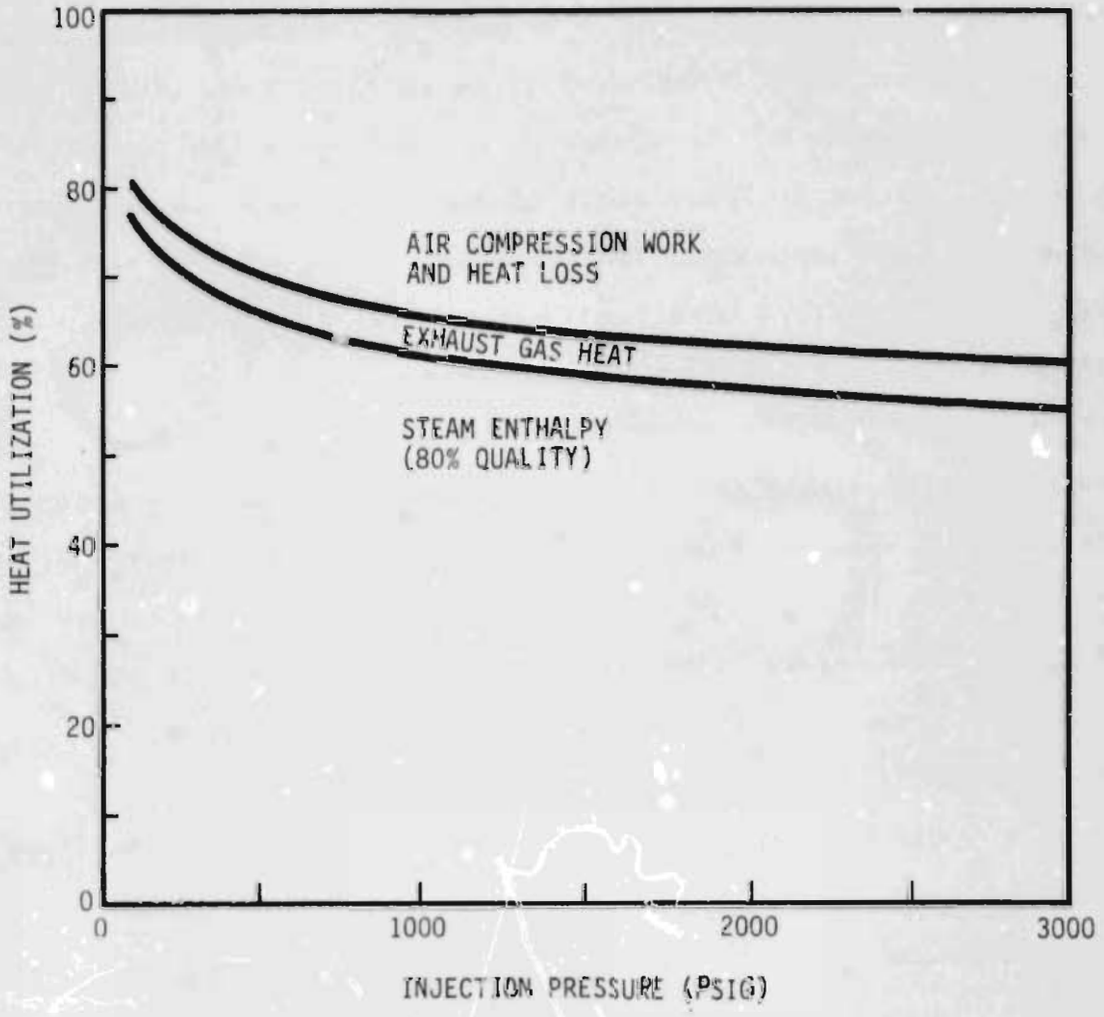

Figure 2-7. Thermal Efficiency of Downhole Steam Generation System

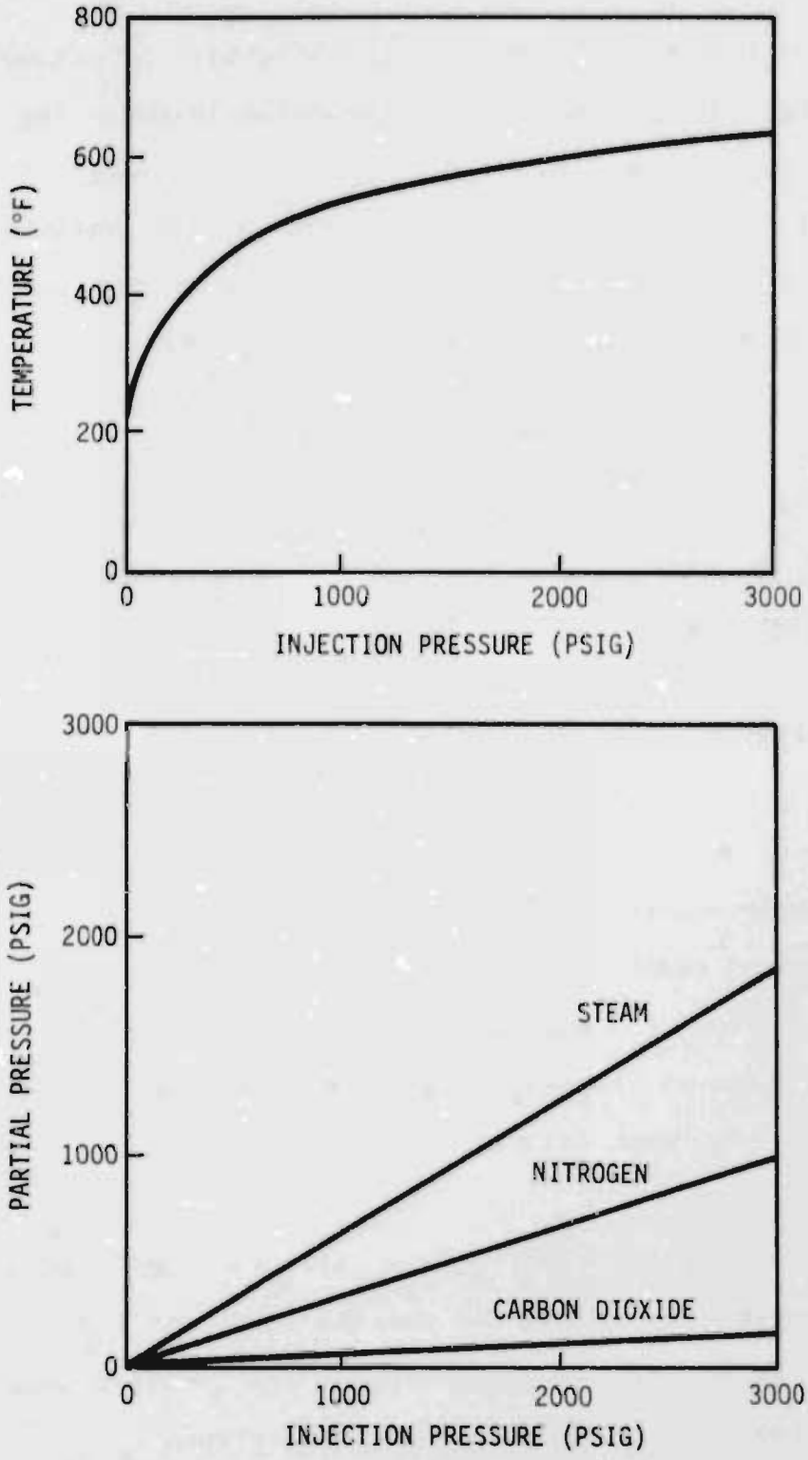

Figure 2-8. Partial Pressure and Temperature of Injected Products

considered. If the heat in the steam and exhaust gas is excluded, the efficiency decreases by about 5%.

b. In high pressure reservoirs, the thermal efficiency of downhole steam -- unlike surface steam -- is not a strong function of the reservoir depth or tubing length, for deviated wells (see Figure 2-7).

c. High downhole steam quality is easily established since it is independent of the depth. With surface steam generation, steam quality decreases with depth, making it difficult to maintain high downhole steam quality in deep wells.

d. Since no hot fluid is transported on the surface, the uphole equipment, including air compressors, can be located remotely and pressurized air, fuel and water piped into the wellhead. With surface steam, remote location of the steam generator is impractical due to excessive heat loss from the surface piping.

e. The absence of steam in the wellbore has two beneficial effects: it eliminates thermal stress in the casing both due to normal heat transfer and due to steam leakage, and it avoids heating the surrounding ground.

f. The amount of pollution control equipment is minimized. The injection of combustion gases into the reservoir eliminates the need for any flue gas scrubbers for the steam generator. If compressor engine exhaust is of concern, then electrically-powered compressors can be considered to eliminate all pollution control equipment and simplify the permitting process.

g. The presence of exhaust gases (CO_2 and N_2) in the injected products could have a positive effect on oil recovery. Under normal conditions, their effects are felt to be minor. However, their influence at high temperature and in combination with steam has not yet been established.

3. STEAM GENERATOR DEVELOPMENT

3.1 Combustor Concept

In order to achieve the design goals discussed in the preceding section, it was necessary to develop a compact combustor that could burn No. 2 fuel oil (and possibly heavier fuels) cleanly without excess air. The conventional approach to this problem would be to use a premixed-prevaporized burner. In this type burner the fuel is atomized, mixed with the combustion air and permitted to vaporize prior to ignition. The air-fuel vapor mixture is ignited and the flame is stabilized by the recirculation flow in the wake of a bluff body or perforated plate. The well mixed air and fuel vapor permit clean burning of the fuel even at the stoichiometric air-fuel ratio. Unfortunately, the requirement that the downhole steam generator combustor must operate at pressures up to 3000 psig, precluded the use of the premixed-prevaporized concept. The high pressure operation brought about the possibility of autoignition of the air-fuel mixture with delay times too short to permit adequate prevaporization and uncertain enough to make proper location of the flameholder impossible. Figure 3-1 plots autoignition delay times of various fuel oils as a function of pressure and temperature. It can be seen that for pressures and temperatures of interest, delay times on the order of 5 to 10 milliseconds could be expected.

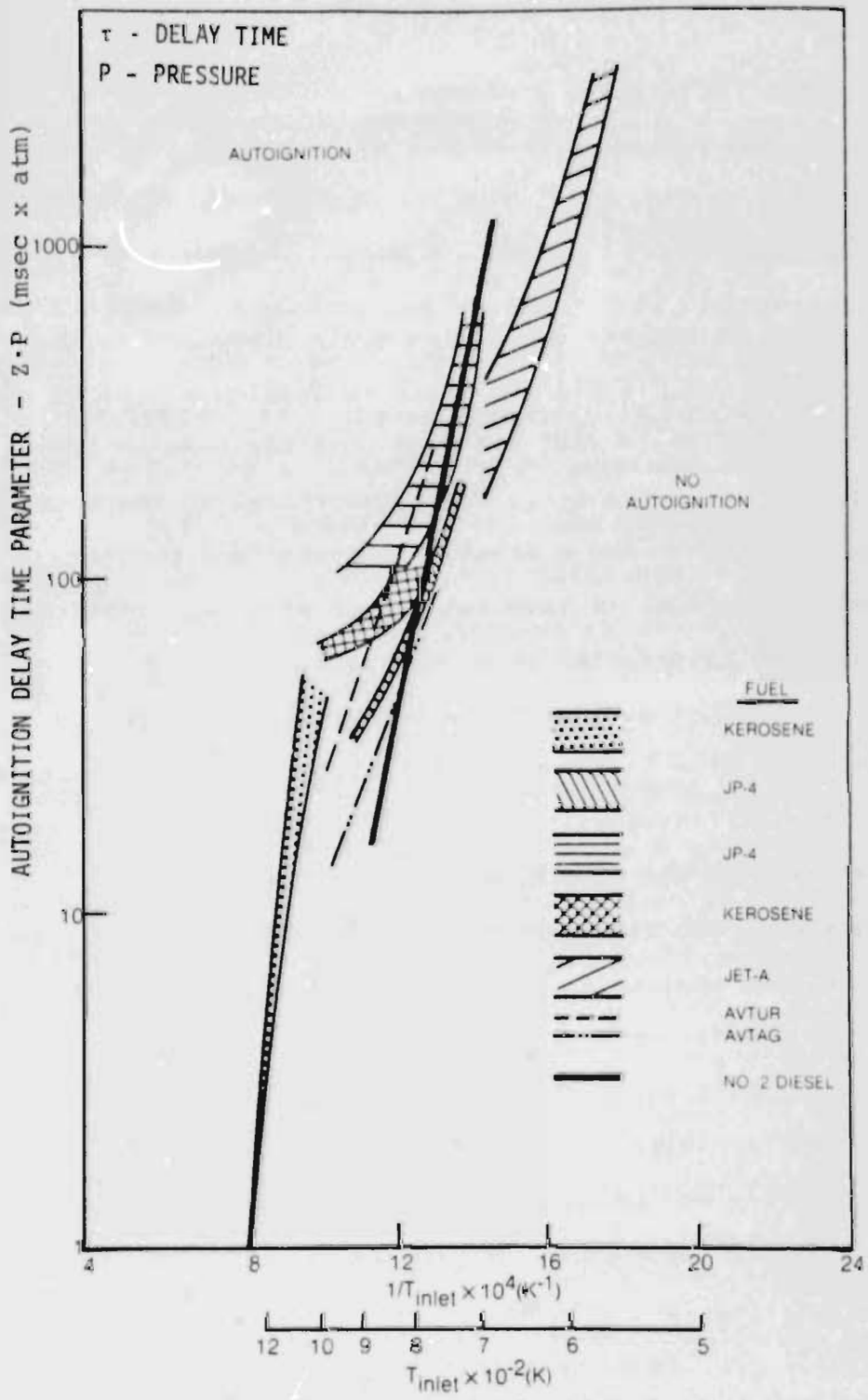

Figure 3-1. Autoignition of Liquid Hydrocarbon Fuel Sprays in Air [1]*

*Numbers in brackets denote references listed at the end of this report.

In order to avoid the problems associated with short autoignition delay times and inadequate fuel vaporization prior to ignition, a concept was generated for a burner which should be relatively insensitive to the degree of fuel prevaporization. This concept is illustrated in Figure 3-2. Fuel is introduced axially through an atomizing nozzle into the mixing chamber where it is subjected to a highly turbulent rotating airflow. The rotating airflow is established by admitting the air tangentially into the mixing chamber. In addition to simply promoting the mixing of fuel and air, the high relative velocity between the two streams creates high shear stresses which aid in the breakup of the larger fuel droplets.

A venturi is located at the discharge of the mixing chamber. The rotating airflow coupled with the divergent section of the venturi creates an expanding vortex. The expanding vortex creates a low pressure zone at its axis; this low pressure zone generates a recirculation zone in which the axial flow of air and fuel is reversed. This recirculation stabilizes the flame front by bringing hot gas in contact with the incoming air-fuel mixture and causing ignition.

Once the air-fuel mixture is ignited, hot combustion products will recirculate back toward the mixing chamber and ignite the air-fuel mixture as it discharges from the chamber. The use of a vortex generated recirculation to stabilize the flame front does

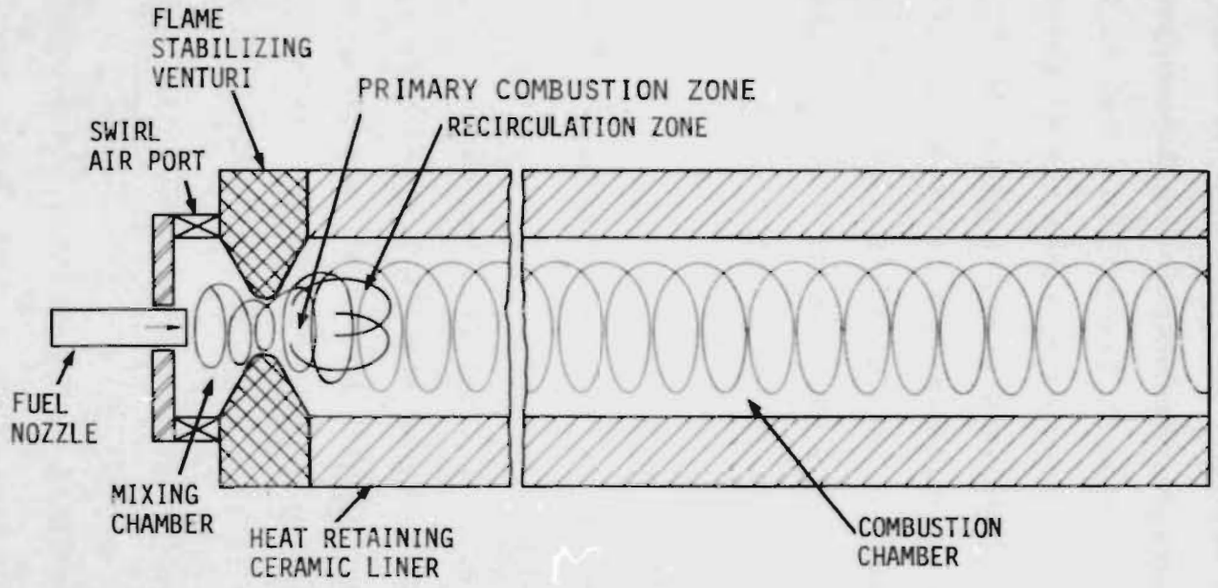

Figure 3-2. Combustor Design Concept

away with the need for a bluff body or perforated plate flame holder. The absence of a flame holder removes sites on which fuel droplets could aglomerate from the burner design and thus increases the probability of soot-free performance.

Some soot will be formed in fuel rich regions of the primary combustion zone which result from fuel droplet size variation caused by uncertainties of the atomization process. Any soot formed will be consumed in the hot walled section of the combustion chamber. The combustion chamber has insulated walls to produce internal temperatures high enough to ensure that combustion reactions are not rate limited and is long enough to provide the residence time for the relatively slow (diffusion controlled) solid-gas reactions to proceed to completion.

For feasibility testing, dense high purity alumina (Al_2O_3) was selected as the fireside liner material of the combustion chamber. This material is quite durable at high temperatures but has poor insulation properties. To overcome this weakness, the alumina liner was backed up with a layer of lightweight, castable alumina refractory insulation. The castable material does not have the structural qualities of the high density material but has an order of magnitude greater resistance to heat flow. The castable material was encased in a metal sleeve in order to give structural strength to the combustion chamber.

3.2 Feasibility Testing

3.2.1 Introduction

An aerodynamically scaled version of the combustor concept designed to operate at atmospheric pressure was fabricated. This model permitted the effect of fuel atomization quality, air velocity and flow rate on the flame stability and the combustion process to be assessed. A photograph of this unit is shown in Figure 3-3.

A series of qualitative tests were run to demonstrate the stable operation of the combustor. Quantitative tests followed to verify that the combustor had performed as well as it had seemed to on visual inspection and to quantify its behavior in terms of fuel-air ratios and emissions.

Emissions were monitored using a Scott continuous sampling gas analysis system which included O_2, CO_2, CO and total hydrocarbon (THC) analysis instrumentation. Soot was measured with a hand-held Dwyer smoke guage which drew a fixed sample volume through a piece of 5 micron filter paper. Particulate level was determined by comparing the color of the used filter paper to a standard. The comparison produced a smoke number ranging from 0 to 10, with 0 corresponding to no detectable soot.

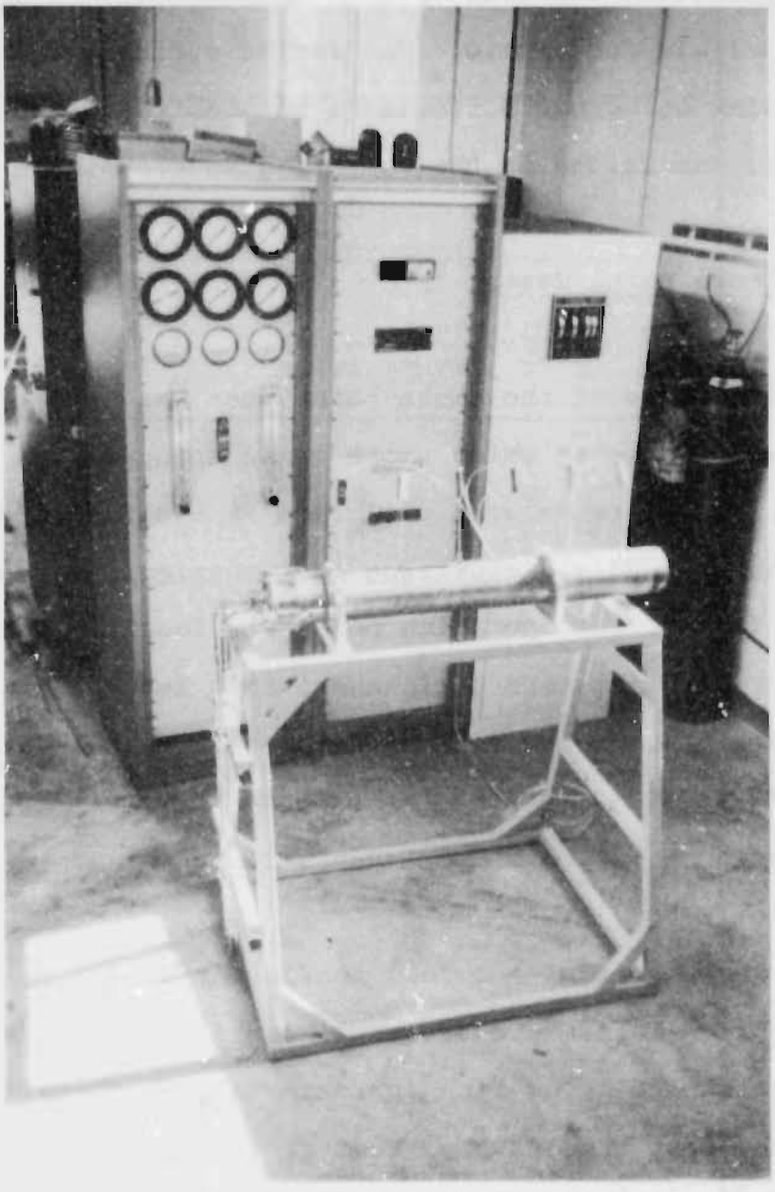

Figure 3-3. Atmospheric Combustor and Controls

Two series of quantitative tests were conducted. The first was smoke point tests which determined the equivalence ratio at which soot became detectable. Equivalence ratio (ε) is defined as the ratio of stoichiometric or theoretical air-fuel ratio to the actual air-fuel ratio. The second series determined the sensitivity of burner performance to atomization quality. These tests are summarized in the following sections.

3.2.2 Smoke Point Tests

The purpose of the smoke point test was to determine the equivalence ratio at which smoke began to appear in the combustor exhaust. These tests were performed at two fuel flow rates using both pressure and air atomizing fuel nozzles. At each fuel flow a clean (soot-free) operating point was found, and then the air flow decreased in steps until measurable amounts of particulates began to appear in the exhaust samples. Typical data from these tests are shown in Table 3-1. A smoke number of 0 indicates that essentially no particles were captured by the 5 micron filter.

A pressure atomizing fuel nozzle was used for these tests. Two fuel flow rates were used: a high flow close to the nozzle design point and a low flow approximately half the nozzle design flow. The test results show that at fuel flows close to the nozzle design point soot free operation could be maintained even with slightly substoichiometric air-fuel ratios ($\varepsilon > 1$). While at the low fuel flow rate a small amount (~0.5%) of excess air

TABLE 3-1. Automization Quality Test Results

Test No.	Fuel Flow lb/hr	lbm air / lbm fuel	Equivalence Ratio ε	Gas Temp °F	CO ppm	CO_2 %	O_2 %	THC ppm	Smoke No.
1	6.34	14.40	.9802	2420	800	15.01	0.52	10	0
2	6.34	14.28	.9882	2440	1000	15.03	0.35	12	0
3	6.34	14.09	1.0014	2440	1700	14.90	0.09	13	0
4	6.34	14.02	1.0063	2395	2300	14.89	0.02	10	0.5
5	6.24	14.00	1.0076	2315	2500	13.91	0.01	17	4
6	3.50	14.45	.9765	2050	600	15.50	0.61	11	0
7	3.68	--	--	2130	--	15.50	--	14	0
8	3.68	14.45	.9765	2110	600	15.50	0.61	11	0
9	3.50	14.18	.9949	2100	1200	14.86	0.21	11	0.5
10	3.50	14.05	1.0043	2050	1900	15.17	0.05	400	8.5

was needed to ensure soot free operation. This somewhat poorer performance at the lower fuel flow rate was attributed to the degraded fuel atomization. However, even at the lower fuel flow, the oxygen concentration in the combustor exhaust was less than 0.5%.

3.2.3 Atomization Quality Tests

The smoke point tests showed that the combustor performance was relatively independent of atomization quality. The purpose of this series of tests was to quantify that behavior. An air atomizing fuel nozzle was used for these tests and atomizing air pressure was varied in order to vary the atomization quality. Smoke measurements were made as in the Smoke Point Tests. The data from these tests are presented in Table 3-2. The combustor operated soot free while atomization air pressure varied from 10 to 3 psig. Operation at the last two points (0 and 1 psig) was sooty: these points corresponded to the poorest fuel atomization. Atomization is directly proportional to the atomizing air pressure with this type nozzle. Observation of the flame during these tests revealed that the flame became less transparent and more luminous as the atomizing air pressure was reduced. This change indicated that more soot was forming in the combustion zone as the atomization was degraded. However, this soot was consumed in the combustor until the atomization quality was severely degraded (i.e. less than 3 psig atomizing air

TABLE 3-2. Automization Quality Test Results

Test No.	Fuel Flow lb/hr	lbm air / lbm fuel	ε	P* (psig)	Gas Temp °F	CO ppm	CO_2 %	O_2 %	THC ppm	Smoke No.
1	8.52	14.28	.9883	10	2500	1000	15.51	0.35	12	0
2	8.52	14.28	.9884	20	2510	1000	15.25	0.35	11	0
3	8.52	14.28	.9880	30	2530	1000	15.18	0.36	11	0
4	8.52	14.25	.9905	5	2530	1000	15.10	0.30	13	0
5	8.52	14.32	.9853	3	2540	900	15.02	0.41	12	0
6	8.52	14.34	.9837	0	2650	1000	15.02	0.45	12	5.5
7	8.42	14.28	.9880	1	2540	1000	15.18	0.36	12	7

*atomizing air pressure

pressure). This characteristic is a key requirement for the ultimate development of a clean burning, heavy fuel combustor.

3.3 Implementation

Once the atmospheric testing had demonstrated the successful operation of the swirl stabilized combustor, the combustor concept was incorporated in the design of a downhole steam generator. A water jacket and steaming section were added to the combustor without changing its basic design. This downhole steam generator concept is shown in Figure 3-4. A prototype steam generator of this design was fabricated and a control system assembled to permit testing of the steam generator at moderate pressures ($\leq$ 500 psig) and firing rates ($\leq$ 5 MMBTU/hr). The control system permitted the steam generator airflow, water flow, fuel flow and operating pressure to be controlled independently. Air,

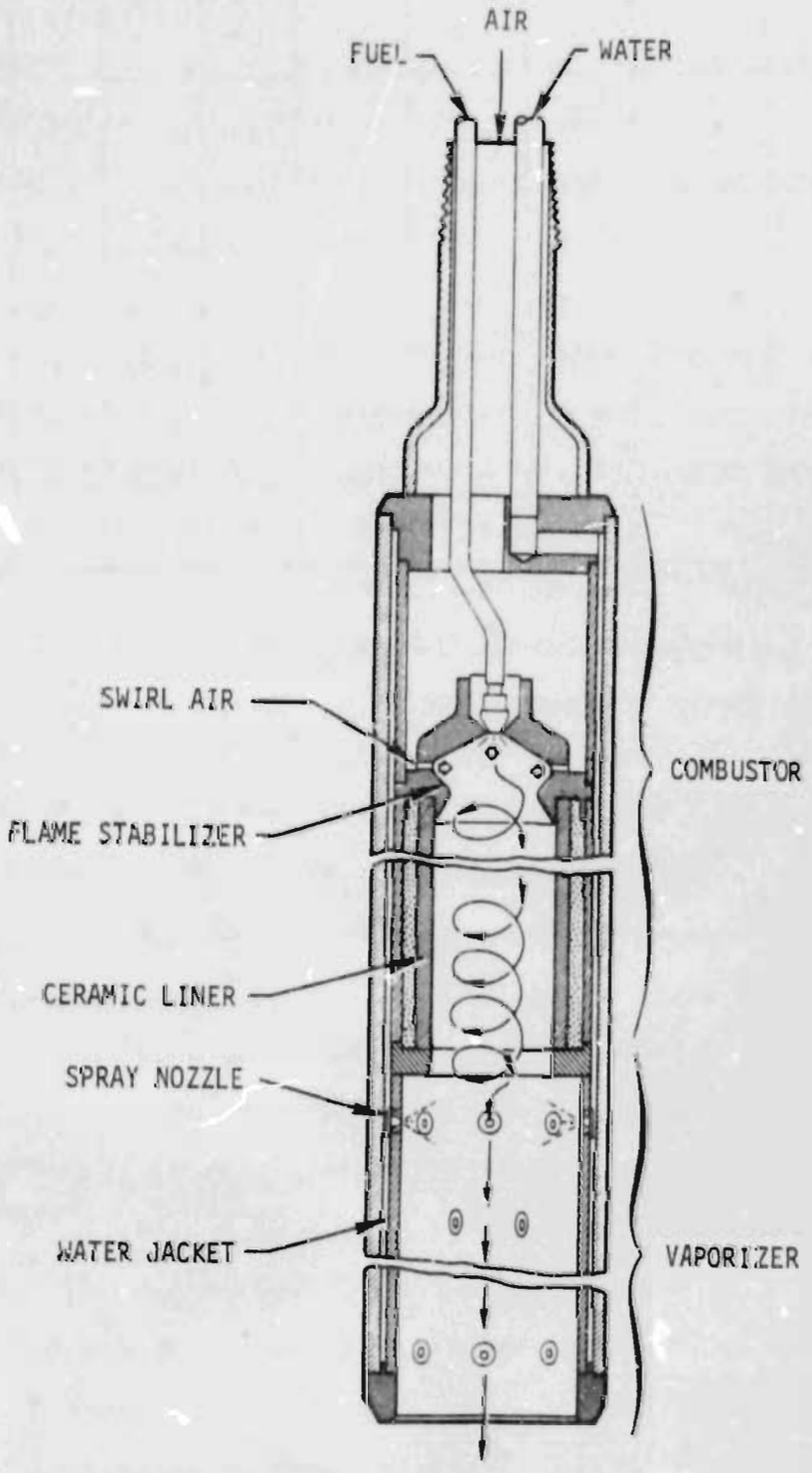

Figure 3-4. The Downhole Steam Generator -- Initial Design

fuel and water were supplied from pressurized tanks. In this blowdown mode of operation, test duration was limited to approximately twenty minutes at the maximum firing rate by tne size of the air accumulator.

During atmospheric testing, the combustor was ignited by inserting an oxyacetylene torch through a thermocouple port located near the combustion zone. This procedure could not be used with the prototype steam generator since the water jacket precluded direct access to the combustion chamber. High voltage spark ignition was considered, but the difficulty expected in maintaining a clean electrode couple with the relatively high dielectric constant of air at the elevated pressures expected in downhole operation led to the selection of a hypergolic ignition system. This system used a hypergolic fluid, triethylborane (TEB) to initiate combustion in the combustion chamber.

In practice, a sample flask filled with a 50-50 mixture of TEB and diesel fuel oil was placed in a piping loop which parallels the primary fuel line. The entire fuel system was filled with diesel fuel oil to purge all air from the system. Air and water flows were established to the steam generator. Fuel flow was then initiated through the sample flask. When the TEB-fuel mixture contacted the air in the combustion chamber, the TEB ignited spontaneously, providing the ignition source for the fuel oil.

This ignition procedure was used throughout the development program. It has the desired feature of requiring no downhole components beyond those needed during steady state combustor operation.

This system was used to conduct the initial elevated pressure testing of the steam generator. It was subsequently modified via the addition of fuel and water pumps and an air compressor connection to permit extended duration testing at pressures up to 1500 psig. The various tests and results are discussed in the following section.

3.4 Prototype Testing

Initial test firings of the steam generator were conducted at 175 psig, a firing rate of 1.25 MMBTU/hr and a steam quality of 80%. In addition to monitoring the air, fuel and water flow rates and steam generator operating pressure, exhaust gas analysis for O_2, CO_2 and CO was performed on the steam generator exhaust. Peridic grab samples of exhaust condensate were taken to determine pH and assess the cleanness of the combustion.

Several tests of 20 to 30 minutes duration were conducted, and the internals of the steam generator were examined after each test to assess any structural changes or damage. The results of these tests were very encouraging. The combustor performance was similar to that observed in the atmospheric pressure tests

in that combustion was stable and clean at stoichiometric conditions. No structural problems were noted and no problems were encountered generating 80% quality steam.

The test conditions were then changed to an operating pressure of 250 psig, a firing rate of 2.5 MMBTU/hr, the 80% quality steam was maintained. Again several tests of 20 to 30 minutes duration were conducted. The operation of the combustor was similar to that at 150 psig with no problems noted. However, examination of the combustor internals revealed several cracks in the aluminum oxide combustion chamber liner after the first of these tests. These cracks were compressive in nature and small pieces of aluminum oxide had been spalled from the edges of each crack. Inspection after subsequent tests revealed a general deterioration of the entire surface of the aluminum oxide. The surface appeared flaky and spalled over its entire surface. At this point it was apparent that the liner design would not satisfy the design goals and testing was stopped. The liner design was reviewed to assess the failure mechanisms and evaluate potential solutions.

The conclusions of this review were that two independent failure mechanisms were at work and that any successful design would have to address both of them. The compressive cracking was caused by the thermal expansion of the liner being restrained by the refractory insulation and water jacket. The temperature of the water jacket is about 600°F less than the metal sleeve

that restrained the atmospheric pressure combustor. The reduced thermal expansion of the metal jacket in the steam generator led to excessively high compressive stresses.

The cause of the general spalling was not as readily determined as that of the compressive stress failure. Examination of pieces of the failed liner by Sandia's Materials Laboratory [3] showed severe chemical attack at the grain boundaries of the aluminum oxide. This attack caused a significant reduction in the strength of the material and made the surface somewhat friable. The conclusion was that the weakened condition of the material coupled with the high compressive stress led to pieces spalling from the surface.

In the course of investigating the liner failure mechanisms an additional series of tests was run using a freely supported liner. The liner tested was an aluminum oxide tube identical to the one cast into the prototype steam generator. This tube was wrapped in a layer of CERABLANKET® ceramic fiber insulation* and inserted inside the steam generator water jacket. The goal was to observe the performance of the aluminum oxide liner in the absence of any externally imposed compressive stress. Four test firings of 20 to 30 minutes duration at a firing rate of 2 MMBTU/hr and pressures of 150-250 psig were made. The liner fractured on the first test into approximately 40 symmetrically shaped pieces (Figure 3-5); the pieces remained in place during the three subsequent firings. The failure mechanism appeared

*A trademark of Johns-Manville

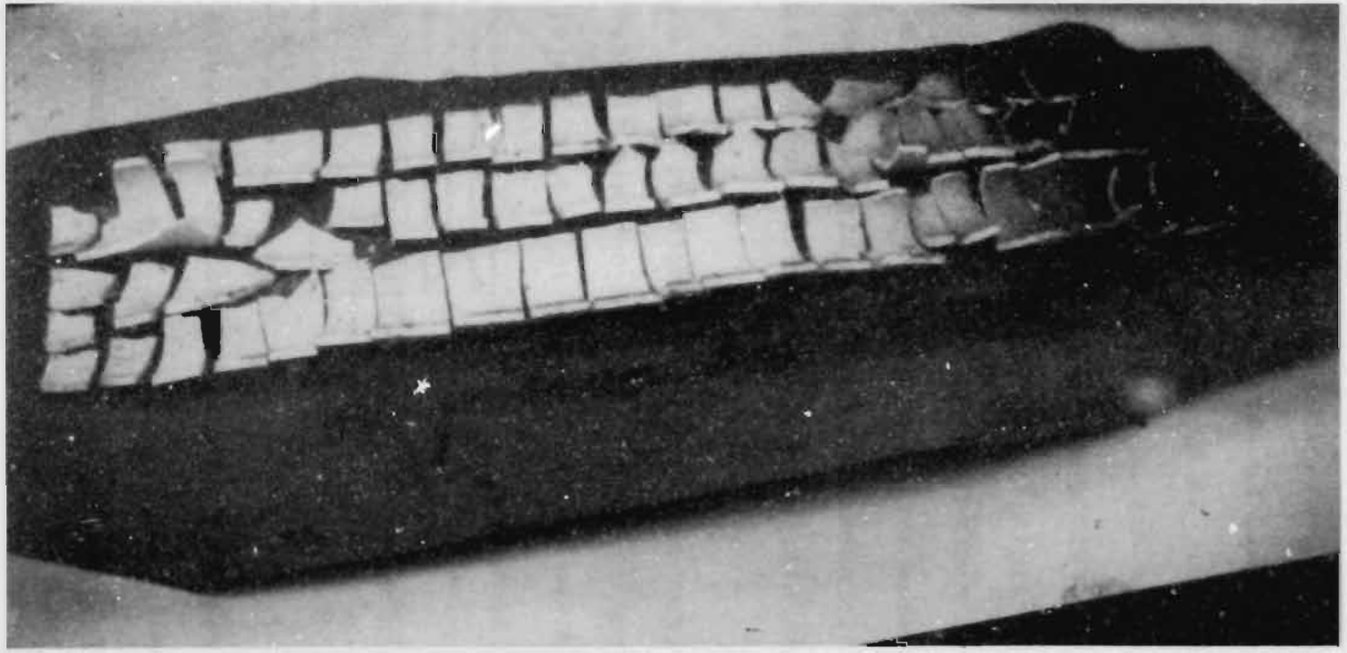

Figure 3-5. Unrestrained Al_2O_3 Combustion Chamber Liner

to have been tensile cracks resulting from thermal shock. However, analysis by Sandia's Material Laboratory [2] indicated that the cracks could be shrinkage cracks produced by sintering of the aluminum oxide. In any event, there were no compressive type failures and there was no spalling of the hot surface of the liner as noted in the prototype. Examination of the aluminum oxide crystals in the vicinity of the cracks revealed evidence of a vapor transport mechanism causing mass transfer of the aluminum oxide and the same type intergranular attack noted in the prototype. This phenomenon would ultimately result in a weakening of the intergranular bonding and failure of the liner.

Two new liner concepts were generated based on the results of the tests of the cast-in-place and ceramic fiber supported liners. The first concept, shown in Figure 3-6(a) incorporated the following features:

- A high density, high purity, segmented aluminum oxide (McDanel 998 Alumina) inner surface
- Reduced insulation compared to previously tested liners
- A metal sleeve to support the aluminum oxide
- An air gap between the liner's metal sleeve and the steam generator water jacket.

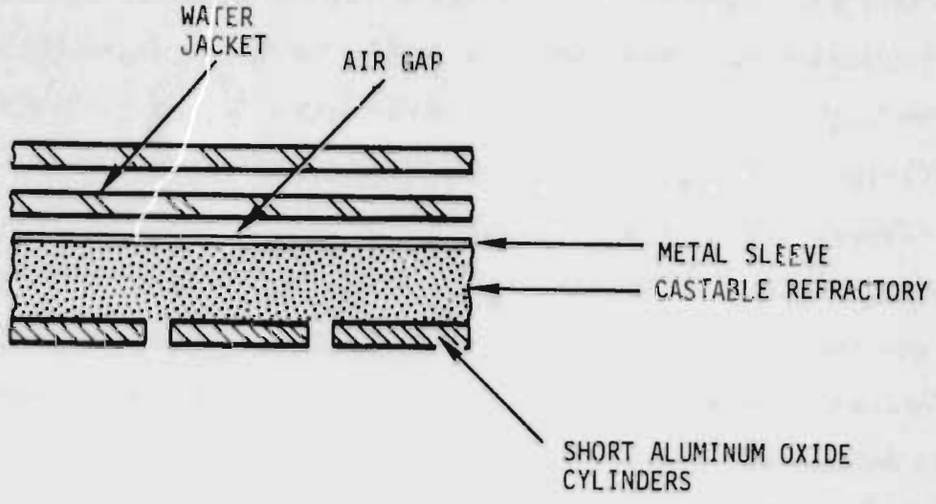

(a) MULTIPLE RING LINER

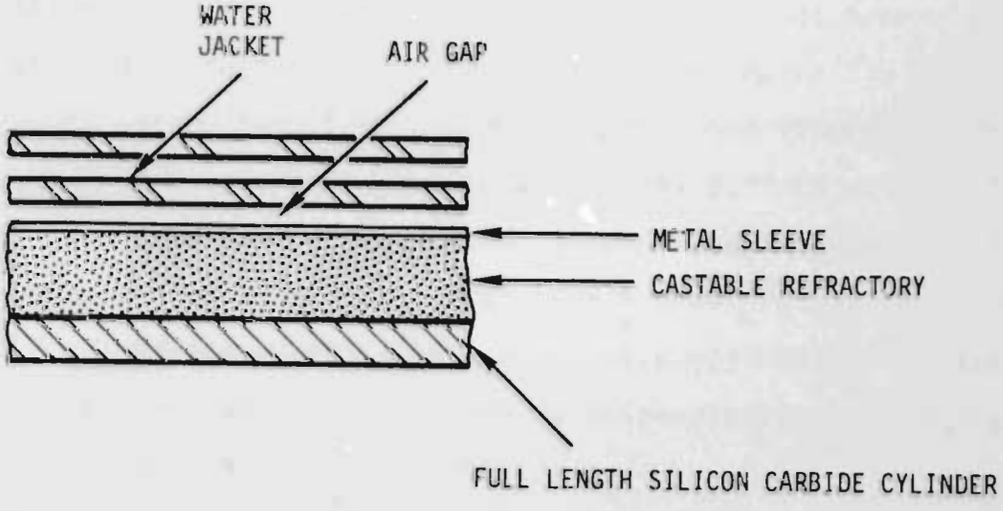

(b) MONOLITHIC LINER

Figure 3-6. Improved Liner Concepts

The higher density and purity of the aluminum oxide would minimize the susceptibility of the material to chemical attack of the grain boundaries. The segments (rings in this case) would reduce the magnitude of thermally induced axial stress. Reducing the insulation (castable refractory) was done to reduce the surface temperature of the aluminum oxide and thus reduce its chemical degradation. The metal sleeve provided structural support for the aluminum oxide and a compressive force to prevent tensile cracks from developing. The air gap permitted the metal sleeve to expand as it heated and thus limit the magnitude of the compressive force to which the aluminum oxide was subjected.

The second concept, shown in Figure 3-6(b), used the metal sleeve and air gap arrangement of the first concept to provide structural support and control compressive forces on the liner. It differed in that silicon carbide (carborundum REFRAX-20) was used to address the problems of thermal stress and chemical stability at hot surface of the liner. Liners of both designs were fabricated and the steam generator modified so that the liners could be interchanged.

A total of 5 test firings (total elapsed time - 4 hours) were conducted using the aluminum oxide liner. Firing rate was varied from 1.25 to 2.5 MMBTU/hr at pressures from 150 to 300 psig. No degradation or structural damage was noted on the aluminum oxide following the first test (1.5 hours at 1.25 MMBTU/hr). However,

inspection after each subsequent test revealed an ever increasing number of hairline cracks in the aluminum oxide. Post test examination of pieces of this aluminum oxide by Sandia's Materials Laboratory [3] indicated that these cracks were tensile in nature and had all started at the inner surface of the liner. The cooldown transient which occurs on shutdown would be the only event which could generate tensile stress at the inner surface of the liner; and, therefore, this thermal transient must be the cause of the cracks. In addition, it was observed that all of the cracks occurred along grain boundaries and that the grain boundaries appeared to have been weakened by chemical attack. This chemical attack was not nearly as aggressive as that noted in the earlier liners.

It was felt that these tensile cracks could be eliminated by some dimensional changes in the liner's metal sleeve which would place the liner in a high state of compression at the start of the cooldown transient. This remedy was not pursued due to concern over the long-term chemical stability of the aluminum oxide and because of the superior performance of the silicon carbide liner in the subsequent series of tests.

A total of 7 test firings (total elapsed time - 7.4 hours) were conducted using the silicon carbide liner during this phase of testing. Again, firing rate was varied from 1.25 to 2.5 MMBTU/hr at 150 to 300 psig. Examination of the liner following

the first test revealed a few hairline cracks with random orientation. In addition, a glaze of silicon dioxide was noted over almost the entire surface of the silicon carbide. The only region not glazed was the first few inches downstream of the inlet venturi. The lack of a glaze in that area is indicative of the lower surface temperature expected in this region due to flow of relatively cool air near the combustion chamber wall.

Inspection after each subsequent test showed essentially no change in the appearance of the liner. Post test examination showed that there had been no dimensional changes nor was there any chemical attack of the silicon carbide liner.

Based on the encouraging results of the tests with the silicon carbide liner, it was incorporated in the design of a steam generator which would be used in long-term, high pressure tests. The design of this steam generator was the same as that used in previous tests with the exception of the location of water injection in the steam generation zone, the method of assembly of the swirler head and the ability to use either a pressure or air atomizing nozzle. As illustrated in Figure 3-7, the multitude of water spray nozzles was replaced with a smaller number of larger orifices located immediately downstream of the combustion chamber. The initial design was modified because of a concern that the small passages in the water spray nozzles would be prone to plugging by corrosion products from the water supply line. The

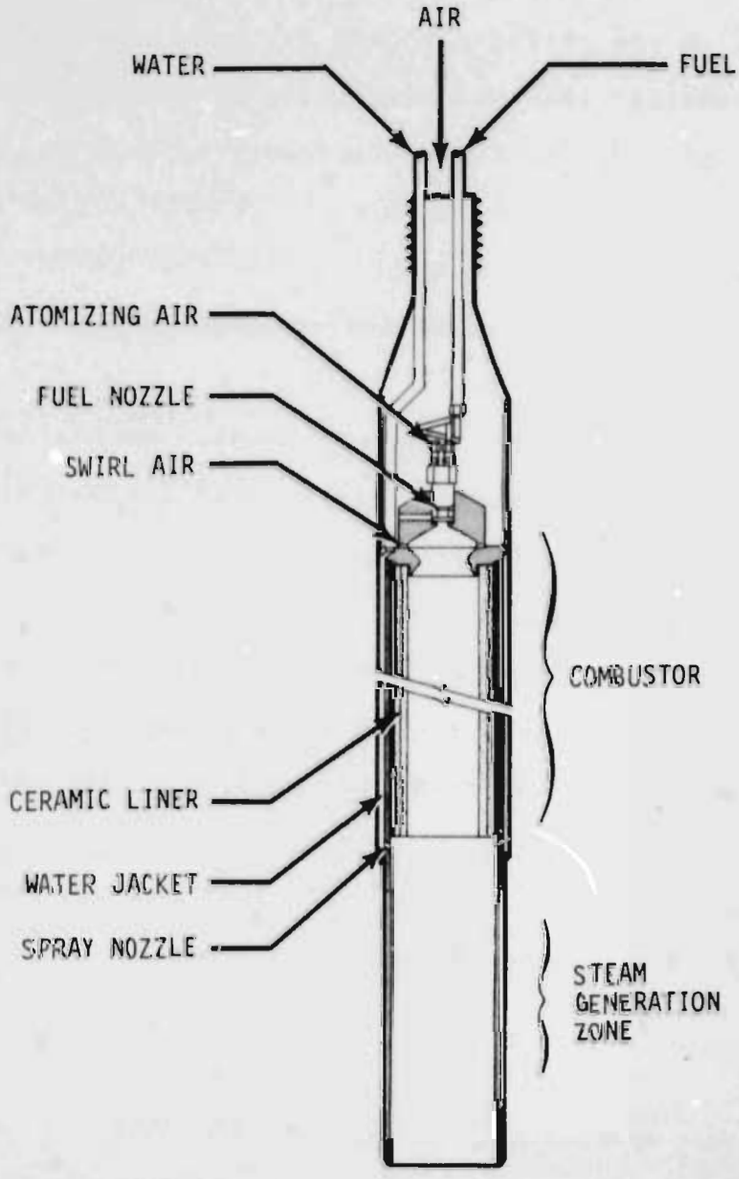

Figure 3-7. The Downhole Steam Generator - Improved Design

larger flow passages in the orifices should let such particulate material pass. The swirler head was fabricated as a two-piece assembly in order to provide the access necessary to weld the water jacket inlet.

Testing of this steam generator is discussed in Section 6 of this report.

4. PACKER DEVELOPMENT

4.1 Background

The function of the packer is to prevent pressurized steam from leaking back up the wellbore. To achieve this end, two distinct subassemblies are usually included in the packer design.

1. A sealing element (usually made from an elastomer or other non-metal) that is expanded radially till it presses against the well casing and prevents flow up the annulus.

2. An anchoring mechanism (usually a set of serrated slips) that is deployed outwards to bite into the casing, resist the pressure force, and hold the packer securely in place.

For the downhole steam application, the packer must seal reliably under the pressure and temperature conditions given below.

- Differential Pressure - up to 3000 psi
- Temperature - up to 650°F

Other requirements include the ability to withstand the corrosive downhole environment, to be retrieved and reused (after redressing), and to be compatible with 7" well casing.

Initially, existing packer technology was assessed to determine whether a commercial unit could be specified and included in the system design. The results indicated that, although "high-temperature" packers were being publicized by several manufacturers, their ratings fell short of the 650°F temperature specification required for the downhole steam system. As a further indication, field experience confirmed that, by and large, the best designs had an upper limit of around 500°F; a temperature at which the sealing element weakened and/or degraded significantly and caused leakage, particularly after thermal cycling (i.e., after repeated heat up and cool down associated with transient and/or intermittent steaming operations). The anchoring mechanism, however, generally worked well, even at the highest temperatures encountered in the field.

The above conclusions indicated that existing commercial packers would be unsuitable for this application. Thus, it was decided to pursue development of an improved unit; one which used a very different approach to the sealing requirement, and which, it was hoped, would overcome the temperature limitations of existing designs. Since conventional anchoring mechanisms appeared to be adequate, it was further decided to develop only an improved seal module and couple it to an existing tubing anchor to form the packer assembly.

The following sections describe the development of the seal module and the design and testing of the packer assembly.

4.2 Concept Development

4.2.1 Description

The seal concept chosen for development is shown in Figure 4-1. It consists of a circular metal sealing ring contained in the packer body and expanded plastically by hydraulic pressure. The key feature of this concept is that the sealing element is entirely metallic and can thus withstand higher temperatures and pressures than existing non-metal packer seals.

In developing this concept further, the first task was to determine the appropriate material(s) and configuration for the ring. The factors that affect ring design include:

- Expansion Pressure. From a practical standpoint, the hydraulic pressure needed to expand the ring must be restricted to a value lower than the pressure rating of the (conventional) tubing used to supply the oil. Recognizing that the ring is to be deployed by a separate small dia. hydraulic line (described later), the allowable expansion pressure should not exceed 20,000 psi.

- Creep Strength. Since the seal must resist the reservoir pressure for a prolonged period, it should have high creep strength to prevent gradual deformation and ultimate failure due to plastic flow.

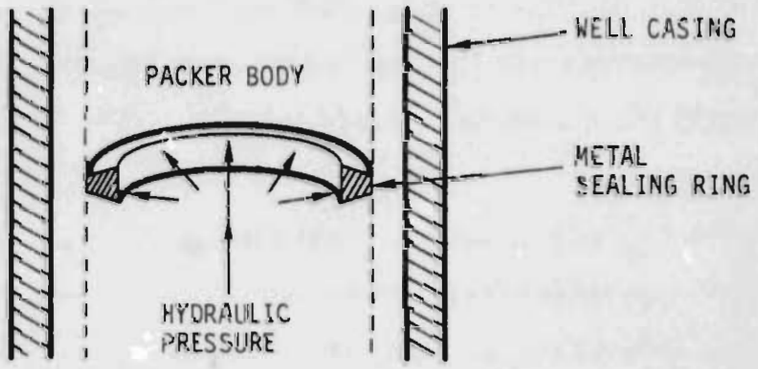

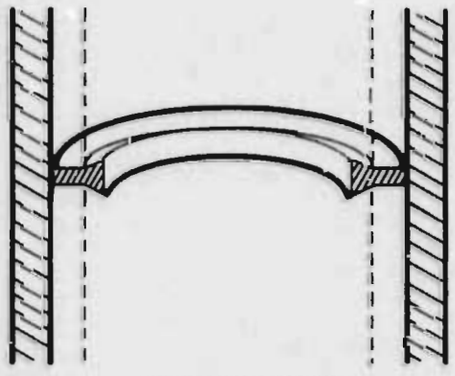

Figure 4-1. Metal Seal Packer Concept

- Ductility. The seal material must be ductile enough to allow the ring to expand and touch the casing without failure. Therefore, as a first order approximation, the elongation-to-failure of the ring material must be greater than the increase in ring circumference (which is about 15% for a 7" well casing packer).

- Corrosion Resistance. The entire sealing ring -- or at least the exposed parts of the ring -- should be made of materials that can resist attack by the corrosive downhole environment, which includes steam, exhaust gases, brine and other reservoir fluids.

A review of the above factors makes it apparent that the ring design must satisfy conflicting requirements. Both expansion pressure and creep strength are closely related to the yield strength of the material. However, a low expansion pressure implies a low yield strength, while high creep strength implies the reverse. The way around this difficulty is to use a composite ring, in which different sections are made of different materials. In this way, that part of the ring which resists the reservoir pressure force can have high strength, while other parts can be made to deform more easily so as to limit the required expansion pressure.

4.2.2 Ring Design

Selection of the appropriate ring configuration and materials was carried out with the help of the seal expansion test fixture

shown in Figure 4-2. The diameter of this fixture corresponds to the body diameter of a 7" casing packer. The fixture consists of a set of dies that are bolted together to hold the ring in place. Pressurized oil from a hand-operated hydraulic pump flows through a passage in the top half of the die set and establishes the required expansion pressure at the inner periphery of the sealing ring. The oil is prevented from leaking past the ring due to the outward taper in the ring crossection. This outward taper (set by the die angle as shown in Figure 4-2) provides an inherent hydraulic seal. Any force that acts to expand the ring also gives rise to a compressive sealing force between the tapered surfaces of the ring and the die. The die angle determines the magnitude of this force and is thus chosen above some minimum value to prevent leakage of hydraulic oil past the ring.

Numerous tests were carried out with this fixture. Three sets of dies were used, each having a different die angle. The objectives of these tests were to:

(a) Verify the feasibility and uniformity of radial ring extrusion.

(b) Confirm the effectiveness of the tapered die in preventing hydraulic leakage.

(c) Determine the expansion pressure as a function of die angle.

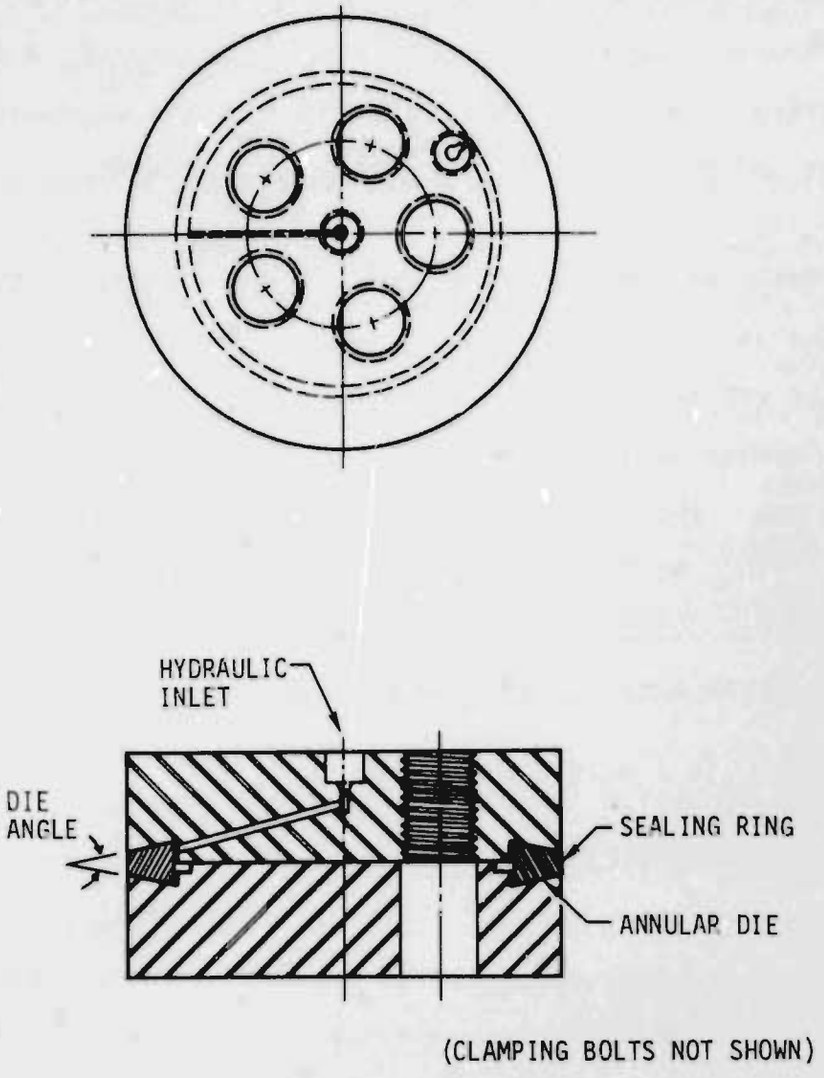

Figure 4-2. Seal Expansion Test Fixture

Initially, tests were carried out with sealing rings made of 1100-0 Aluminum (commercially pure annealed aluminum). This material was chosen for the initial tests due to its low yield stress and high ductility. The tests confirmed the feasibility of the extrusion process. They also demonstrated that the radial expansion was very uniform. This high uniformity is felt to occur due to the strain hardening property of the metal; any incipient non-uniformity causes the ring to be harder (stronger) where the strain is higher, thus slowing down the expansion in this region and decreasing the original non-uniformity.

Test data were obtained for three different die angles: 16°, 26° and 36°. With these die angles, there was no leakage of hydraulic oil past the die. However, it was recognized that hydraulic leakage would occur at some angle below 16 degrees, and in any case, when the die surfaces were parallel (zero die angle).

Other characteristics were also noted:

(a) The hydraulic pressure did not remain constant during the test, but increased gradually as the ring expanded. This increase is due to strain hardening (and other factors) and, as mentioned earlier, promotes extrusion uniformity. Expansion pressure values presented subsequently correspond to measurements taken when the outer diameter of the ring had grown by 15% (which represents the fully expanded condition for a 7" casing packer).

(b) Upon removal of the hydraulic pressure, the outer diameter of the (expanded) ring was found to reduce slightly due to "elastic springback". This springback, measured by a dial gauge, was in the range of 0.005 to 0.01 inches. The effects of springback on seal operation are discussed in Section 4.2.3.

The measured expansion pressure as a function of die angle (for an aluminum ring) is shown in Figure 4-3. As expected, this pressure was lower for smaller die angles, because the area contraction is smaller. The minimum pressure occurs at zero die angle when the ring expands without extrusion. This pressure was estimated by extrapolation.

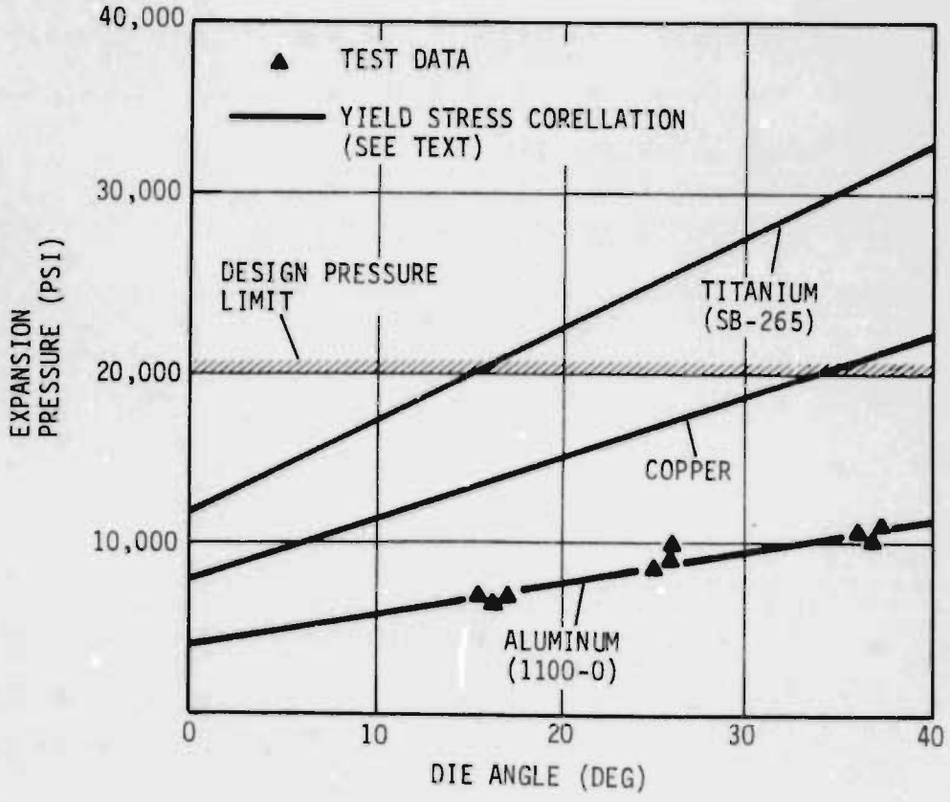

Figure 4-3. Seal Expansion Pressure

The expansion pressure data for aluminum were used as the baseline for estimating the expansion pressures for other candidate ring materials (copper, titanium). As a first order approximation, the pressure to extrude metal through a die is directly proportional to the yield stress. Thus, the expansion pressure for another metal is obtained by multiplying the expansion pressure for aluminum by the ratio of the yield stress.

Material	Specification	Yield Stress Ratio
Aluminum	1100-0	1
Copper		≈ 2
Titanium	SB-265	≈ 3

The expansion pressure curves for the above metals (copper and titanium) are also shown in Figure 4-3.

Table 4-1 shows the seal expansion pressure for the candidate ring materials and presents data on other relevant characteristics (maximum elongation, corrosion resistance, and creep strength). The expansion pressure is shown for two key values of the die angle: 0° and 16°. The zero die angle case is important because it requires the lowest expansion pressure. However, for this die angle, the system does not establish its own hydraulic seal, and a separate hydraulic seal would thus be necessary. The 16° die angle case requires higher expansion pressure, but results in a system that provides its own hydraulic seal.

Table 4-1. Seal Material Evaluation

Material	Expansion Pressure		Maximum Elongation %	Corrosion Resistance	Creep Strength
	0° Die Angle	16° Die Angle			
Aluminum	4,000	7,000	35	Good	Low
Copper	8,000	14,000	50	Good	Medium
Titanium	12,000	21,000	55	Excellent	High

Table 4-1 illustrates why no single material can satisfy all the packer seal requirements. Aluminum and copper do not have the necessary strength, while titanium -- though strong enough -- requires an excessive expansion pressure (21,000 psi) when the die angle is high enough (16°) to assure a reliable hydraulic seal. The requirements can however be met with a composite sealing ring; one in which different parts are made of different materials, as shown in Figure 4-4. In this design, the ring is made up of three concentric sections: the hydraulic seal (aluminum), the main load-carrying member (titanium) and the soft outer lip (copper). The hydraulic seal prevents oil from leaking past the die. This seal is achieved by choosing a very soft material (aluminum) and providing a high die angle (30°) for this part of the ring. In this way, the compressive sealing force between seal and die is maximized. The main load-carrying member resists the reservoir pressure force. Titanium provides the necessary high-temperature strength and creep resistance. Titanium also has high corrosion resistance against steam, exhaust gases and reservoir fluids. Since the hydraulic seal is provided by the aluminum element, the titanium section can have zero die angle. The expansion pressure for this section is thus reduced from 21,000 psi to 12,000 psi. Finally the serrated outer lip, made of a soft metal (copper), serves as a deformable member that, when expanded, presses against the (harder) steel casing and conforms to its surface features to form the casing seal.

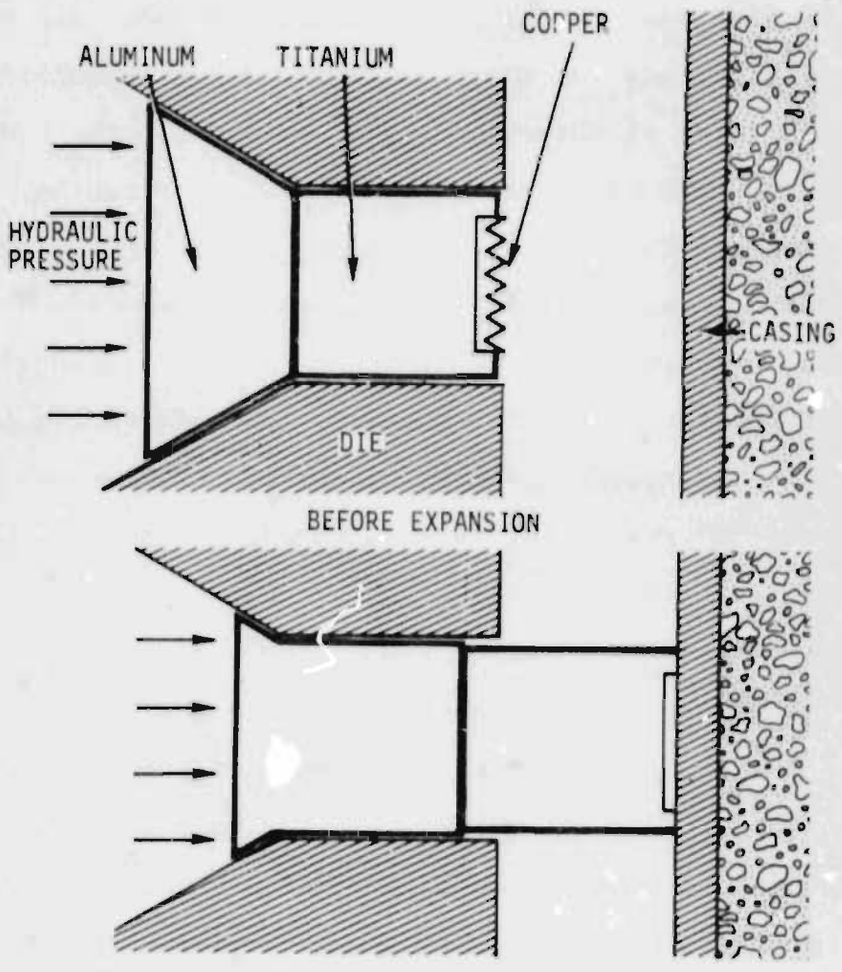

Figure 4-4. Cross-Section of Sealing Ring

Several composite rings were fabricated and tested in the seal expansion test fixture. The results confirmed that the ring expansion pressure was well below the 20,000 psi design pressure limit. In fact, the expansion pressure for the composite ring was about 15,000 psi. This pressure can be represented as the sum of the pressures needed to expand the three sections of the ring. Additional tests (with partial sections) indicated that the pressure components were approximately as follows.

Section	Material	Expansion Pressure Component
Hydraulic Seal	Aluminum	4,000 psi
Main Load-Carrying Member	Titanium	11,000 psi
Outer Lip	Copper	Negligible

The results also confirmed that hydraulic leakage did not occur and demonstrated the uniformity and repeatability of the seal expansion process.

4.2.3 Feasibility Testing

The seal was tested for leakage in the fixture shown in Figure 4-5. This fixture consists of a short piece of 7" well casing that stands on a metal base. The sealing ring, retained

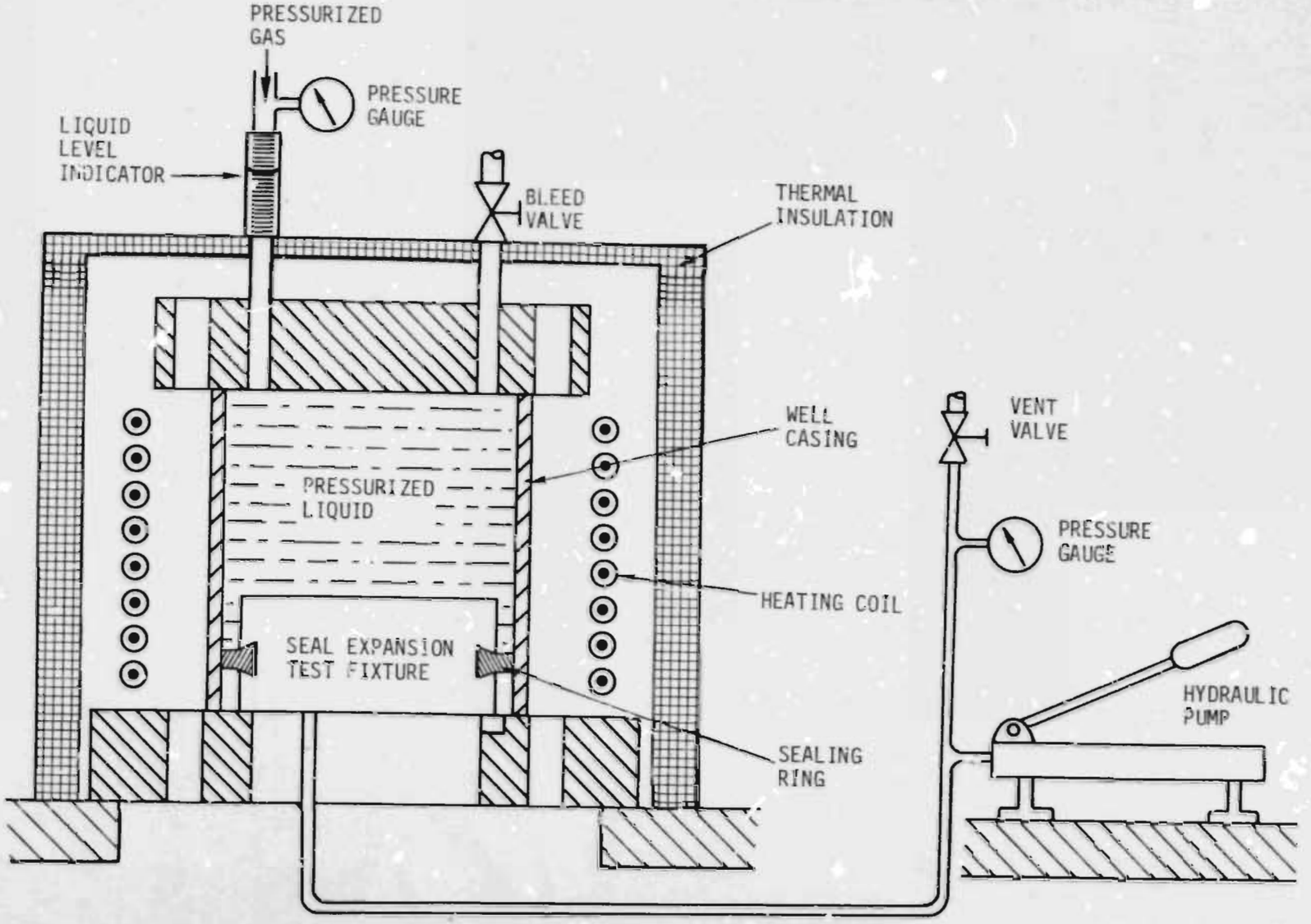

Figure 4-5. Seal Leakage Test Fixture

in the expansion test fixture, is placed inside the casing as shown. The top end of the casing is covered by a cover plate, with a graphite gasket placed in between. Bolts (not shown) are inserted through the base and cover plate to force the latter against the casing and prevent leakage around the top.

The sealing ring is deployed by pressurized hydraulic oil from a hand-operated pump. After the ring has expanded, the hydraulic pressure is increased by about 3,000 psi to force the outer lip against the casing and ensure that it is in intimate contact along the entire periphery. The enclosed casing volume is then filled with liquid (silicone oil) and pressurized by connection to a regulated high-pressure gas cylinder. Pressure gauges are provided to monitor the hydraulic and gas pressures. A liquid level indicator (sight glass) is also provided as shown to monitor any leakage of fluid across the packer seal. A thermostat-controlled electric heating coil surrounds the casing and is used to establish a given ambient temperature. The entire assembly is covered by thermal insulation.

Several tests were carried out with this fixture to establish the feasibility of sealing against high pressure and confirm that leakage could indeed be prevented under conditions representative of field use (high-temperature, cyclic operation). A typical test record is shown in Figure 4-6. The key parameters monitored during the test are the hydraulic pressure, temperature and differential pressure across the seal (gas pressure). The test

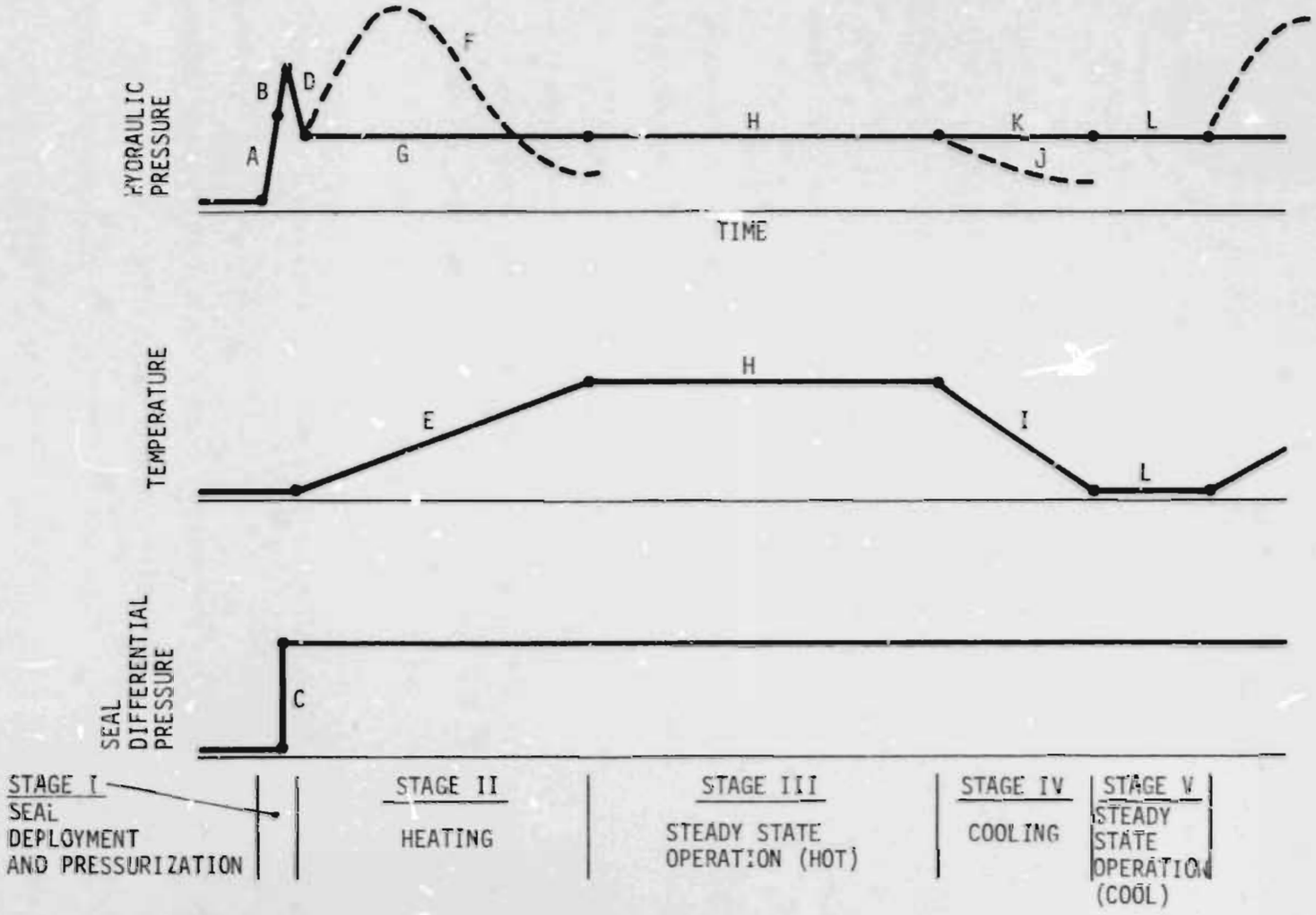

Figure 4-6. Typical Test Record -- Seal Leakage Testing

has five stages. Operations within each stage are denoted by the letters A through L as marked in Figure 4-6 and referenced in the discussion below.

Stage I - Seal Deployment and Pressurization

(A) The seal is expanded till it touches the casing by pressurization to about 15,000 psi with the hydraulic pump.

(B) The pressure is then raised by an additional 3,000 psi to ensure that the sealing ring is in initimate contact with the casing over the entire periphery. Raising the pressure causes the serrations in the outer lip of the ring to be crushed, and forces the soft metal to conform to any irregularities in the casing surface.

(C) The gas pressure is then applied to establish the required seal differential pressure (1,500 psi).

(D) The hydraulic pressure can now be reduced (to 7,000 psi) without seal leakage. This operation is carried out by opening the vent valve.

Stage II - Heating

(E) The electric heater is activated to bring the temperature up to the specified level (650°F).

(F) If no external action is taken, the effects of the temperature rise are as follows. First, the hydraulic oil expands and causes the hydraulic pressure to increase. Then, as the yield strength of the sealing ring is reduced, additional plastic deformation takes place to lower the hydraulic pressure. Because of the different time lags associated with these effects, the hydraulic pressure first rises and then falls.

(G) In order to prevent initial overpressurization and subsequent pressure loss, the pressure is controlled manually. When the pressure is rising, the vent valve is opened; when it is falling, the pump is activated. By such actions, the pressure is kept constant in spite of the temperature changes.

Stage III - Steady-State Operation (Hot)

(H) After thermal equilibrium is achieved (at 650°F), the hydraulic pressure remains constant without external action.

Stage IV - Cooling

(I) The electric heater is turned off and the system begins to cool down.

(J) The drop in temperature causes the hydraulic oil to contract. Without external action, the hydraulic pressure would decrease and seal leakage would occur.

(K) Therefore, as the system cools down, the pump is activated periodically to keep the pressure constant.

Stage V - Steady-State Operation (Cool)

(L) After thermal equilibrium is achieved (at room temperature), the hydraulic pressure remains constant without external action.

Stages II to V are repeated to evaluate the effects of thermal cycling on seal performance.

The following conclusions emerged from the tests.

a. The composite ring consistently established a leak-free seal in several types of casings, including rough, worn, and eccentric sections. Seal operation was verified at pressures up to 1,500 psi (the design limit of the test fixture) and temperatures up to 650°F.

b. The soft metal lip (including the serrated edge) of the sealing ring played an important role in forming the seal.

Tests with rings that did not have serrations were not as successful; the seal could not usually be established in rough casing. Roughness resulting from surface corrosion was sufficient to prevent sealing. It was concluded that significant plastic deformation of the soft metal lip was necessary to effect a tight seal.

c. To prevent elastic springback and loss of sealing capability, the hydraulic pressure had to be maintained throughout the test. No method was found to maintain the seal without hydraulic pressure.

d. The seal survived thermal cycling. It was, however, necessary to maintain constant hydraulic pressure during the thermal transients as described earlier.

4.3 Protctype Design

The prototype metal-seal packer is shown in Figure 4-7. As discussed in Section 4.1, it consists of two components: a tubing anchor and a seal module.

The tubing anchor is of conventional design; almost any commercial hydraulic-set unit can be used. Initially, the anchoring system of an Otis Type RH hydraulic set packer was chosen.

The seal module (Figure 4-8) is fastened to the tubing anchor by a threaded coupling. The module consists of a set of annular dies that hold two metal sealing rings. It was felt that two rings would increase seal reliability without compromising the simplicity of the design. The rings and die set are held together by means of a threaded cap. This cap also serves to compress the rings in the dies and prevent hydraulic leakage. The necessary compression is established by tightening the cap to a specified torque with a torque wrench. Hydraulic leakage across the annular mating surface between dies is prevented by metal 'C' rings (not shown). Thus, there are no elastomeric or other non-metal elements in the seal module that can fail at high temperature. The tube supplying hydraulic fluid to the seal module is attached to the top die as shown. This tube, which runs to the surface as a separate hydraulic line, is part of the tube string described in

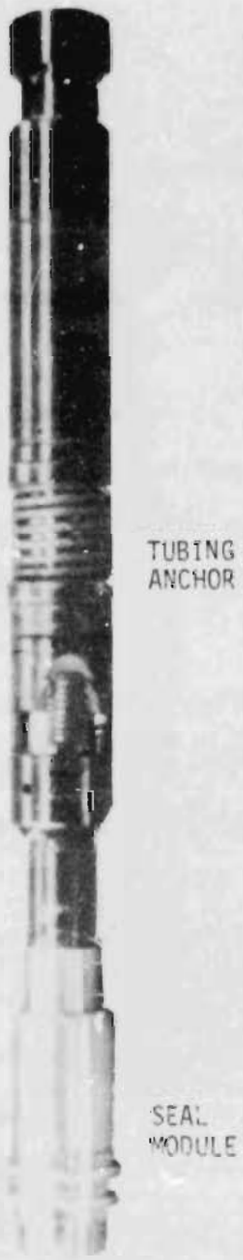

Figure 4-7. The Prototype Metal-Seal Packer

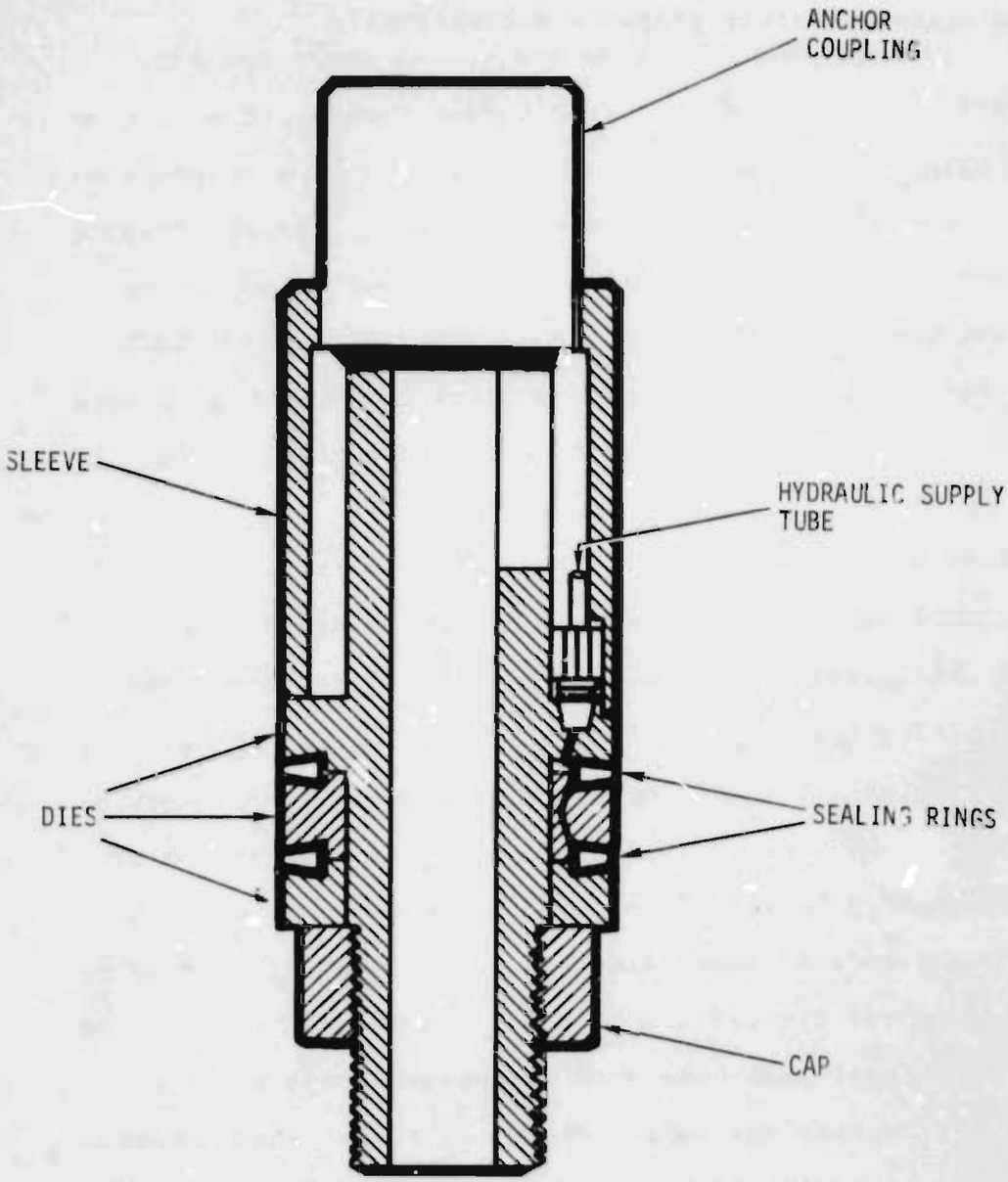

Figure 4-8. The Seal Module

Section 6. The seal is deployed from the surface by means of a hydraulic system (pump and accumulator) that expands the rings and then maintains constant pressure automatically.

4.4 Prototype Testing

4.4.1 Laboratory Testing

The prototype packer was tested in the laboratory with the help of a full-scale packer test rig (Figure 4-9). The rig consists of a 10 ft. section of well casing surrounded by a pressure vessel. Thermostat-controlled electric heaters are strapped around the pressure vessel, and the entire assembly is covered by thermal insulation. A suitable base and cap are also included in the system, along with a pressure relief valve to prevent accidental overpressurization.

The packer is lowered into the casing (Figure 4-10) until a plug on the lower end of the seal module drops into a recess at the bottom of the rig. The cap is then installed, together with the hydraulic line that supplies the seal module. The seal is deployed by pressurization with the hydraulic pump. This part of the test sequence is similar to that shown in Figure 4-6 (Stage I). The casing is then partly filled with water through an opening in the cap. A pressure gauge is then attached to this opening as shown. The electric heaters are activated to bring the system temperature to a specified level. As the temperature rises, steam is formed inside the casing, its pressure being governed by the temperature. (In this respect, the test sequence differs from that shown in Figure 4-6, since the seal differential pressure rises gradually with temperature). When

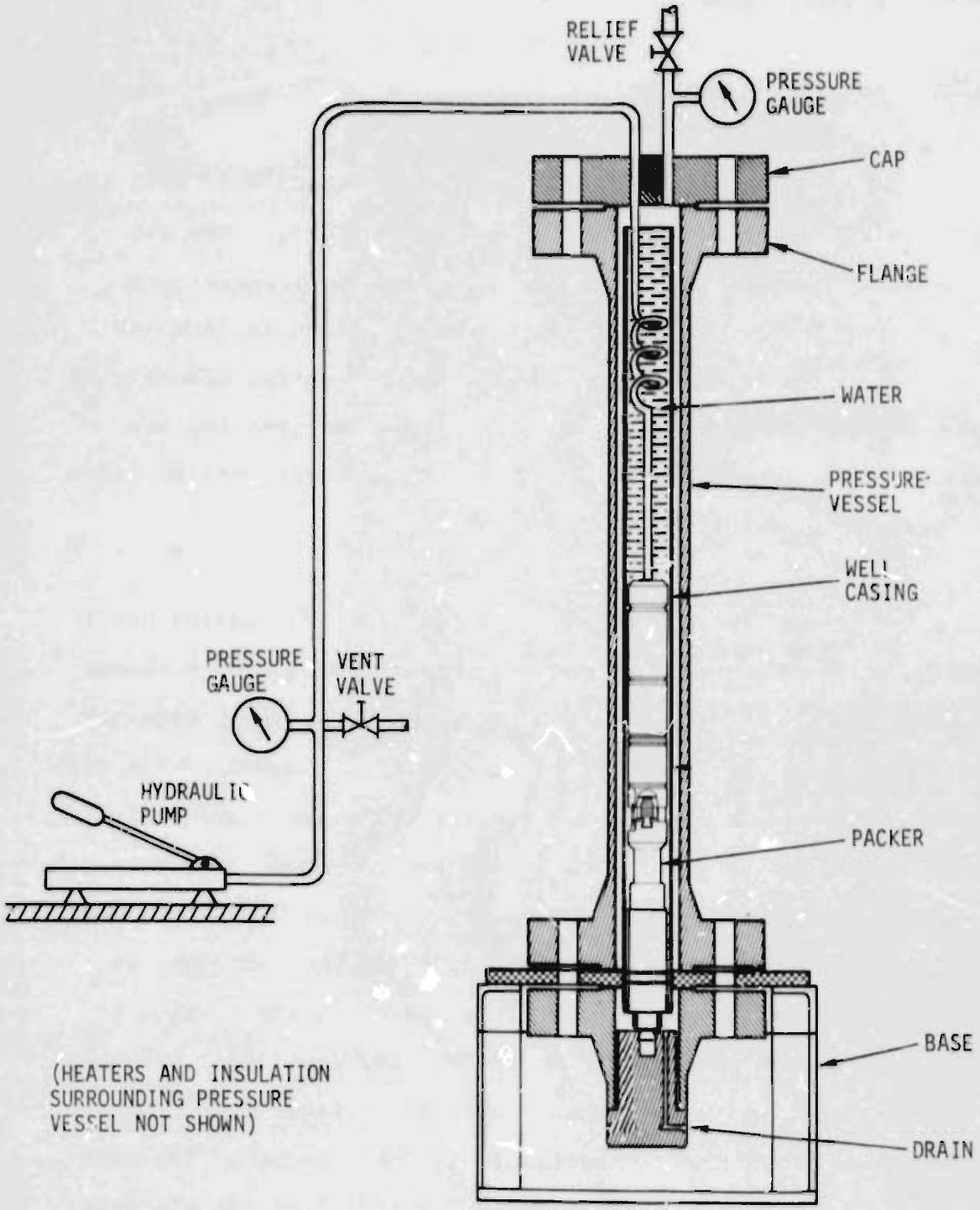

Figure 4-9. Packer Test Rig

Figure 4-10. Packer Installation (Laboratory Testing)

the temperature is rising, the hydraulic pressure is kept constant by using the vent valve and pump, as described in Section 4.2.3. Throughout the test, seal leakage is monitored by measuring the outflow from the drain. After a period of steady-state operation, the electric heaters are switched off and the system begins to cool down. The seal differential pressure (steam pressure) begins to decrease with temperature. During this stage, the hydraulic pressure is kept constant by using the pump. After the system has cooled down, the test sequence is repeated to evaluate the effects of thermal cycling.

A summary of the tests carried out with the rig is presented in Table 4-2. The first two tests were performed at low temperature and pressure (about 500°F and 500 psi). In the longer of these two tests, satisfactory seal operation was observed for a two-week period that included three thermal cycles. Subsequent tests were carried out at high temperature and pressure (640°F, 2000 psi). During the first test in this series (Test #3 in Table 4-2), a weld in the test rig started to leak, so the test was terminated. After the faulty weld had been repaired, the test was restarted (Test #4 in Table 4-2) and ran for 60 days without seal leakage. During this period, the seal underwent three thermal cycles.

In all cases, packer removal from the casing took place without difficulty. The initial upward pull (breakaway force) was about 15,000 lbs. The force then dropped down to about 3000 lbs as the packer was pulled up through the casing.

Table 4-2. Packer Test Summary

Test No.	Duration (days)	Pressure (psi)	Temperature (°F)	No. of Thermal Cycles	Remarks
1	7	500	470	1	No leakage across seal
2	14	600	490	3	No leakage across seal
3	7	2000	640	-	Test terminated due to test fixture failure
4	60	2000	640	3	No leakage across seal

Additional tests of the seal module were carried out using live steam and exhaust gas. These tests, undertaken as a part of the overall steam generation system test, are described in Section 7.

5. CONTROL SYSTEM

5.1 Background

The steam generator control system carries out four functions:

a. It allows the operator to activate/deactivate the system and set the independent variables (airflow, and air-fuel, and air-water ratios) that control firing rate (steam output) and steam quality.

b. It establishes and regulates automatically the air, fuel, and water flows so that the desired firing rate and steam quality are obtained.

c. It displays and records key system parameters and alerts the operator to any anomaly or malfunction by means of a set of alarms.

d. In certain cases, it takes action automatically, either to maintain the fuel and water flow (automatic transfer from malfunctioning pump to backup pump) or to avoid catastrophic failure (automatic shutdown due to major deficiency in water flow).

The system consists of two equipment skids (one for air, and one for fuel and water) and a control console. The entire system is synthesized from standard commercial components, and implements a conventional feedback control strategy using analog devices. A schematic diagram of the system is shown in Figure 5-1; photographs of the hardware are shown in Figure 5-2.

5.2 The Air Skid

The air skid controls the airflow. A schematic diagram of the air supply system is shown in Figure 5-3. Flow from a high-pressure air compressor is regulated by a dump valve that vents any excess air to the atmosphere. The valve is operated pneumatically from a 30 psi instrument air supply. The electrical signal from the control console modulates the pneumatic supply through a current-to-pressure (I-to-P) converter that is part of the valve installation. The dump valve is part of a closed loop controller; valve excursions around a reference position are proportional to the difference and an integral of the difference between the required airflow (as set by the operator) and the actual airflow. This control strategy is implemented by a commercial proportional-and-integral (P-and-I) analog control module. The airflow is determined from a conventional orifice flowmeter mounted on the skid. The pressure and temperature upstream of the orifice and the pressure drop across it are measured, and the signals transmitted to the control console for processing. The

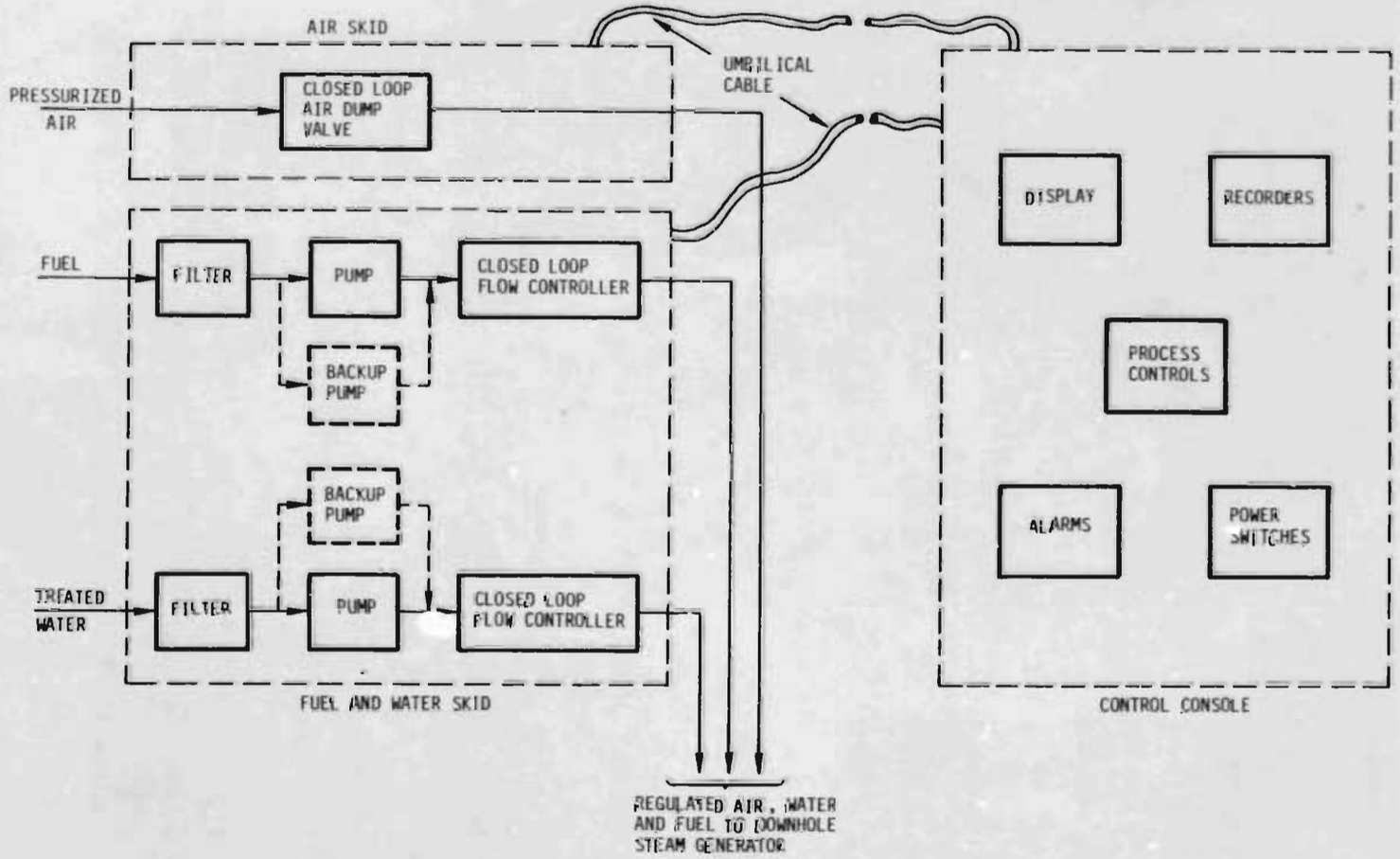

Figure 5-1. The Control System

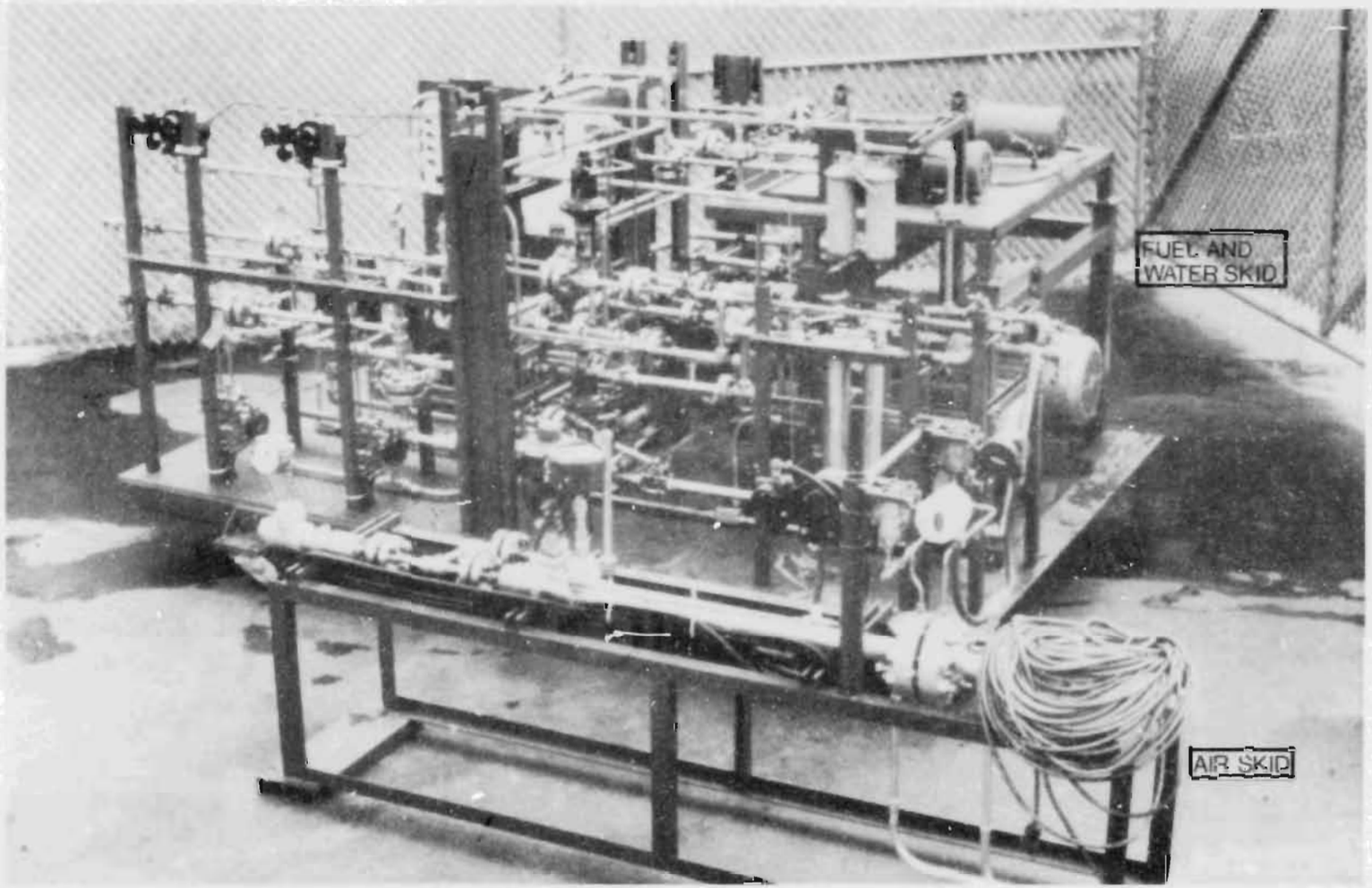

(a) The Equipment Skids

Figure 5-2. The Control System -- Overall View

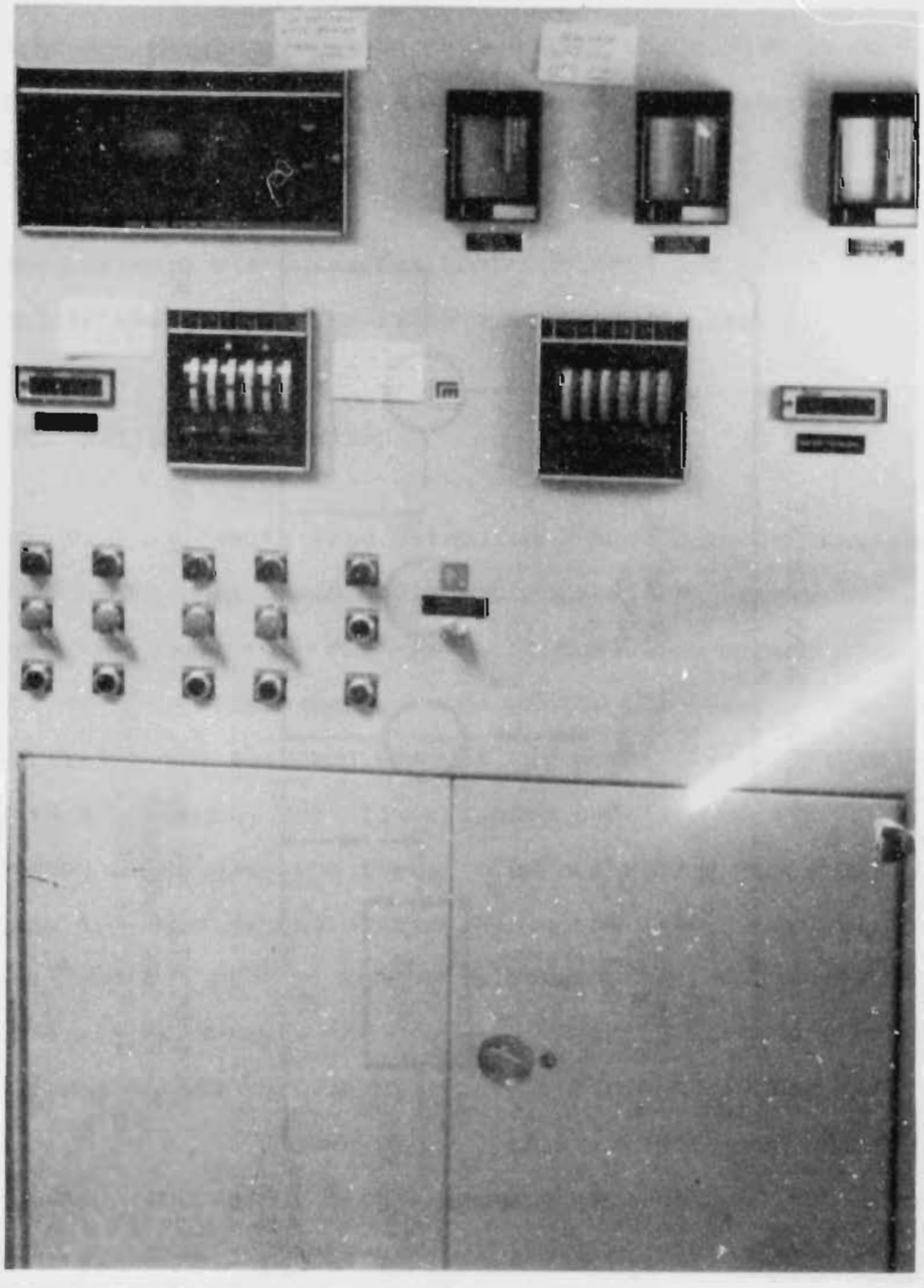

(b) The Control Console

Figure 5-2. (Cont.) The Control System -- Overall View

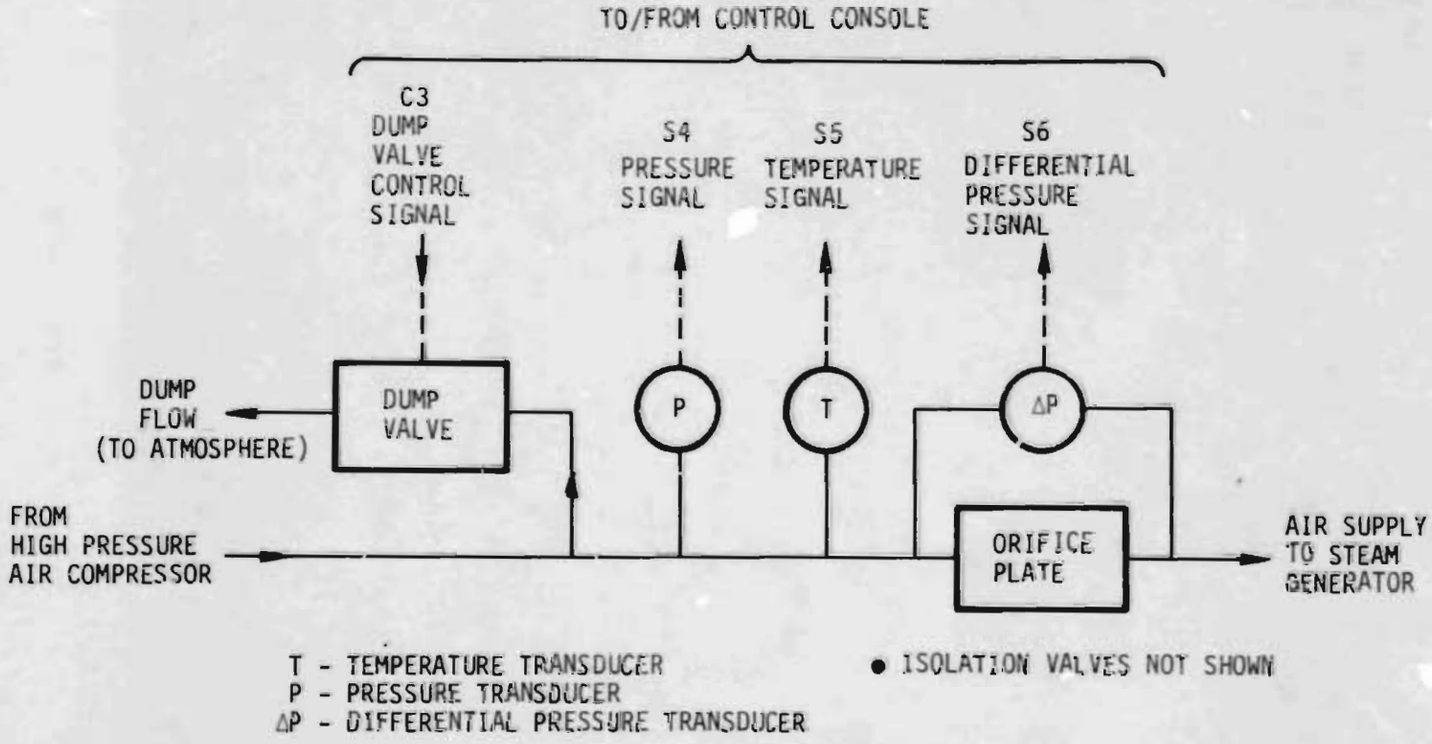

Figure 5-3. Schematic Diagram of Air Supply System

pressures are measured with diaphragm-type capacitive transducers; the temperature is sensed by a resistance-temperature detector (RTD).

The air skid also includes hand-operated isolation valves to shut off the flow and to isolate the transducers.

5.3 The Fuel and Water Skid

The fuel and water skid establishes and controls the fuel and water flow. A schematic diagram of the fuel supply system is shown in Figure 5-4. Fuel from the fuel tank passes through a filter system to the suction side of the fuel pump. The filter strains the fuel and removes any particulates larger than 3 to 5 microns. The filter system consists of two independent cartridge-type filter elements with a means of switching the flow manually from one to the other. In this way, when any one element begins to get blocked (clogged), the flow is diverted through the other so that the blocked element can be replaced and kept on standby. Incipient blockage is sensed by a pressure switch (relay) that is activated when the pressure drop across the filter element exceeds a preset level (10 psi). This switch activates an alarm at the control console to alert the operator to impending filter blockage.

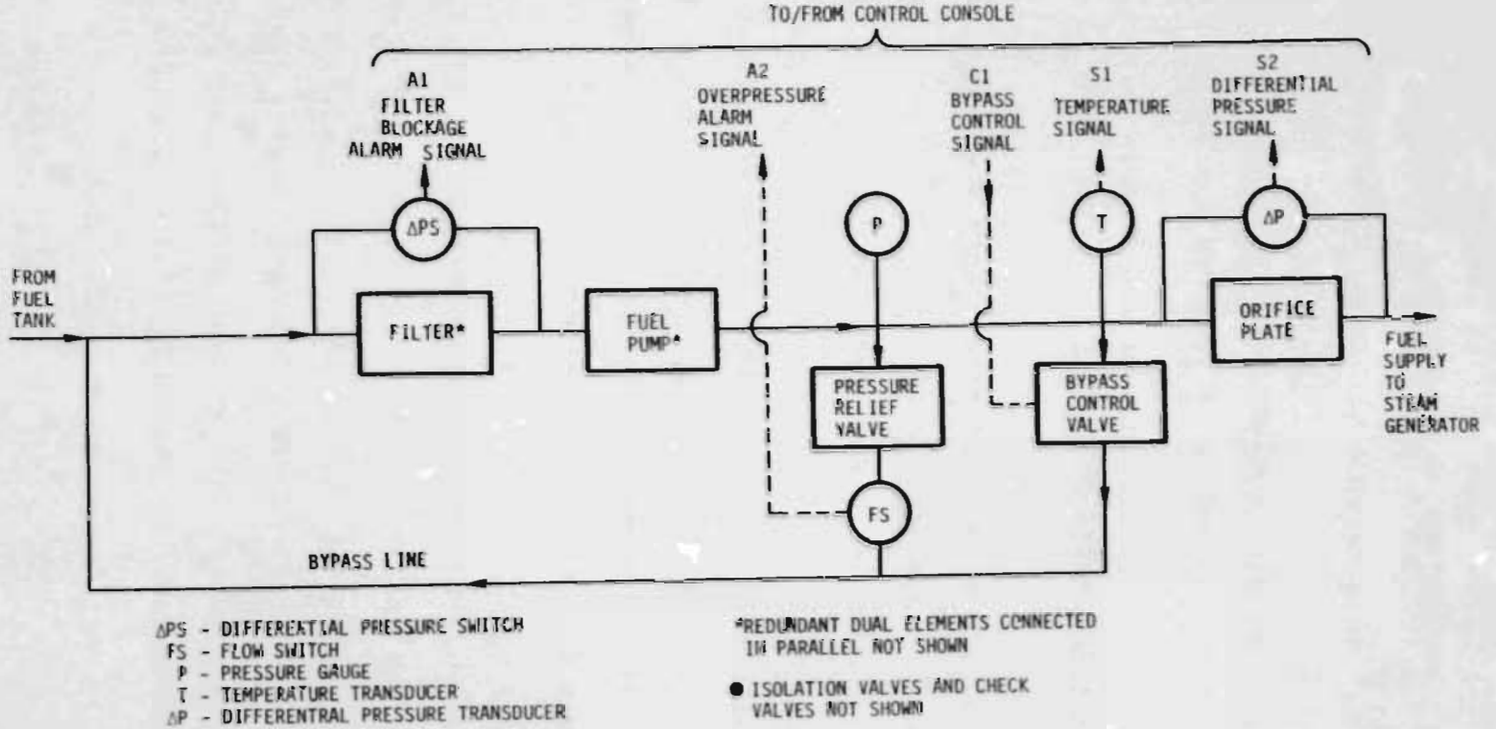

Figure 5-4. Schematic Diagram of Fuel Supply System

The fuel pump is a gear pump rated for a flow of 1 gpm and a maximum pressure of 1500 psi. Although two such pumps are provided, only one operates at any given time while the other remains on standby. In case of flow deficiency, pump transfer takes place automatically; the malfunctioning pump is taken out of service and the standby pump put into operation. The fuel pump is driven at constant speed by an electric motor so that the output flow is (nominally) constant regardless of the pressure. Flow control is achieved by diverting excess flow back to the suction side of the pump through a bypass line. The bypass flow is regulated by a bypass control valve. Like the air dump valve, the bypass control valve is operated pneumatically; the electrical signal from the control console modulates the pneumatic supply through an I-to-P converter. Also, like the air dump valve, this valve is part of a closed loop controller that includes a P-and-I analog control module.

To prevent the pump from experiencing high backpressure, a pressure relief valve is connected between the pump discharge and the bypass line. Any overpressure is now relieved as the valve opens and diverts flow into the bypass loop. A flow switch connected in series with the valve senses any valve flow and activates an alarm (at the console) to alert the operator to the overpressure condition.

Fuel flow is determined by a conventional orifice flowmeter. The temperature upstream of the orifice and the pressure drop

across it are measured, and the signals transmitted to the control console for processing.

The fuel supply system also includes hand-operated isolation valves and check valves that prevent reverse flow.

A schematic diagram of the water supply system is shown in Figure 5-5. This system is very similar to the fuel supply system, and includes dual filters with filter blockage alarm, dual pumps, a pressure relief valve with overpressure alarm, a bypass control valve, and an orifice flowmeter. Notable differences are the filter rating (40 micron cutoff), type of pump (piston pump vs. gear pump), its rating (16 gpm and 2000 psi max), and the absence of a temperature transducer.

Although the flow is a weak function of the temperature, a temperature transducer for the water system has been omitted because the water flow does not have to be controlled as accurately as the fuel flow. The latter has to be particularly accurate since it affects the air-fuel ratio, and hence the cleanness and efficiency of combustion.

5.4 The Control Console

The system is operated from the control console. The console accepts operator inputs, carries out the signal processing, and interacts with the skids to establish the required air,

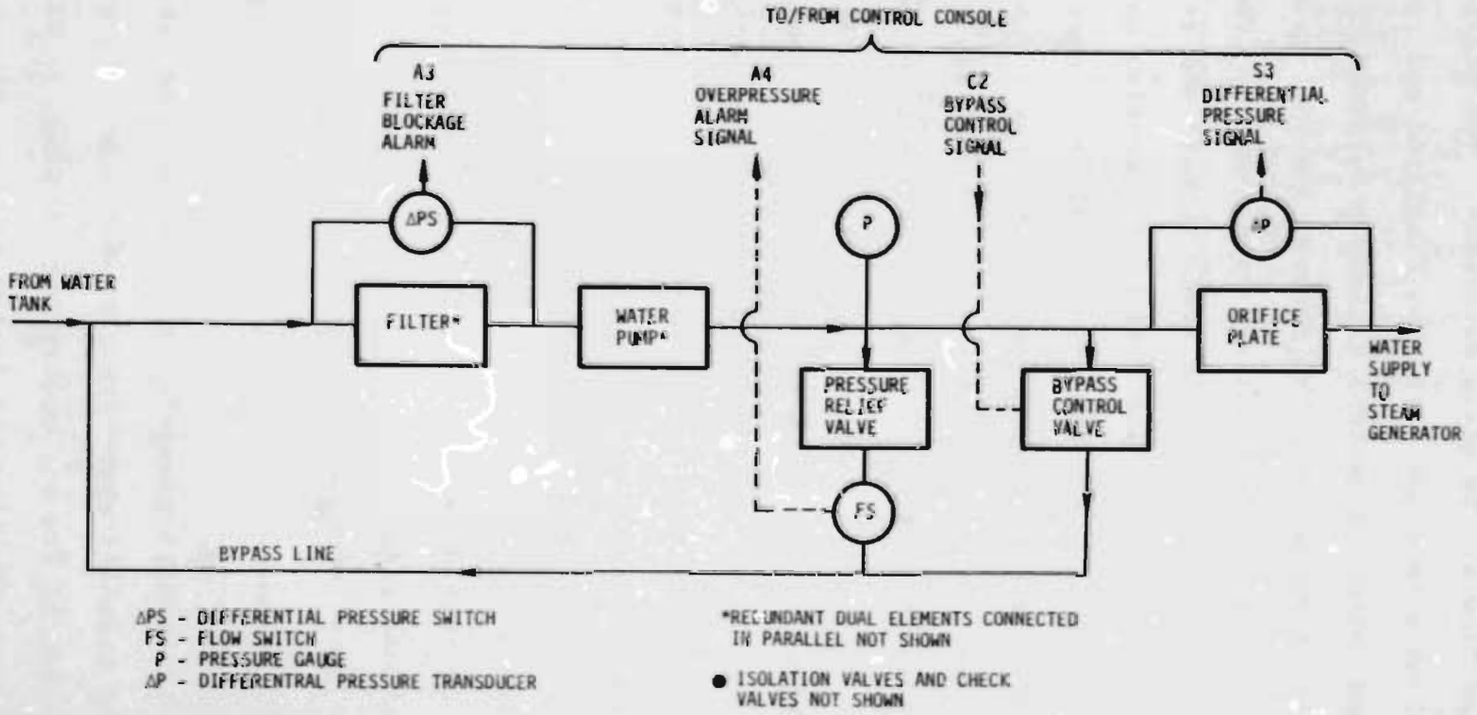

Figure 5-5. Schematic Diagram of Water Supply System

fuel and water flow to the steam generator. The primary control variables, along with other variables displayed and recorded, and the alarms and automatic control actions programmed in the system are summarized in Table 5-1. The primary control variables are the airflow and the air-fuel and air-water ratios. These variables set the firing rate (or steam output) and steam quality, respectively. The air-fuel ratio can also be adjusted in case the type or composition of the fuel is changed. The control variables are set by the operator at the front panel by means of a thumbwheel adjustment. About a dozen key variables are monitored and indicated (displayed) on the front panel by a meter readout or digital display; several of these variables are recorded on strip chart recorders for a permanent record. Seven alarms are provided to alert the operator to abnormal air, fuel and water flows, water and fuel supply overpressure, and water and fuel filter blockage. The alarm system is implemented by means of a panel-mounted annunciator that provides an audible and visual alerting signal to indicate the existence and type of alarm condition that prevails. Finally, the system is programmed to act automatically and bring about pump transfer (due to low fuel or water flow) or shutdown (due to a major deficiency in water flow).

The control console consists of controllers for the air, fuel and water, and miscellaneous circuitry for other functions. A schematic diagram of the air controller is shown in Figure 5-6. Three signals from the air skid -- temperature, pressure and

Table 5-1. Summary of Variables and Alarms

Primary Control Variables	Displayed Variables	Recorded Variables	Alarms	Automatic Control Actions
Airflow (Firing Rate or Steam Output)	Air Pressure[2]	Air Pressure	Fuel Filter Blockage	Water Pump Transfer (Low Water Flow)
Air-Water Ratio (Steam Quality)	Fuel Pressure	Air Flow Rate	Water Filter Blockage	Fuel Pump Transfer (Low Fuel Flow)
Air-Fuel Ratio[1] (Stoichio-metric Level)	Water Pressure	Fuel Flow Rate	Fuel Overpressure	Pump Shutdown (Continued Low Water Flow)
	Air Flow Rate	Water Flow Rate	Water Overpressure	
	Fuel Flow Rate	Air-Fuel Ratio	High/Low Fuel Flow	
	Water Flow Rate	Firing Rate	High/Low Water Flow	
	Total Fuel Flow[3]	Steam Quality	High/Low Air Flow	
	Total Water Flow	System Temperatures		
	Air-Fuel Ratio			
	Air-Water Ratio			
	Firing Rate			
	Steam Quality			
	System Temperatures			
	Steam Injection Rate BBL/Day			

1. Adjustment capability for change in fuel type or composition.
2. Injection pressure.
3. Total fuel consumption (GALS.).

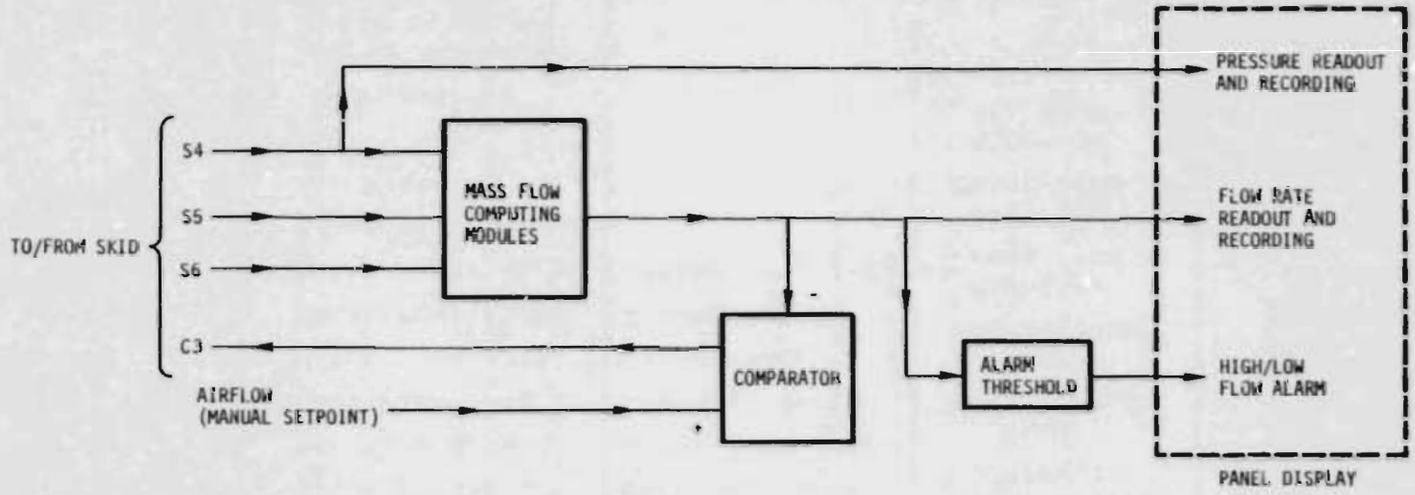

Figure 5-6. Schematic Diagram of Air Controller

orifice pressure drop -- are processed to determine the mass flow rate according to the following relationships.

$$W_a = K_a\sqrt{\rho_a \Delta P_a}$$

$$\rho_a = P_a/RT_a$$

where W_a - Mass flow of air

T_a - Upstream orifice temperature

P_a - Upstream orifice pressure

ΔP_a - Orifice pressure drop

K_a - Orifice constant

ρ_a - Air density

R - Gas constant

The measured airflow signal is then subtracted from the airflow setpoint and further processed in the P-and-I controller to generate a signal that controls the skid-mounted air dump valve.

The measured airflow signal also is processed by a threshold module to generate a high/low airflow alarm signal. The alarm is activated when the airflow is either below a preset level (200 scfm) or above another preset level (2000 scfm). The former condition represents the lower bound for which airflow control accuracy can be assured, the latter condition represents the maximum flow that the system is designed to handle.

A schematic diagram of the fuel controller is shown in Figure 5-7. Two signals from the fuel skid -- temperature and orifice pressure drop -- are processed to determine the mass flow rate according to the following relationships.

$$W_f = K_f \sqrt{\rho_f \Delta P_f}$$

and $$\rho_f = \rho_o \left\{1 + C_f (T_f - T_o)\right\}$$

where W_f - Mass flow of fuel

ΔP_f - Fuel orifice pressure drop

ρ_f - Fuel density at temperature

ρ_o - Fuel density at temperature T_o

T_f - Fuel temperature

T_o - Reference temperature

K_f - Fuel orifice constant

C_f - Thermal expansion coefficient for fuel.

The desired fuel flow (derived setpoint) is found by multiplying the air-fuel ratio setpoint by the measured airflow signal generated by the air controller. The measured fuel flow signal is then subtracted from its derived setpoint and further processed in the P-and-I controller to generate a signal that controls the skid-mounted bypass control valve.

Improper operation of the fuel system is indicated by a fuel flow alarm. The ratio of the actual and desired fuel flow

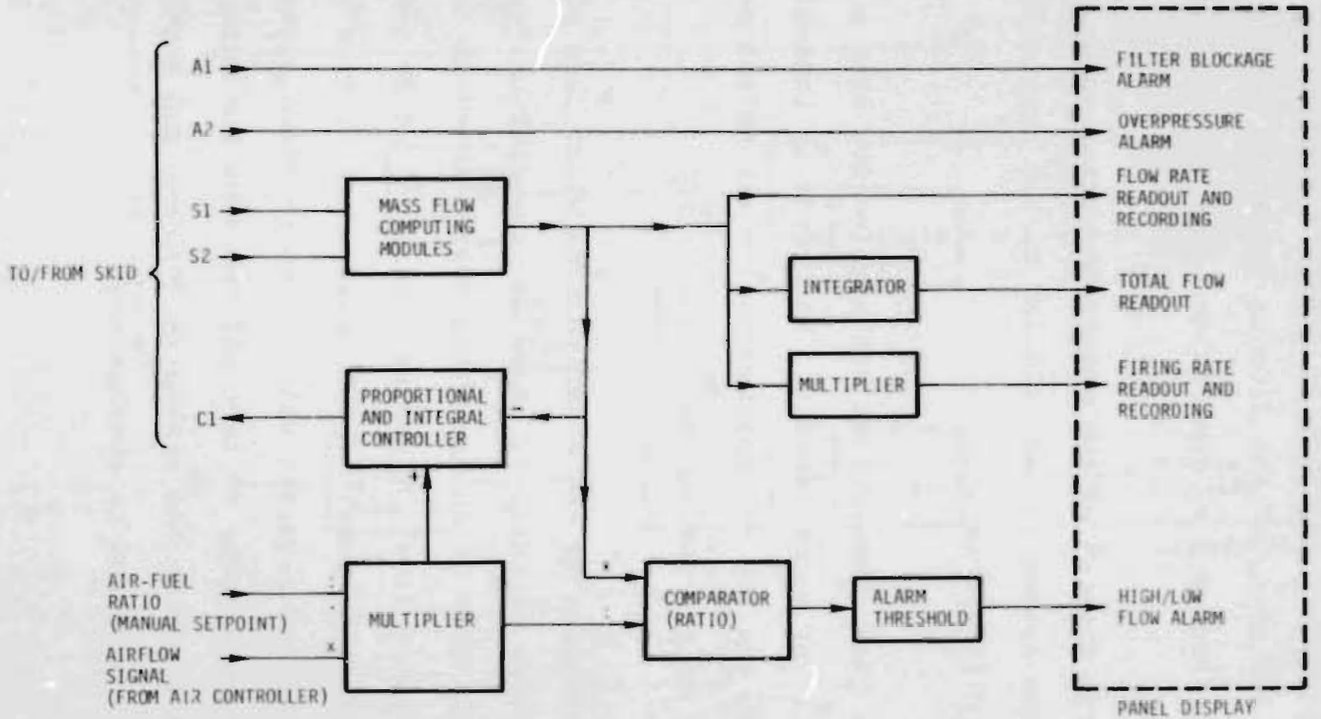

Figure 5-7. Schematic Diagram of Fuel Controller

is processed by a threshold module to generate a high/low alarm signal. The alarm is activated whenever the actual fuel flow differs (positively or negatively) from its setpoint by more than 10%. In addition, if the flow is below its setpoint, transfer to the backup fuel pump takes place automatically.

A schematic diagram of the water controller is shown in Figure 5-8. The system is very similar to the fuel controller; the principal differences are:

(a) Mass flow computations are carried out with a constant value for water density. The error in indicated steam quality is expected to lie within the uncertainty band of the quality calculation; and

(b) In addition to the high/low flow alarm (and pump transfer circuitry), there is an additional safeguard in the form of an automatic system shutdown due to low water flow. A second threshold module generates a shutdown signal if the measured water flow is below 50% of its required value. The shutdown signal acts through a relay to turn off the fuel and water pumps, thus stopping the combustion process and preventing failure caused by overheating.

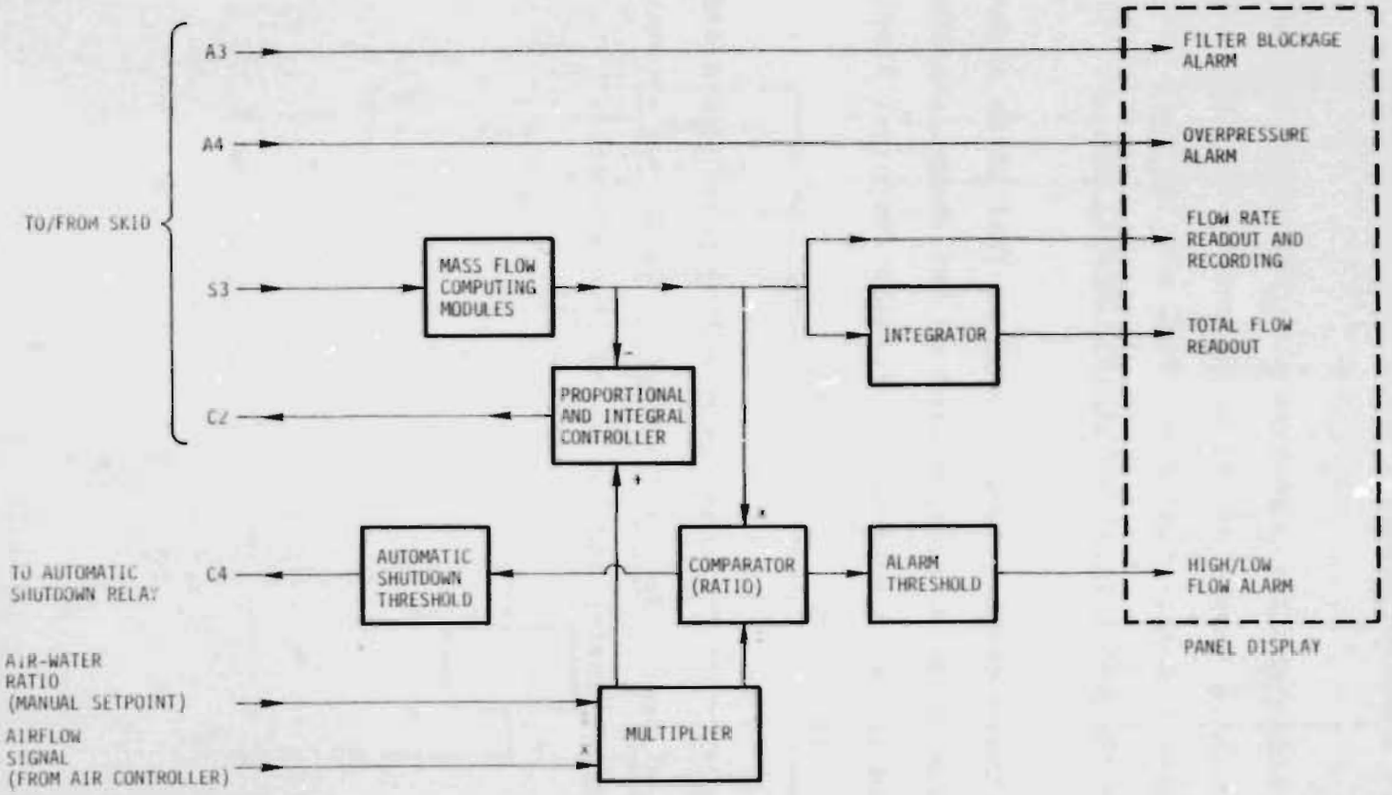

Figure 5-8. Schematic Diagram of Water Controller

A schematic diagram of certain miscellaneous control console subsystems is shown in Figure 5-9. These subsystems include:

- A steam quality computing algorithm that infers downhole steam quality by balancing the heat liberated through combustion of the fuel and the heat absorbed by the water as it turns into steam.

- A thermocouple signal processor that takes signals from thermocouples mounted on the steam generator and provides temperature signals for panel display and recording.

- Power circuits that energize the pump motors and instrumentation, and relays to carry out automatic pump transfer and low water flow shutdown.

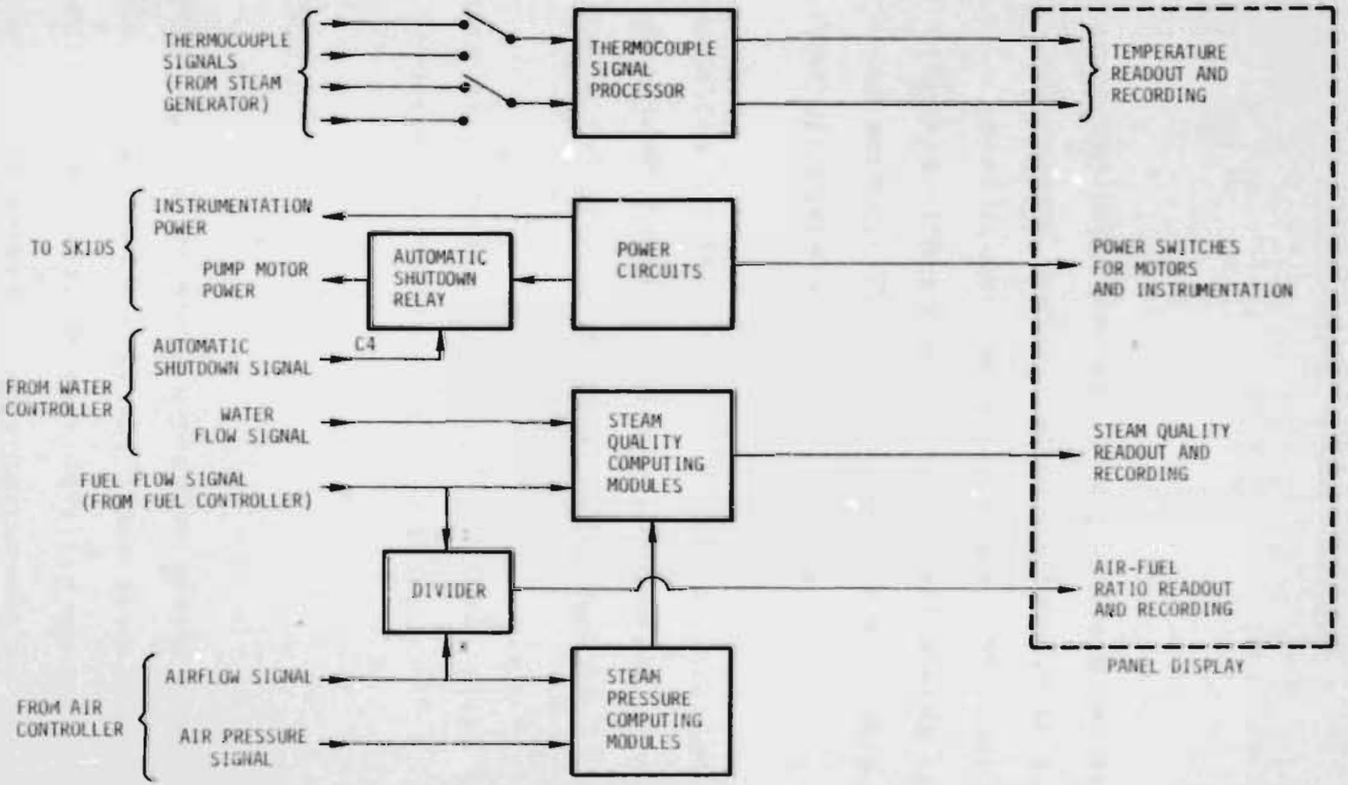

Figure 5-9. Schematic Diagram of Miscellaneous Circuitry

6. EXTENDED SYSTEM TESTING

6.1 Introduction

In order to evaluate how the prototype steam generator (and the control and support systems) would perform in an oil field environment, a quasi field test was planned. The test was conducted at Sandia with a goal of continuous system operation over a five-day period. The steam generator was operated in a simulated downhole environment.

In preparation for this test, a series of extended laboratory test runs of several hours duration was conducted at Foster-Miller's facility in Waltham, Massachusetts.

The extended laboratory tests and the quasi field test are described in detail in the following sections.

6.2 Extended Laboratory Tests

The complete downhole steam generator system (controls, support skids, metal seal packer and steam generator) was tested at Foster-Miller's Waltham, MA test facility during July 1981. The packer and steam generator were positioned in a pressure vessel, as shown in Figure 6-1. The pressure vessel

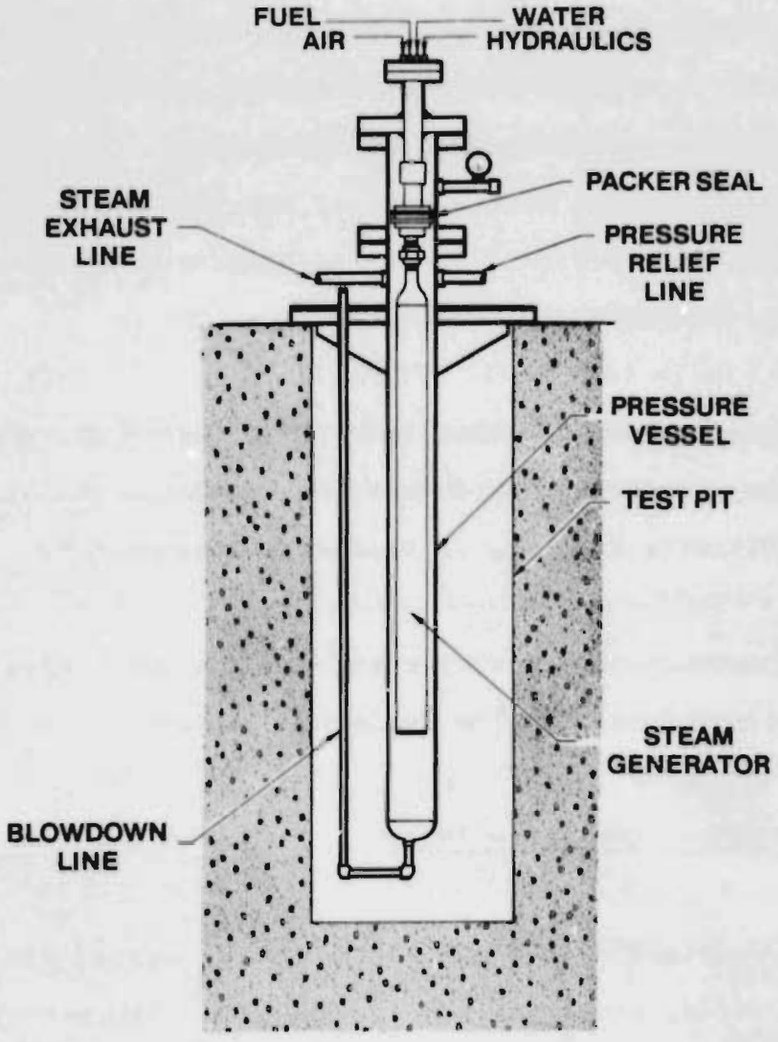

Figure 6-1. Downhole Component Test Facility

permitted the high pressure (up to 1500 psig) downhole oil well environment to be simulated during testing. The test set up permitted the packer to be continuously monitored for leakage. Two Ingersoll-Rand trailer mounted compressors (one primary and one booster) were used to supply the high pressure combustion air. These compressors were capable of delivering airflow sufficient to maintain a 5 MMBTU/HR firing rate. Although the booster unit had a rated discharge pressure of 1500 psig, packing problems with its high pressure stage limited operation to less than 900 psig.

The downhole steam generating system was run for a total of 30 hours during these tests. Test runs varied in length from 1.5 to 7 hours. Operating parameters typical of those monitored during these tests are listed in Table 6-1.

Table 6-1. Typical System Operating Parameters

Firing Rate		5.0 MMBTU/HR
Airflow		830 scfm
Fuel Flow		.62 gpm
Water Flow		8 gpm
Operating Pressure		250-1000 psig
Steam Generator Discharge Analysis	O_2	0.2 - 0.7%
	CO	500 - 2000 ppm
	NO_x	50 - 700 ppm

During these tests, both pressure and air atomizing fuel nozzles were used. Operation with the pressure atomizing nozzle was cleaner than with the air atomizing nozzle. This result was the opposite of that experienced during testing of the atmospheric burner. Although time did not permit an in-depth study of operation with the air atomizing nozzle, it is expected that precise control of the atomizing air pressure and flow rate is needed to optimize performance.

The system operated trouble free with the exception of a fatigue failure of the feedwater control valve stem. Despite the trouble free operation of the system, several forced shutdowns were experienced and significant time was lost due to problems with the air compressors and steam leaks in the packer test spool piece. These steam leaks were not related to the packer which performed flawlessly throughout these tests.

6.3 Quasi Field Test

6.3.1 Introduction

This test which ran from Wednesday, November 4, 1981 through Tuesday, November 10, 1981 was conducted in a simulated well at Sandia. The test well consisted of a 122 ft length of 7 inch well casing cemented in a vertical borehole. The bottom of the

casing was capped and vented back to the surface through a 2.5 inch pipe. A manually-operated back pressure control valve in the vent line was used to establish the pressure at which the steam generator would operate. The steam generator was suspended from a flange at the top of the cased hole in a manner similar to that used during the Extended Laboratory Tests. Figure 6-2 shows the steam generator being lowered into the test well. Trailer-mounted Ingersoll-Rand compressors were used to provide high pressure combustion air to the downhole steam generator. For firing rates up to 5 MMBTU/HR (airflow of 830 scfm), one primary unit and one booster unit were used. Operation at firing rates between 5 and 10 MMBTU/HR required two primary units and one booster unit. The compressors, fuel tanks and instrument trailer used during these tests are shown in Figure 6-3.

During this test, the downhole steam generator system operated for ~111 hours out of an elapsed time of ~156 hours, for an availability of 71 percent. The firing rate varied from 4 to 10.2 MMBTU/HR and steam quality varied from <75 percent to 250°F superheat. Overall performance of the system was quite satisfactory, except for a problem caused by deposition of calcium salts in the cooling water passages. We know now that this problem is avoidable (by different water treatment), but it was responsible for 65 percent of the downtime experienced during the test.

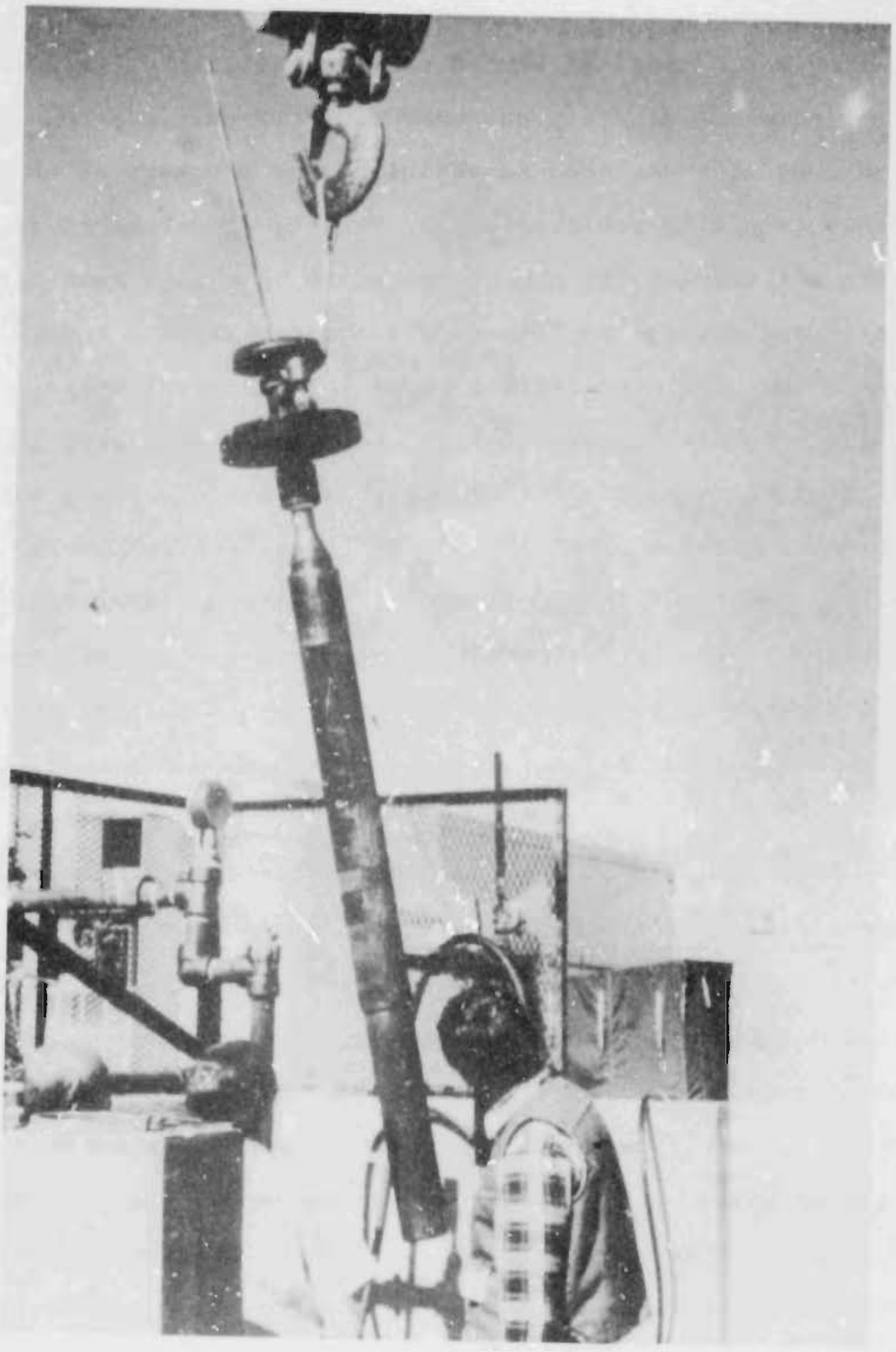

Figure 6-2. Steam Generator Being Placed in Test Well

Figure 6-3. Air Compressor, Fuel Tanks, and Instrument Trailer

6.3.2 Test Log

Startup at 10:15, Wednesday, November 4. Except for a 1.5 hour shutdown to repair a compressor fuel line leak, the steam generator ran continuously for 42 hours at 3.5-5 MMBTU/HR, 900-1300 psi. During this run, the firing rate was limited by the indicated compressor airflow output, which dropped off late at night to as low as 600 scfm (low airflow readings discussed below).

The water pump discharge pressure began to increase during the last 4 hours of the run, eventually opening the water pressure relief valve and causing automatic shutdown of the steam generator. This excessive pressure was apparently caused by salt buildup in the water spray nozzles.

During shutdown, sulfamic acid was poured down the waterline to dissolve the salt deposits, then the waterline was flushed with water for over 1 hour. Total downtime was over 12 hours.

Startup at 16:55, Friday, November 6. The steam generator ran for 8 hours at approximately 5 MMBTU/HR, 1100 psi. Again, clogged water nozzles caused an automatic shutdown. Shortly before shutdown, an attempt to cool the water jacket by reducing the firing rate from 4.5 to 4.2 MMBTU/HR failed to relieve the high water pressure.

After shutdown, the waterline was flushed with water. Total downtime was ~1.5 hours.

Startup at 02:25, Saturday, November 7. The steam generator ran for 4+ hours at ~5 MMBTU/HR, 900-1300 psi. Again, clogged water nozzles caused an automatic shutdown.

While the steam generator was down, a defective pressure gauge at the water filter discharge was replaced. The water flow control valve, which had been leaking, was tightened. The water pressure relief valve, which also had been leaking, was tightened.

The compressor air hoses were uncoupled, and it was noticed that the inner walls of the hoses were coated with an oily substance, with a mustard-like consistency. This substance effectively reduced the diameter of the air hose by about 1/3. The airflow orifice was then disassembled and inspected. It, too, was covered with the substance. The tubes leading to the airflow transmitter were partially clogged. This probably caused the low airflow readings at night when the temperature was low and the substance was more likely to congeal in these tubes. The airflow orifice and transmitter piping were cleaned and reassembled. To prevent a reoccurrence of this problem, the air skid was covered and heated during the remainder of the test.

An attempt to start up was made, but there was no control over the water flow. The water flow control valve was disassembled, and it was discovered that loss of control was caused by a worn plug. Several of the worn parts were replaced. Total downtime was ~8-1/2 hours.

Start-up at 14:55, Saturday, November 7. The steam generator ran for 2 hours at ~5 MMBTU/HR, 1200 psi. The water nozzles started to clog, and the steam generator was shut down manually.

Three quarts of sulfamic acid were poured down the waterline, and the waterline was flushed with 11 gpm of water for 1 hour. Total downtime was ~2 hours.

Start-up at 19:25, Saturday, November 7. The steam generator ran for 12 hours at 4.5 MMBTU/HR, 100 psi. During this run, it was very difficult to maintain adequate caustic flow. The pH was ~3 for the last 5 hours of the run. Numerous steam leaks developed during this time. Due to severe corrosion in the exhaust line, the steam generator was shut down.

The leaks were repaired and the exhaust manifold piping was replaced. Total downtime was ~4 hours.

Start-up at 11:30, Sunday, November 8. The steam generator ran for 20 minutes at 5 MMBTU/HR, 1200 psi. Right after

start-up, attempts to increase caustic flow failed. The water supply pressure was high enough (80 psi) that the chemical addition pumps were unable to pump against it. The water supply pressure regulator was found to be inoperative. The steam generator was shut down while the water supply pressure regulator was replaced. Total downtime was ~1 hour.

Start-up at 13:05, Sunday, November 8. The burner did not light. Apparently there was not enough triethylborane (TEB) in the TEB bottle. The TEB supply cylinder at the TEB filling station was replaced and a new, full TEB bottle was installed at the burner. Total additional downtime was 2+ hours.

Start-up at 15:10, Sunday, November 8. The steam generator ran for ~21 hours at 5 MMBTU/HR, ~1200 psi. Caustic flow was adequate to maintain the pH above 7 until 03:00, Monday, November 9. At that time, the pH began to fluctuate rapidly between 3 and 7. By 10:00, the pH failed to rise above 3. Constant attention to the caustic addition pumps failed to remedy the problem, so at 12:35 the steam generator was shut down to prevent severe corrosion.

Many chrystals had formed at the bottom of the caustic supply drum and at the inlet filter to the caustic addition pump, completely clogging the filter and preventing flow to the pump.

The caustic supply drum was replaced with a fresh drum which was then kept heated. The caustic addition pumps were cleaned and primed. Caustic pump #2 (from Foster-Miller) was replaced with a DMT pump (same type as caustic pump #1). A leak which had developed on the pressure reducing valve union in the steam generator exhaust line was welded. Total downtime was 3 hours.

Start-up at 15:40, Monday, November 9. The steam generator ran for ~1 hour at 6.3 MMBTU/HR, 1100 psi. A higher firing rate was attempted, but fuel flow was limited by the 24 gph fuel nozzle. The steam generator was shut down to replace the fuel nozzle with a 40 pgh, 80° hollow nozzle. Total downtime was 2 hours.

Start-up at 19:00, Monday, November 9. The steam generator ran for ~7 hours at ~8 MMBTU/HP, 1000 psi. Clogged water nozzles caused an automatic shutdown.

The waterline was flushed with water. The leak on #1 water pump inlet was repaired. Total downtime was 2 hours.

Start-up at 03:30, Tuesday, November 10. The steam generator ran for 1 hour at 4 MMBTU/HR, 1000 psi. The fuel nozzle appeared to be clogged which prevented a higher firing rate. The steam generator was shut down to clean the fuel nozzle. Total downtime was ~3 hours.

Start-up at 07:20, Tuesday, November 10. The steam generator ran for ~2 hours at 8 MMBTU/HR, 1000 psi. The water nozzles began to clog, so the steam generator was shut down and the waterline was flushed with water. Total downtime was 1 hour.

Start-up at 10:05, Tuesday, November 10. The steam generator ran for 10 minutes at 5 MMBTU/HR, 100 psi. The fuel nozzle had clogged again, so the steam generator was shut down and the fuel nozzle cleaned.

At the same time, 3 more quarts of sulfamic acid were poured down the waterline. Total downtime was ~2 hours.

Start-up at 12:00, Tuesday, November 10. The steam generator ran for 4 hours at ~8 MMBTU/HR, 1000 psi. At 16:10, the firing rate was increased gradually. While the firing rate was being increased, the water flow control valve broke in the closed position. All control over water flow was lost. With both water pumps on, the flow was 21 gpm. This high flow caused the pump inlet pressure to drop to 0 psig, even with flow through both sets of new filters. At this constant water flow rate, the firing rate was increased to 10 MMBTU/HR, 900 psi, where it was held for most of the next 6+ hours (two 15-20 minute periods of running at a reduced firing rate, 5 MMBTU/HR, were required to combat water nozzle clogging by changing water filters and stopping caustic addition). At 1800, the firing rate was

increased as much as possible. A maximum firing rate of 10.2 MMBTU/HR was attained. The burner was limited from a higher rate by the airflow output from the compressors. The water nozzles began to clog, and the steam generator was shut down.

6.4 Test Summary and Conclusions

A summary of the system performance during the test is shown in Table 6-2 and Figure 6-4. Causes of all shutdowns, automatic and operator initiated, during the test are summarized in Table 6-3. Operating hours and shutdown times for various causes are presented in Table 6-4.

As can be seen from Tables 6-3 and 6-4, 7 of 14 shutdowns were caused by salts deposited by the precipitation of calcium carbonate in the water passages of the steam generator. Figure 6-5 shows the $CaCO_3$ deposit present in the water jacket of the steam generator at the conclusion of the test. During the course of the test it was felt that this problem was caused by leakage of excess calcium through the water softener. Further investigation after the tests indicated that the problem was actually caused by the introduction of the sodium hydroxide used to control the pH of the wet steam into the feedwater. The feedwater pH was increased to about 11 before it was delivered to the steam generator. At this pH the solubility limit of calcium in water is less than 1 ppm. Heating the water in the steam

Table 6-2. Test Summary

Firing Rate (MMBTU/HR)	Pressure (psig)	Steam Quality	Steam Output (bbl/day)	Operating Time (hr)	Startup/ Shutdown Cycles
4.0 to 5.5	900 to 1300	85% to Superheat	190 to 300	89.5	7
7.5 to 8.0	900 to 1300	75% to Superheat	400 to 550	14.5	5
10.0 to 10.2	750 to 1000	75%	700	7	1

Table 6-3. Shutdown Summary

Cause of Shutdown
1. Air Compressor Fuel Line Leak
2. *Clogged Water Nozzles and Compressor Failure
3. *Clogged Water Nozzles
4. *Clogged Water Nozzles
5. Clogged Water Nozzles
6. Corrosion of Exhaust Piping
7. Defective Water Supply Pressure Regulator
8. Inability to Control pH
9. Fuel Nozzle Too Small
10. *Clogged Water Nozzles
11. Clogged Fuel Nozzle
12. Clogged Water Nozzles
13. Clogged Fuel Nozzle
14. Clogged Water Nozzles
* Automatic Shutdown

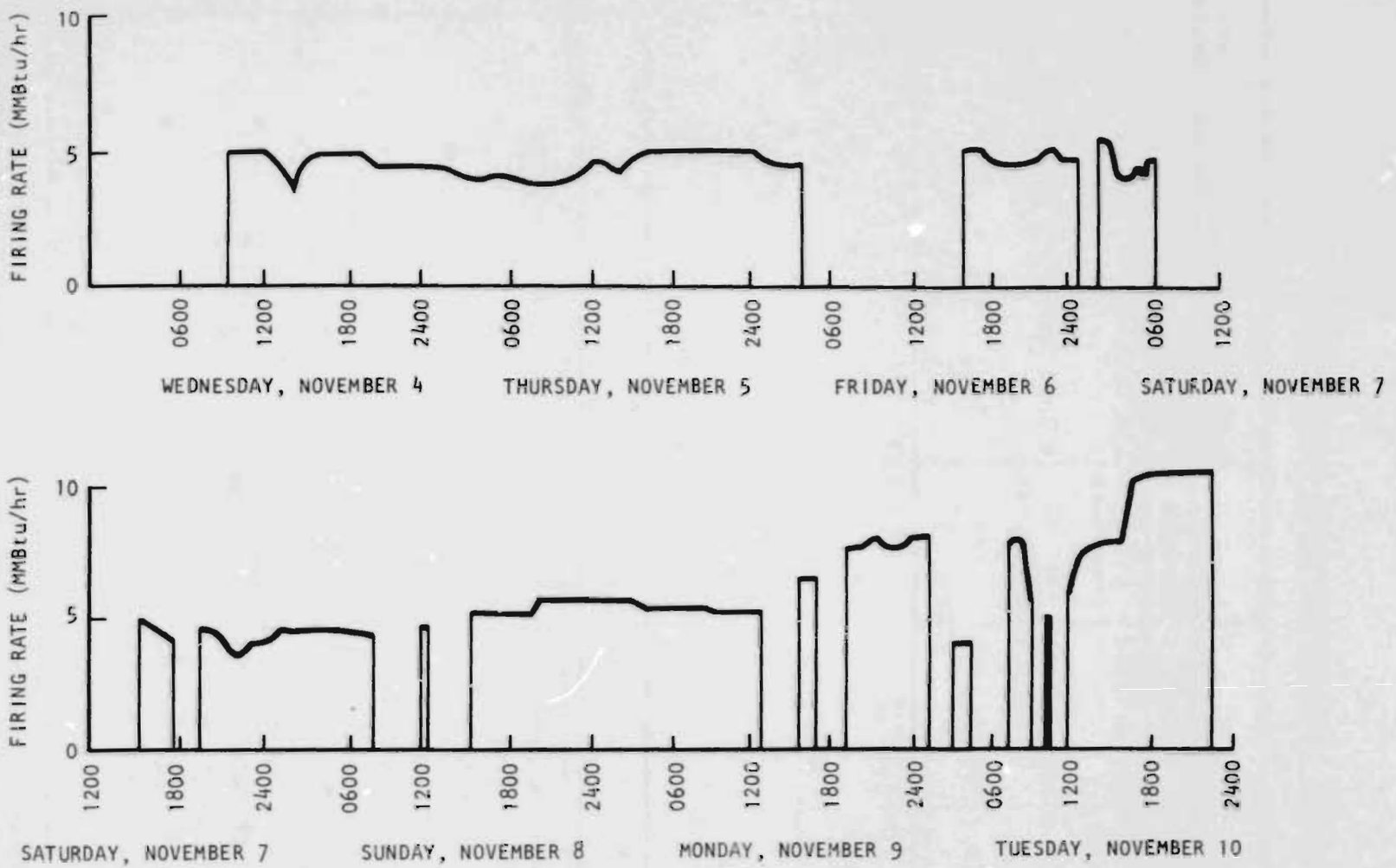

Figure 6-4. Quasi Field Test Operating Profile

TABLE 6-4 OPERATING/SHUTDOWN TIMES

TOTAL HOURS			156.2 hrs
OPERATING TIME AT VARIOUS FIRING RATES:	4.0 - 5.5 MMBTU/hr:	89.5 hrs	
	7.5 - 8.0 MMBTU/hr:	14.5 hrs	
	10.0 - 10.2 MMBTU/hr:	7.0 hrs	
TOTAL		111.0 hrs	
PERCENT OPERATING TIME:			71%

SHUTDOWNS

CAUSE	INCIDENTS	HOURS DOWN	% TOTAL DOWNTIME
Clogged water nozzles	7 & Final	29.1	65
Water supply/ treatment problems	2	6.3	14
Clogged fuel nozzle	2	4.6	10
Exhaust pipe corrosion	1	3.7	8
Compressor problems	1	1.5	3
TOTALS	14	45.2	100

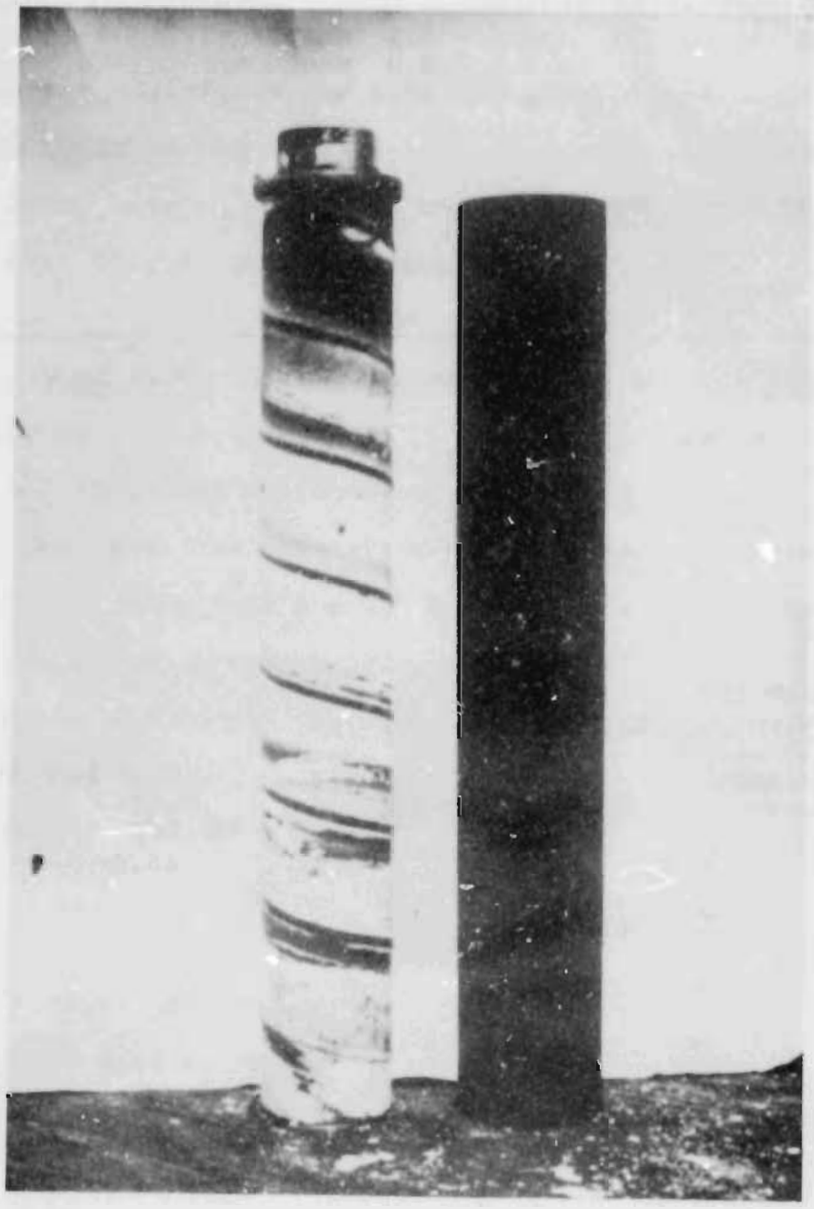

Figure 6-5. Water Jacket Scale Deposits

generator water jacket reduced the solubility limit even further, thus, even trace amounts of calcium would precipitate, making plugging inevitable.

This problem could be avoided by using deionized water or by using a high pressure chemical injection pump and introducing the sodium hydroxide directly into, or downstream of, the steam generation zone of the steam generator.

The practicality of the hot wall ceramic combustion chamber was demonstrated during this test. The sectioned ceramic (Carborundum REFRAX) combustion chamber is shown in Figure 6-6. Visual examination of the combustion chamber prior to disassembly revealed a crack pattern of 1-2 cm separation over most of the interior surface. On disassembly it was determined that many of the cracks extended through the tube wall. Glass (silicon dioxide) produced by oxidation of the ceramic covered most of the inner surface and bridged the cracks at the inner surface of the tube.

The glass layer had a rippled appearance and varied in thickness from 1-2 mm in most areas to several mm at the thickest point. The rippled appearance of the glass was evidently due to flow of the molten glass caused by the high velocity gas moving over the surface. The glass layer appears to be chemically stable in the combustor environment, and it acts as a barrier to

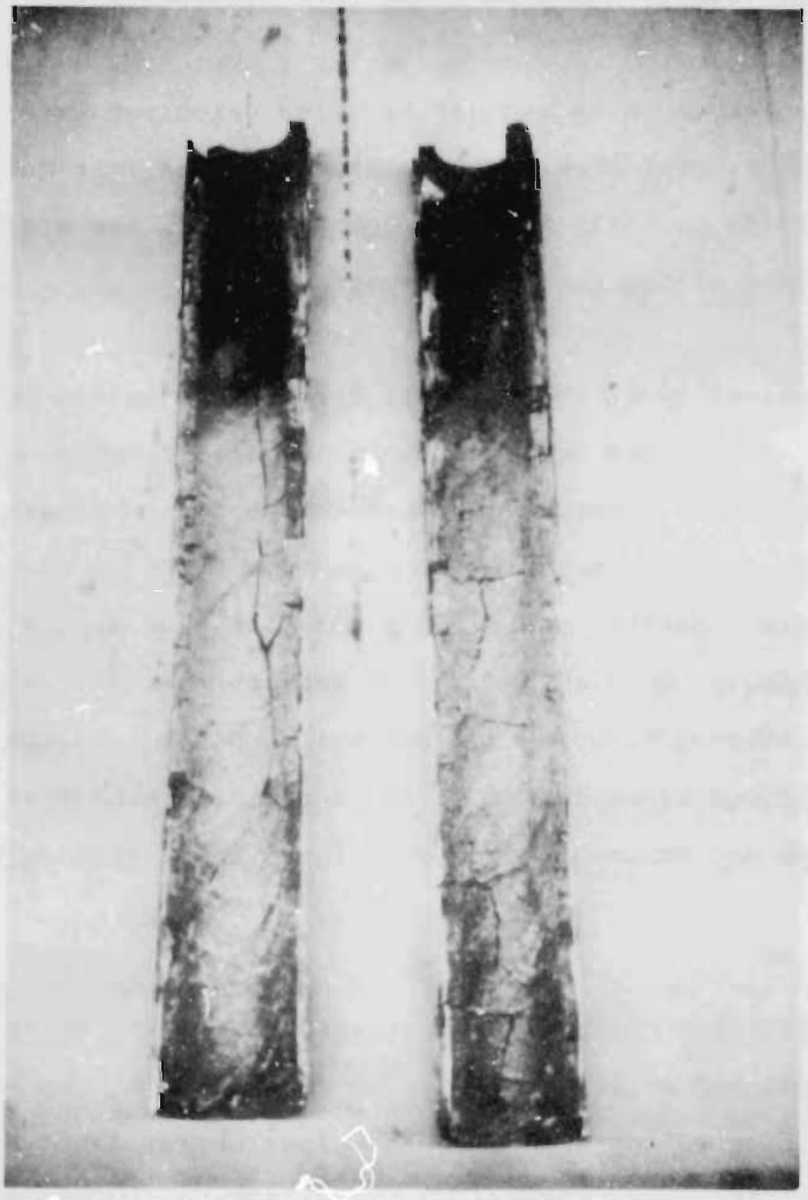

Figure 6-6. Silicon Carbide Combustion Chamber Liner

prevent chemical attack and further oxidation of the ceramic. Spalling of the glass produced local recession of the tube walls in some areas. This spalling occurred during cooldown of the liner. Differences in the coefficients of thermal expansion of glass and silicon carbide resulted in the glass layer being placed in compression and spalling during cooldown; this spalling was most severe in the vicinity of the cracks in the ceramic tube.

The cracking of the ceramic tube and the spalling of the glass layer did not adversely affect the performance of the combustor nor is it felt that they would significantly reduce the operating life of the steam generator. The most severe damage to the combustion chamber was the loss of a 3 inch section from the downstream end. This type failure would be unacceptable if it propagated up the liner. Incorporation of an end restraint in the liner design should prevent this type failure.

The overall performance of the silicon carbide combustion chamber liner was very good and certainly much superior to any other liner tested during the program. A more detailed analysis of the liner performance can be found in Sandia's report entitled "Performance of Ceramic Combustion Tubes in Enhanced Oil Recovery Steam Generators," [4].

Aside from the calcium scaling problem, the only disappointing aspect of this test was the inability to attain the

soot free combustion seen in previous tests. Soot was present in the steam generator exhaust regardless of air-fuel ratio. Post test examination revealed a gap in the burner swirl head which permitted some combustion air to bypass the tangential air inlets and deflect the atomizing fuel spray against the combustion chamber wall. This disruption of the fuel distribution pattern prevented clean combustion. A return to the one-piece swirler head designs at the sacrifice of ease of assembly would remove the potential for a gap opening and eliminate this problem in future units.

7. CONCLUSION

This program was undertaken to develop the technology base for downhole steam generation, and to demonstrate the feasibility of key system components. These objectives have now been achieved.

Basic system components (steam generator, packer, tube string and controls) have been designed. Testing of the steam generator and packer (including the controls) have confirmed overall feasibility. (A tube string design similar to the one described herein was tested independently by Sandia.) Thus, all system components have successfully undergone prototype testing. An integrated system can now be assembled and tested in the field.

Specific conclusions drawn from the technical development are as follows.

Steam Generator

- The diesel-fired, ceramic-lined combustor operates reliably and efficiently at high pressures under stoichiometric conditions

- The direct-injection vaporizer downstream of the combustor is capable of producing steam of a quality that can be varied from wet to superheated

- The use of demineralized or unbuffered feedwater is necessary to prevent salt buildup and clogging of the steam generator water passages

- The ceramic liner of the combustor enables the system to operate efficiently and cleanly in spite of poor fuel atomization (caused by high pressure, for instance). The concept thus appears to be capable of ultimate use with heavy fuels.

Packer

- The expanding metal seal packer seals reliably at high pressures and temperatures

- The composite aluminum-titanium-copper sealing rings provide the necessary ductibility, creep strength and corrosion resistance needed for downhole use

- A standard tubing anchor used in conjunction with the metal seal module is adequate.

Control System

- Accurately metered air, water and fuel to the steam generator is essential for clean combustion and predictable steam generation

- Air-fuel ratio control is particularly important to prevent generation of soot in the exhaust products

- A closed-loop analog control system assembled from commercial off-the-shelf components provides adequate control.

Tube String

- A multi-string tubing system, based on designs used in offshore risers, appears to be within the state-of-the-art.

System Analysis

- The overall thermal efficiency of the downhole steam generation process lies between 55-65%

- Downhole steam quality is independent of depth

- The casing and wellbore are not subject to thermal stress

- The amount of pollution control equipment is minimized.

A brief applications study indicates that downhole steam generation is likely to be the favored system for certain unconventional steam flooding operations where limitations restrict the use of surface steam generators. Some key applications and the reasons for choosing downhole steam over surface steam are given below.

APPLICATIONS	ADVANTAGES OF DOWNHOLE STEAM
1. Deep wells	No wellbore heat loss High downhole steam quality
2. Environmentally impacted areas	No exhaust emissions. Minimum surface impact (with remote equipment location)
3. Arctic applications	No thermal impact on completion and surroundings
4. Offshore applications	High downhole quality in long (deviated) wells. No wellbore heat loss. Reduced platform space constraints (with remote equipment location)

8. REFERENCES

1. TeVelde, J.A., Spadaccini, L.J., "Autoignition Characteristics of No. 2 Diesel Fuel," Prepared for National Aeronautics and Space Administration, Report No. NASA CR-165315, DOE/NASA/0066-2, June 1981.

2. Beauchamp, E.K., "Failure Analysis of Alumina Liners for Downhole Steam Generator Combustion Tube," Memo Dated August 6, 1980 to D.R. Johnson, Sandia National Laboratories, Albuquerque, New Mexico.

3. Beauchamp, E.K., "Post Test Analysis of Fragments from Foster-Miller Combustor Tube," Memo Dated February 16, 1981 to A.B. Donaldson, Sandia National Laboratories, Albuquerque, Mew Mexico.

4. Beauchamp, E.K., "Performance of Ceramic Combustion Tubes in Enhanced Oil Recovery Steam Generators," SAND83-1863, Sandia National Laboratories, Albuquerque, New Mexico.

5. Loomis, A.W., Compressed Air and Gas Data, 3rd Edition, Ingersoll-Rand Co., Washington, N.J., 1980.

APPENDIX A

Analytical Model of Downhole Steam Generation System

The thermodynamic model of the downhole steam generation system is given in Figure A-1. Applying the First Law of Thermodynamics during steady state operation to the control volume shown leads to the following relationship

$$(w_s h_s + w_e h_e) - (w_a h_a + w_w h_w + w_f h_f) - w_f h_{rf} = Q + (P_a + P_f + P_w) \qquad (A\text{-}1)$$

where the symbols are as follows:

w	-	mass flow of fluid entering or leaving control volume
h	-	enthalpy (per unit mass) of fluid entering or leaving control volume
h_r	-	"heat value" of fuel
Q	-	rate of heat transfer into control volume
P	-	power delivered to control volume

and the subscripts are defined below:

$( )_s$ - steam $( )_w$ - water

$( )_e$ - exhaust gases $( )_f$ - fuel

$( )_a$ - air

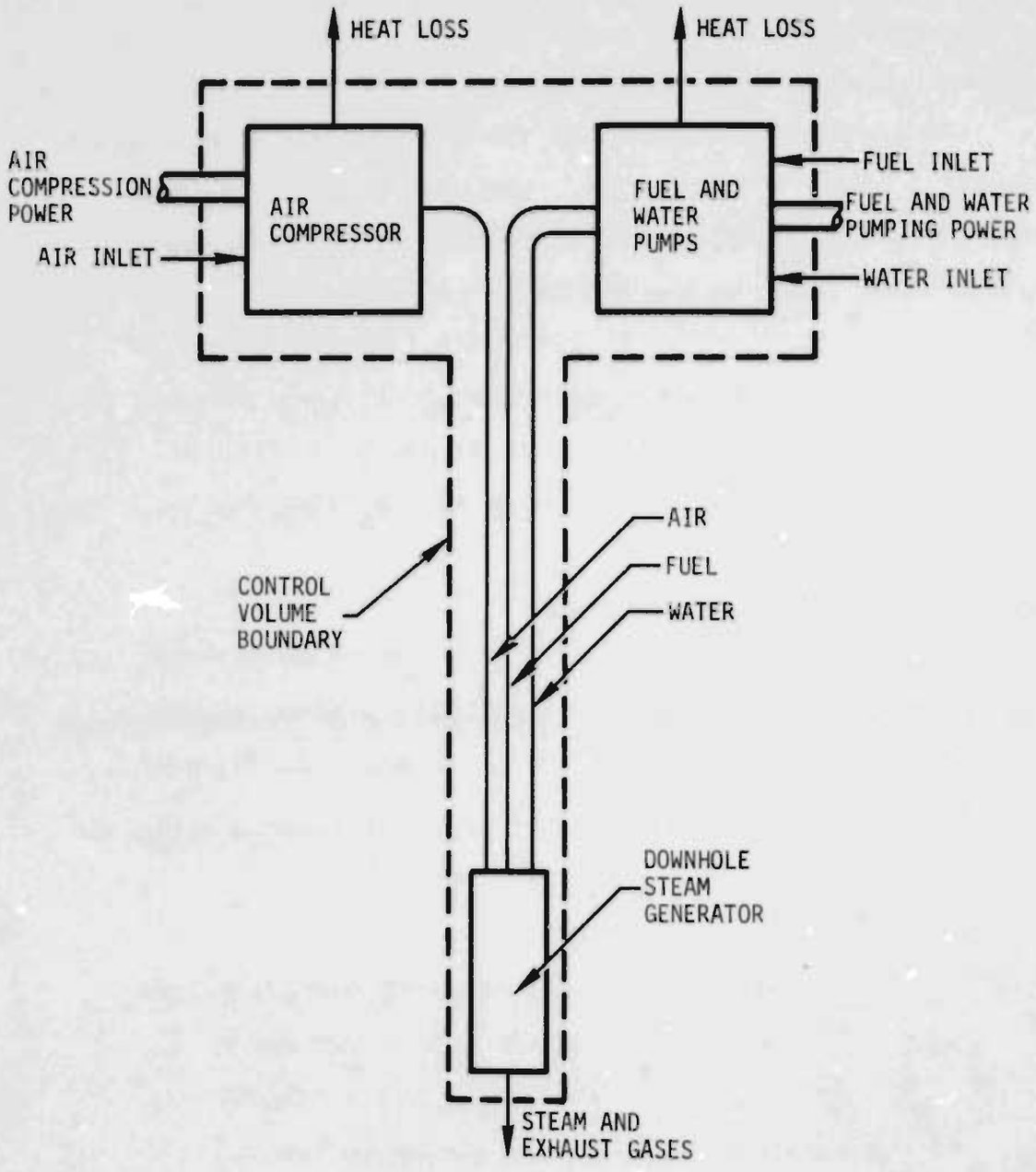

Figure A-1. Thermodynamic Model of Downhole Steam Generation System

Eqn. (A-1) is the fundamental relationship from which thermal efficiency and other data presented earlier have been found. In evaluating this equation, the following assumptions have been made.

1. Fuel is supplied to establish the required firing rate. The fuel burns completely in the steam generator, and all the heat liberated is transferred to the products of combustion and water which increase in enthalpy and leave the control volume. The relevant properties of the fuel (#2 fuel oil) are as follows:

Upper Heat Value	140,000 BTU/gal
Stoichiometric Air/Fuel Ratio:	14.41 lb/lb
Combustion Products (by weight):	20.7% CO_2, 7.6% H_2O, 71.7% N_2
Density:	7.17 lb/gal

2. Air is supplied to maintain the stoichiometric air/fuel ratio.
3. Water is supplied to maintain a steam quality of 80% at the generator outlet.
4. The air, fuel and water entering the control volume have a temperature of 77°F.

5. The steam and exhaust gases (N_2&CO_2) leaving the control volume are in thermal equilibrium (uniform temperature). The partial pressures of the steam and exhaust gases are proportional to their respective mole fractions (Daltons Law of Partial Pressures). The total pressure of the mixture equals the injection pressure.

6. The volume of the liquid phase in wet steam is neglected in comparison to the volume of the vapor phase.

7. The fuel and water pumping power and friction loss is neglected.

8. Enthalpy change due to height change and velocity change is neglected.

9. There is no pressure change between the air compressor outlet and the steam generator exhaust. Both gravity head and friction loss are neglected.

10. The air compression power (P_a) per unit airflow at delivery pressure p_d (atmospheric pressure p_a) is given by [5]

$$P_a = 0.278 \ln (p_d/p_a) \quad hp/scfm$$

11. The efficiency of the engine driving the air compressor is 35%.

DISTRIBUTION:

D. Uthus, Director
Office of Oil, Gas, & Shale
U. S. Dept. of Energy
FE-33, GTN
Washington, DC 20545

U. S. Department of Energy (3)
FE-32, D-128 GTN
Washington, DC 20545
Attn: G. Parker
G. Stosur
Kishore Parekh

Ronald S. H. Thoms
Div. of Geothermal Energy
U. S. Dept. of Energy
CE-324, 5G-030 FORSTL
Washington, DC 20585

Dr. R. J. Braitsch, Jr.
Office of Planning & Tech.
Assessment
U. S. Dept. of Energy
FE-13, C-125 GTN
Washington, DC 20545

Office of Deputy Asst. Secretary (2)
for Oil, Gas & Shale Technology
U. S. Dept. of Energy
Mail Stop D-107
Washington, DC 20545
Attn: R. Avellanet
E. Burwell

Morgantown Energy Tech. Center (3)
U. S. Dept. of Energy
P. O. Box 880
Morgantown, WV 26505
Attn: P. R. Wieber
H. D. Shoemaker
J. W. Martin

L. Dockter
U. S. Dept. of Energy
P. O. Box 3395, Univ. Sta.
Laramie, WY 82071

R. Folstein, Director
Bartlesville Project Office
U. S. Dept. of Energy
P. O. Box 1398
Bartlesville, OK 74003

U. S. Dept. of Energy (3)
San Francisco Operations Office
1333 Broadway
Oakland, CA 94612
Attn: J. Keenan, Director
H. J. Lechtenberg
G. D. Peterson

A. A. Pitrolo
US/DOE, METC
P. O. Box 880
Morgantown, WV 26505

U. S. Dept. of Energy (2)
Energy Research & Technology
Albuquerque Operations Office
Albuquerque, NM 87115
Attn: D. L. Krenz
Capt. John Hanson

Joseph T. Hamrich
Aerospace Research Corp.
5454 Jae Valley Road
Roanoke, VA 24014

R. E. McCluskey
Amoco Production Co.
P. O. Box 591
Tulsa, OK 74102

T. S. Buxton
Amoco Production Co.
P. O. Box 591
Tulsa, OK 74102

B. Ferguson
Amoco Prod. Research
P. O. Box 591
Tulsa, OK 74102

C. Birnie
Amoco Production Co.
P. O. Box 591
Tulsa, OK 74102

Elton B. Hunt, Jr.
Amoco Production Co.
Research Center
P. O. Box 591
Tulsa, OK 74102

M. W. Smith
Arco Oil & Gas Co.
PRC-R115
P. O. Box 2819
Dallas, TX 75221

A. L. Barnes
Arco Oil & Gas Co.
Box 2819
Dallas, TX 75221

F. Hernandez
Arco Oil & Gas Co.
PRC-R138
Box 2819
Dallas, TX 75221

G. Youngren
Arco Oil & Gas
P. O. Box 2819
Dallas, TX 75221

D. B. Burnett
Burnett Research Assoc.
2081 Hutton, Suite 111
Carrollton, TX 75006

James Irvine, Manager
Oil Recovery Division
Chevron Oil Field Research Co.
P. O. Box 446
La Habra, CA 90631

Wes Densmore
Cities Services Co.
Box 300
Tulsa, OK 74102

J. C. Mundis
Cities Services Co.
Box 3908
Tulsa, OK 74102

W. M. Pusch
Cities Service Co.
Box 12016
Jackson, MS 39211

R. C. Ellis
Completion Technology Co.
4200 Westheimer Rd., Suite 211
Houston, TX 77027

W. L. Martin
Conoco, Inc.
P. O. Box 1267 (NT 100)
Ponca City, OK 74603

Dr. Thomas J. Gilligan III
Diamond Shamrock Corp.
T. R. Evans Research Center
P. O. Box 348
Painesville, Ohio 44077

P. A. Leonard
Exxon Prod. Research Co.
P. O. Box 2189
Houston, TX 77001

M. E. Rodgers
Exxon Production Research
P. O. Box 2189
Houston, TX 77001

B. Willman
Exxon Prod. Research Co.
P. O. Box 2189
Houston, TX 77001

Steve Pursley
Exxon Production Research Co.
3120 Buffalo Speedway
Houston, TX 77001

J. S. Aronofsky
Gafney Cline Assoc.
630 Fidelity Union Tower
Dallas, TX 75201

Vernon Hill
Gas Research Institute
8600 West Bryn Mawr
Chicago, IL 60631

B. F. Birdwell
Getty Oil Co.
Exploration & Prod. Research
3903 Stoney Brook
Houston, TX 77063

Getty Oil Co. (2)
1601 New Stine Road
P. O. Box 10269
Bakersfield, CA 93389
Attn: R. A. Shore
R. L. Williams

A. E. Trimble, Manager
Petroleum Recovery Research
Getty Oil Co.
3903 Stoney Brook
Houston, TX 77063

Gibbons Geotechnical
528 Carlisle NE
Albuquerque, NM 87106

J. V. Howard
Greenwich Oil Corp.
Suite 200
6750 Hillcrest Plaza Dr.
Dallas, TX 75230

John C. Fair, Director
Production Engineering Section
Gulf Research & Development Co.
P. O. Drawer 2038
Pittsburgh, PA 15230

C. C. Cala
Gulf R&D Co.
Bldg. 5-407
P. O. Box 2038
Pittsburgh, PA 15230

J. P. Benton
Gulf Oil E&P Co.
P. O. Box 16735
Houston, TX 77251

P. L. Terwilliger
Gulf Oil E&P Co.
P. O. Box 1392
Bakersfield, CA 93302

Dr. Paul Kydd
HCR R&D Center
P. O. Box 6047
Lawrenceville, NJ 08648

R. C. Wilson
Husky Oil Co.
P. O. Box 1869
Santa Maria, CA 93456

R. F. Meldau
Husky Oil Ltd.
P. O. Box 1869
Santa Maria, CA 93456

W. H. Fairfield
Husky Oil Co.
P. O. Box 1869
Santa Maria, CA 93456

A. Erickson
Koch Exploration Co.
P. O. Box 2256
Wichita, KS 67201

R. J. Miller
Koch Exploration Co.
P. O. Box 2256
Wichita, KS 67201

A. J. Leighton
1816 Holland Dr.
Walnut Creek, CA 94596

D. R. Stephens
Lawrence Livermore Natl. Lab.
L-200
Livermore, CA 94550

K. D. Dreher
Marathon Oil Co.
P. O. Box 269
Littleton, CO 80160

B. G. Holmes
Mobil R&D Corp.
P. O. Box 900
Dallas, TX 75221

W. R. Shu
Mobil R&D Corp.
P. O. Box 900
Dallas, TX 75221

W. D. Lyle
Mobil FRL
P. O. Box 900
Dallas, TX 75221

K. J. Touryan
Mount Morich Trust
6200 Plateau Drive
Englewood, CO 80111

G. N. Buttram, Opr. Mgr.
Attn: J. L. Turney
Occidental Petroleum, Inc.
5000 Stockdale Highway
Bakersfield, CA 93309

George B. Miller
Occidental Research Corp.
P. O. Box 19601
Irvine, CA 92713

J. A. Slater
Occidental E&P Co.
5000 Stockdale Hwy.
Bakersfield, CA 93309

Bill Rumbaugh
Otis Engineering
P. O. Box 34380
Stop D-O
Dallas, TX 75234

Michael Fahy
Public Service Co. of NM
P. O. Box 2267
Albuquerque, NM 87103

T. M. Counihan
Santa Fe Energy Co.
10737 Shoemaker Ave.
Santa Fe Springs, CA 90670

P. J. Closmann
Shell Development Co.
Box 481
Houston, TX 77001

W. Carey Hardy
Sun E&P Co.
P. O. Box 2880
Dallas, TX 75221

J. T. Moss
Tejas Petroleum Engr., Inc.
2809-B Allen Street
Dallas, TX 75204

P. D. White
Tejas Petroleum Engr.
2809-B Allen Street
Dallas, TX 75204

E. H. Garthoffner
Tenneco Oil
P. O. Box 9909
Bakersfield, CA 93389

Dr. W. Somerton
Mechanical Engineering Dept.
Univ. of California/Berkeley
Berkeley, CA 94306

Dr. L. Handy, Chairman
Petroleum Engineering Dept.
University of Southern Cal.
Los Angeles, CA 90007

Ali Ghalambor
Univ. of SW Louisiana
P. O. Box 44408
Lafayette, LA 70504

Charles H. Ware
5457 Jae Valley Road
Roanoke, VA 24014

Roger Paul
WIDCO
101 Big Hanaford Rd.
Centralia, WA 98531

Jim Fowler
Xadar Corporation
5554 Port Royal Rd.
Springfield, VA 22151

S. M. Farouq Ali
University of Alberta
Dept. of Mineral Engineering
Edmonton, Alberta T6G 2G6
CANADA

T. B. Kimmel
Pengalta R&D Ltd.
4425 - 64th Ave. SE
Calgary, Alberta T2C 2C8
CANADA

Petro Canada (5)
P. O. Box 2844
Calgary, Alberta, CANADA T2P 3E3
Attn: K. Kisman
D. W. Ruth
L. E. Hajdo
B. F. Hawkins
L.D.L. Vorndran

Prof. Maurice B. Dusseault
Dept. of Earth Sciences
Univ. of Waterloo
Waterloo, Ontario N2L 3G1
CANADA

D. A. Best
Esso Resources Canada Ltd.
339 50th Ave SE
Calgary, Alberta T2G 2B3
CANADA

Dr. M. F. Mohtadi
University of Calgary
2920 24th Avenue NW
Calgary, Alberta T2N 1N4
CANADA

J. K. Donnelly
BP Exploration Canada Ltd
333 Fifth Avenue SW
Calgary, Alberta T2P 3B6
CANADA

J. P. Batycky, Section Head
Esso Resources Canada Ltd.
339 50th Ave. SE
Calgary, Alberta
CANADA T2G 2B3

M. Kryska
Husky Oil Operations, Ltd.
Hwy #6 East
Lloydminster, Sask. S9V 0Z8
CANADA

R. Scarborough
Dome Petroleum Ltd.
P. O. Box 200
Calgary, Alberta T2P 2H8
CANADA

J. Burger
Institut Francais Du Petr.
1&4 Ave. De Bois Preau
Rueil Malmaison, FRANCE 92500

Mr. C. H. Dodwell
Attn: Dr. J. E. Preedy
BP Coal Limited
Britannic House, Moor Lane
London EC2Y9BU
UNITED KINGDOM

D. H. Desty
British Petr. Research Centre
Chertsey Road
Sunbury-on-Thames
Middlesex, TW16 7LN
UNITED KINGDOM

D. S. Hughes
UN Kingdom Atomic Energy
AEE Winfrith
Dorchester DT2 8DH
UNITED KINGDOM

Pierre Lichaa
INTEVEP, S. A.
Apartado 76343
Caracas 1170
VENEZUELA, S.A.

END OF

PAPER